New Directions for *Bis*-Adamantane Chemistry and Reactivity

by

Yumeela Ganga-Sah

B. Sc. (Hons.), University of Mauritius, 2011

Thesis Submitted in Partial Fulfillment of the
Requirements for the Degree of
Master of Science

in the
Department of Chemistry
Faculty of Science

© Yumeela Ganga-Sah 2017

SIMON FRASER UNIVERSITY

Spring 2017

Approval

Name: **Yumeela Ganga-Sah**

Degree: **Master of Science (Chemistry)**

Title: ***New Directions for Bis-Adamantane Chemistry and Reactivity***

Examining Committee: **Chair:** Dr. Charles J. Walsby
Associate Professor

Dr. Daniel B. Leznoff
Senior Supervisor
Professor

Dr. Andrew J. Bennet
Co-Supervisor
Professor

Dr. Robert N. Young
Supervisor
Professor

Dr. Jeffrey J. Warren
Supervisor
Assistant Professor

Dr. Peter D. Wilson
Internal Examiner
Associate Professor

Date Defended/Approved: January 27, 2017

Abstract

Bulky chiral ligands have gained tremendous attention in metal coordination chemistry as they influence greatly coordination geometry and reactivity and are critical features of asymmetric catalysts. In this thesis, the design and synthesis of sterically congested chiral alcohol and amine ligands based on a *bis*-adamantane framework, are explored. Optimization of the ligand synthesis and purification were conducted on the racemic ketone, while the chiral synthetic pathway utilized an enzymatic hydrolysis as the key step.

In another aspect of *bis*-adamantane chemistry, the bromonium ion of adamantylideneadamantane (Ad=Ad) has provided valuable mechanistic information about electrophilic addition of bromine and undergoes a fast "Br^+" transfer process to alkenes. However, the Ad=Ad isomer SesquiAdAd only reacts with [AdAdBr$^+$] and not with Br_2. This thesis also investigated the rearrangement of SesquiAdAd to Ad=Ad catalyzed by [AdAdBr$^+$] via the formation of the potentially high energy intermediate SesquiAdAdBr$^+$, probed by ^{1}H NMR spectroscopy and kinetics. Data analysis involved a series of ^{1}H NMR spectral deconvolutions.

Keywords: *Bis*-adamantane; sterically congested chiral ligands; synthesis; bromonium ion; rearrangement; ^{1}H NMR spectroscopy

To my father

for believing in me and always supporting my dreams…

To my mother

for your care and unconditional love…

To my little brother

for being my sunshine…

To my beloved grandmothers

for inspiring me to be an independent and strong woman…

Acknowledgements

A special thanks to my dear friend Melissa for her friendship and support, and Om for his unwavering love and care. Thank you for always being present despite the crazy twelve-hours time difference.

This journey would not have been possible without the support and love of my family. Words cannot express how grateful I am to my parents for their care, encouragement, sacrifices, trust, and above all, their unconditional love.

.

Table of Contents

List of Tables

List of Figures

List of Abbreviations and Acronyms

$[\alpha]_{589}^{20}$	Specific optical rotation at the sodium D line (589 nm) at 20 °C
a	Axial
Å	Angstrom; 10^{-10} m
°C	Degrees Celsius
Ad=Ad	Adamantylideneadamantane
Aq	Aqueous
Ar	Aryl
Ar_F	$3,5\text{-}(CF_3)_2Ph$, C_6F_5
Anal.	Analysis
BINAP	2,2'-*bis*(diphenylphosphino)-1,1'-binaphthyl
br	Broad (NMR)
Bn	Benzyl
^{t}Bu	*Tert*-butyl group -$C(CH_3)_3$
Bz	Benzoyl
Calc.	Calculated
CTC	Charge Transfer Complex
COD	1,5-Cyclooctadiene
d	Dextrorotary
d	Doublet
DEPT	Distortionless Enhancement by Polarization Transfer
DIOP	*O*-Isopropylidene-2,3-dihydroxy-1,4-*bis*(diphenylphosphino)butane
DIPAMP	Ethane-1,2-diyl*bis*[(2-methoxyphenyl)phenylphosphane]
Dr	Diastereomeric ratio
e	Equatorial
Ee	Enantiomeric excess
eq.	Equivalents
Et_2O	Diethyl ether
EtOAc	Ethyl acetate
EtOH	Ethanol
FT-IR	Fourier Transform-Infrared
g	Gram(s)
GSD	Global Spectral Deconvolution
H	Hour(s)
HOAc	Acetic acid
HPLC	High Performance Liquid Chromatography

HRMS	High Resolution Mass Spectroscopy
Hz	Hertz
^{i}	Iso
IR	Infrared
IS	Internal standard
IUPAC	International Union of Pure and Applied Chemistry
k	Rate constant
K	Kelvin
KIE	Kinetic Isotope Effect
k_{obs}	Observed rate constant
L	Levorotary
L	Litre
L-DOPA	L-3,4-dihydroxyphenylalanine
L/G	Lorentzian to Gaussian ratio
Lit.	Literature
L-selectride®	Lithium tri-*sec*-butyl(hydrido)borate
M	Multiplet
m	milli
M	Molar (mol/L)
Me	Methyl
m/z	Mass to charge ratio
mCPBA	*meta*-Chloroperoxybenzoic acid
m.p.	Melting point
Me	Methyl
MeOH	Methanol
mmol	Millimol(s)
mol	Mole(s)
MS	Mass Spectrometry
N	Normality, equivalent per litre
NBS	*N*-Bromosuccinimide
NCS	*N*-Chlorosuccinimide
NMR	Nuclear Magnetic Resonance
Nu	Nucleophile
OTf$^-$	Triflate anion
ORTEP	Oakridge thermal ellipsoid plot
Ph	Phenyl

pH	-log[H$^+$]
pK_a	Negative base-10 logarithm of the acid dissociation constant
^{i}PrOH	Isopropanol
POV-Ray	Persistence of vision raytracer
ppm	Parts per million
pyr.	Pyridine
QNP	Quattro Nucleus Probe
RDS	Rate Determining Step
r^2	Coefficient of determination
r.t.	Room temperature
R	Generic chemical group
rac	Racemic
s	Singlet
SesquiAdAd	Sesquihomoadamantene
SDS	Sodium Docecyl Sulphate
t	Triplet
tt	Triplet of triplets
TCI	Triple Resonance NMR 'inverse' Probe
THF	Tetrahydrofuran
TLC	Thin Layer Chromatography
TMS	Tetramethylsilane
TS	Transition State
UV	Ultraviolet
v/v	Volume to volume
Δ	Heat

Chapter 1.   General Introduction

The research reported in this thesis focuses on the *bis*-adamantane system with particular interests in:

1) The design and synthesis of highly sterically congested chiral ligands. Bulky chiral ligands have gained tremendous attention in metal coordination chemistry especially for catalysis and the adamantane system has been shown to offer the desired steric bulk. However, ligands based on a *bis*-adamantane framework have never been explored. As such, this research project has as an objective the design and synthesis of bulky chiral amine and alcohol molecules to be used as monomeric anionic ligands and their eventual incorporation into ligand-bridged frameworks.

2) The investigation of the formation of a high energy intermediate of an isomer of the *bis*-adamantane Ad=Ad from a bromonium "Br^+" ion transfer and the rate of the subsequent skeletal rearrangement to form Ad=Ad.

1.1. Adamantane

1.1.1. Background

Adamantane is a colourless crystalline solid, consisting of fused cyclohexane rings (Figure 1.1), and it is known to be strain free.[1] This hydrocarbon is the most thermodynamically stable of the numerous possible $C_{10}H_{16}$ alkane tricyclic isomers.[2] X-ray and electron diffraction studies reveal that all C-C bonds are 1.54 Å, which is similar to that found in diamond and all C-C-C bond angles are 109.5°.[1] This diamondoid type compound has an unusually high melting point for a simple hydrocarbon of 270 °C.[3]
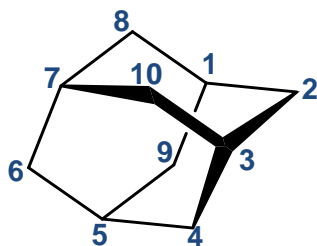
Figure 1.1   Structure and numbering of adamantane.

Adamantane, whose IUPAC name is tricyclo[3.3.1.1³,⁷]decane, was discovered in 1933 by Stanislav Landa in petroleum.[4] It was first prepared by Vladimir Prelog in 1941, by a multistep synthesis that used Meerwein's ester as the starting material.[1, 4] In 1957, adamantane was obtained from a Lewis acid catalyzed rearrangement of fully hydrogenated dicyclopentadiene by Paul von Ragué Schleyer (Figure 1.2).[3] We now know that any saturated cyclic $C_{10}H_{16}$ isomer, in the presence of a Lewis acid, will rearrange to give adamantane.[2]
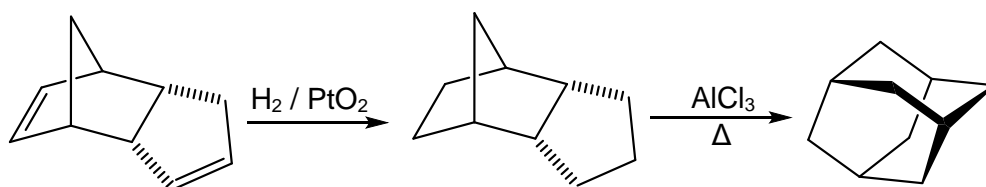
Figure 1.2   First reported synthesis of adamantane.[3]

1.1.2.   Functionalization of the Adamantane Skeleton

The adamantane framework can be functionalized via carbocationic or free radical-based chemistry. A prime example is Barton's Gif chemistry.[5] However, tertiary 1-adamantyl derivatives are formed preferentially when adamantyl compounds are subjected to this type of free-radical chemistry. Nevertheless, due to the thermodynamic stability of the ring, 2-adamantyl derivatives such as 2-adamantanone *(1)* can be obtained by heating adamantane or 1-adamantanol in concentrated sulphuric acid. The proposed mechanism for this oxidation reaction involves an intermolecular hydride transfer between tertiary and secondary carbocations (Figure 1.3).[6, 7]
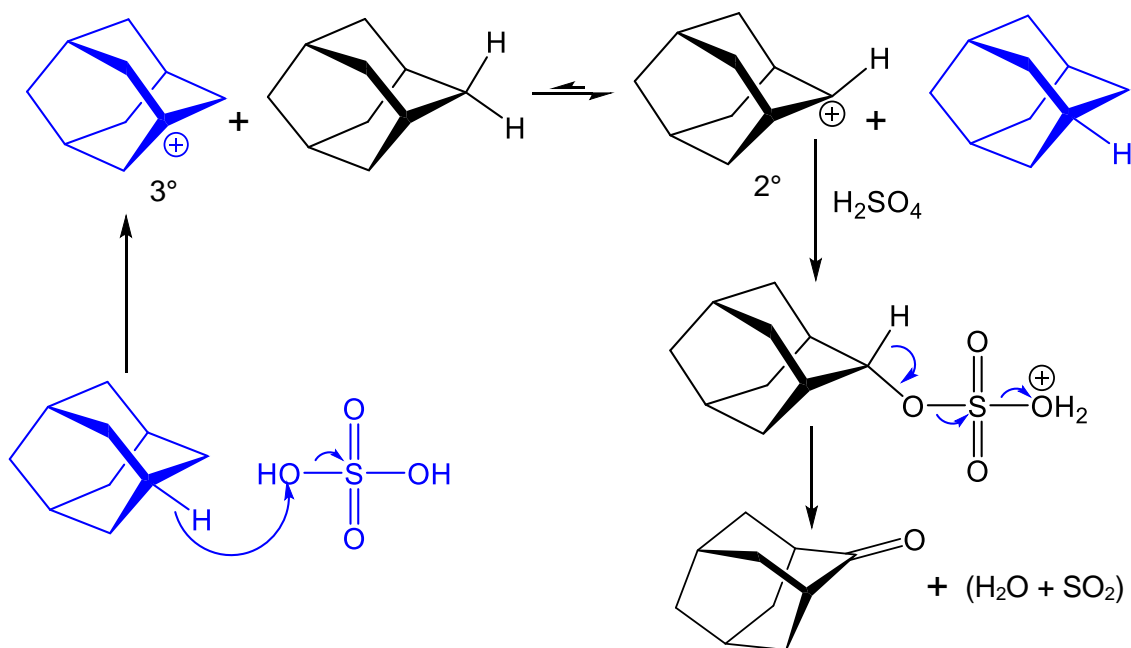
Figure 1.3   Mechanism for the formation of 2-adamantanone from adamantane in concentrated sulphuric acid.

1.2. Adamantylideneadamantane

1.2.1. General Background

Adamantylideneadamantane (Ad=Ad) is a white solid comprised of two adamantane molecules that are connected via a double bond (Figure 1.4). The IUPAC name for Ad=Ad is 2-(tricyclo[3.3.1.1^{3,7}]decylidene)tricyclo[3.3.1.1^{3,7}]decane.
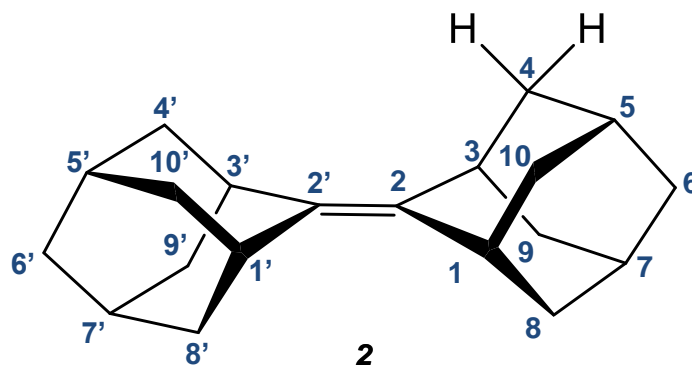
Figure 1.4   Structure and numbering scheme of adamantylideneadamantane (Ad=Ad, **2**).

1.2.2. Synthesis of Ad=Ad

In 1970, Strating and coworkers reported the first synthesis of this sterically congested alkene via the photolysis of 2-adamantyl ketene dimer (Figure 1.5).[8] Furthermore, access to Ad=Ad via the rearrangement of spiro[adamantane-2,4'-homoadamantan-5'-ol] with Lewis acids was also reported.[9,10] This 1971 study also reported that a second $C_{20}H_{28}$ isomer, namely sesquihomoadamantene (SesquiAdAd) was formed in addition to Ad=Ad (Figure 1.6).[10]
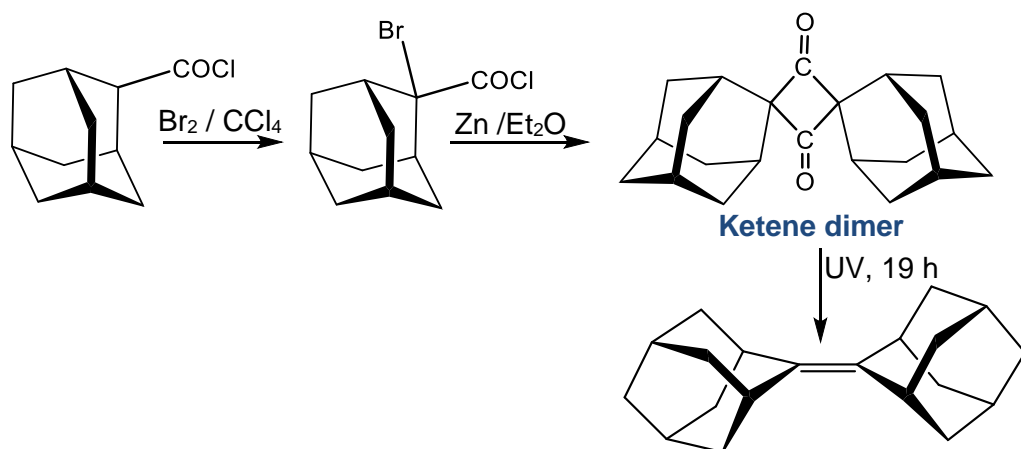
Figure 1.5   Synthesis of Ad=Ad via 2-adamantyl ketene dimer.[8]

Sesquihomoadamantene (*3*)   Adamantylideneadamantane (*2*)
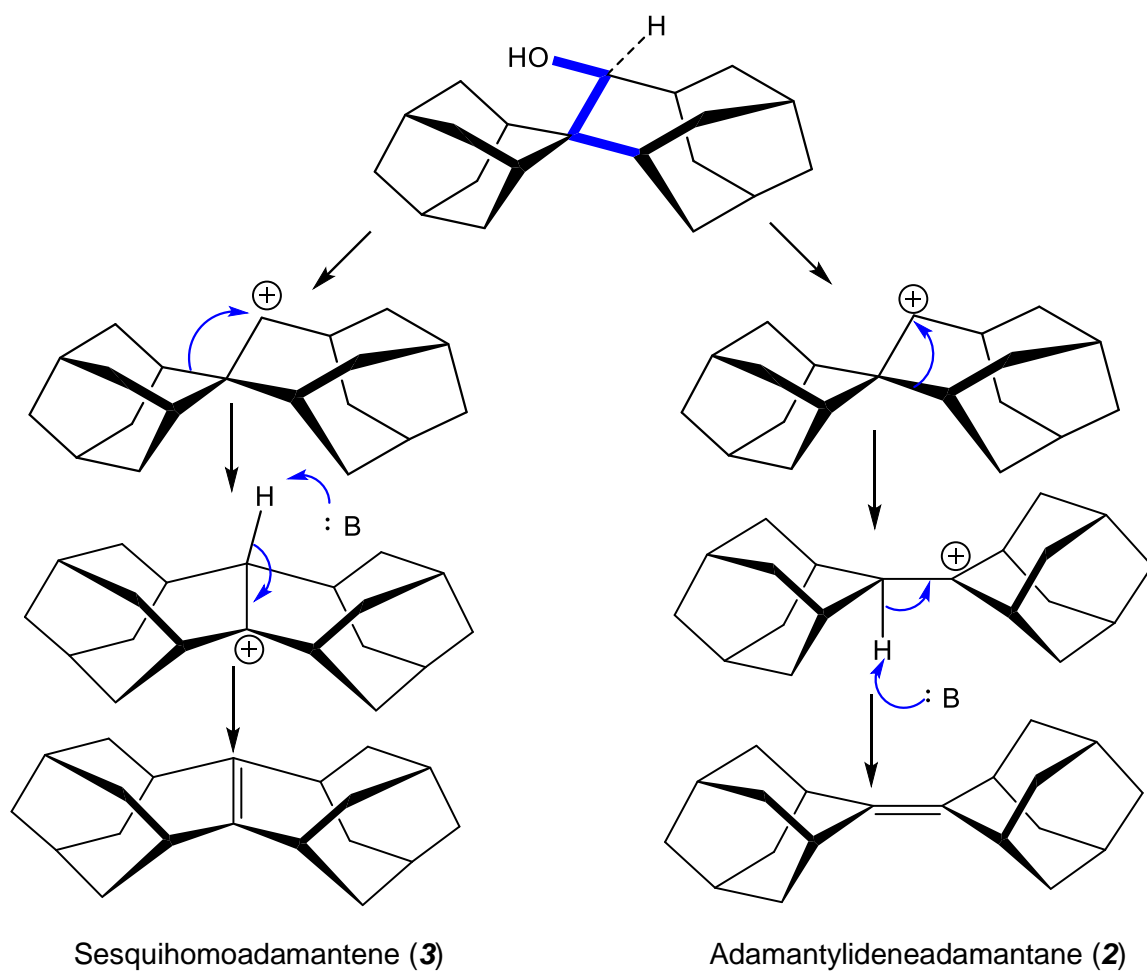
Figure 1.6   Concurrent synthesis of Ad=Ad and sesquiAdAd from spiro[adamantane-2,4'-homoadamantan-5'-ol].[10]

Notably, in 1983, McMurry reported a one-step synthesis of Ad=Ad from 2-adamantone using his low valent titanium reagents (Figure 1.7).[11]
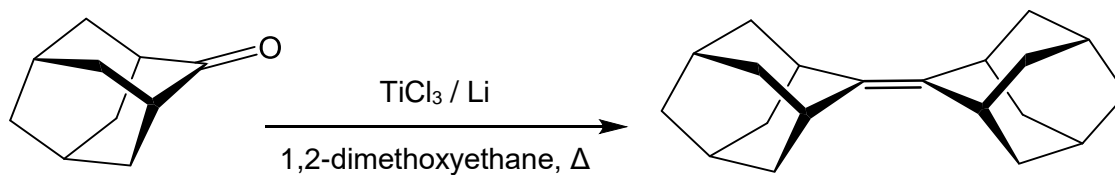
Figure 1.7   One step synthesis of Ad=Ad via a McMurry coupling reaction.

1.2.3.   Reactivity of Ad=Ad

This tetrasubstituted alkene, Ad=Ad, displays some unusual properties during electrophilic reactions because of its steric encumbrance. It is known that Ad=Ad reacts with several electrophilic reagents such as *N*-chlorosuccinimide,[12] benzenesulfenyl chloride,[13] and benzeneselenyl chloride[12] to yield a homoallylic substitution product Ad=Ad-Cl (**4**), instead of the usual addition products (Figure 1.8).[14]
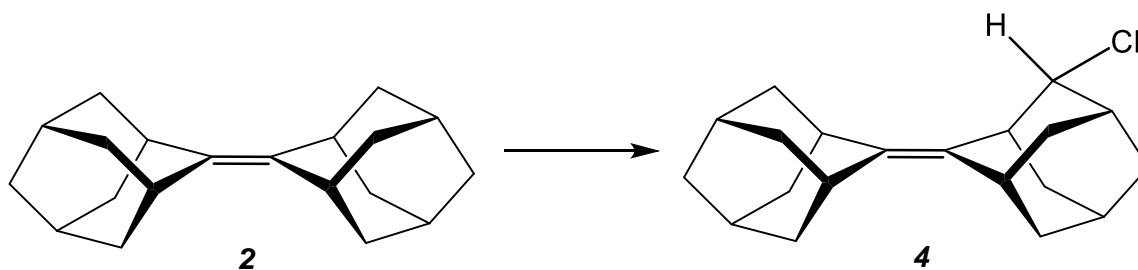
Figure 1.8   Synthesis of Ad=Ad-Cl via homoallylic halogenation.[14]

In 1969, the unusual reactivity of Ad=Ad was highlighted by the observation that it gave a stable bromonium ion tribromide salt (**5**) (Figure 1.9) when treated with bromine, instead of the expected dibromide product.[15] This novel salt has been characterized by single X-ray crystallography.[16,17]

5
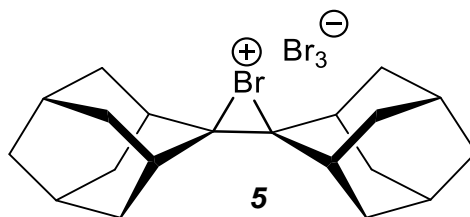
Figure 1.9   Structure of the bromonium ion tribromide salt.

Although the tribromide salt is sparingly soluble in halogenated solvents, Brown and coworkers reported that the Br_3^- counterion could be easily replaced by the triflate anion (OTf^-) (Figure 1.10) to give a soluble salt.[18]

This observation led to the design of an organic bromonium ion with a non-coordinating anion in as $[AdAdBr]^+[B(Ar_F)_4]^-$ (Ad adamantyl; Ar_F= 3,5-$(CF_3)_2Ph$) where its formation, by reaction of Br_2, Ad=Ad and $NaB(Ar_F)_4$ in CH_2Cl_2, is driven by the precipitation of NaBr from solution.[19] Bromonium ions such as these have also been identified as oxidants by virtue of their ability to transfer "Br^+" to acceptors.[18-20]
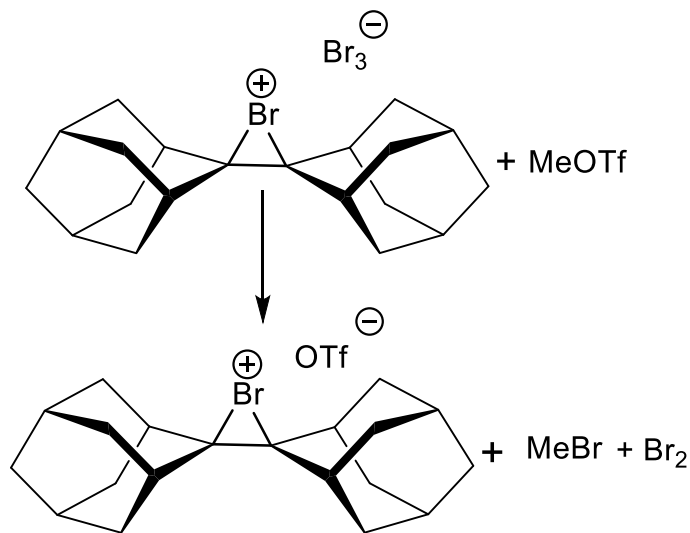
Figure 1.10   Synthesis of the bromonium ion triflate salt of Ad=Ad.[18]

1.2.4. Reactions of Adamantyl Based Cations

In 1998, Chou *et al.,* reinvestigated a reaction reported by Boelema and coworkers on the homoallylic alcohol of Ad=Ad in strongly acid media.[21, 22] Chou *et al.,* showed that a stereospecific acid-catalyzed 1,4-hydride rearrangement occurs when alcohol *6-H* is heated in a mixture of concentrated sulphuric acid and acetic acid to give the saturated ketone *7* (Figure 1.11).[22] These authors used isotopic labelling experiments and kinetic isotope effect (KIE) measurements to show that the mechanism involved a stereospecific protonation of the double bond, followed by an intramolecular 1,4-hydride shift from the C-H of the secondary alcohol to the other carbon of the alkene (Figure 1.12), rather than the initially proposed 1,3-hydride shift.[21]
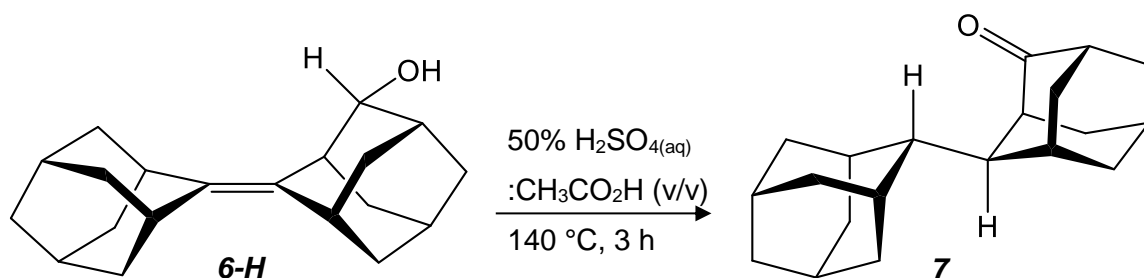
Figure 1.11   Acid-catalyzed 1,4-Hydride shift rearrangement of Ad=Ad-OH.[22]
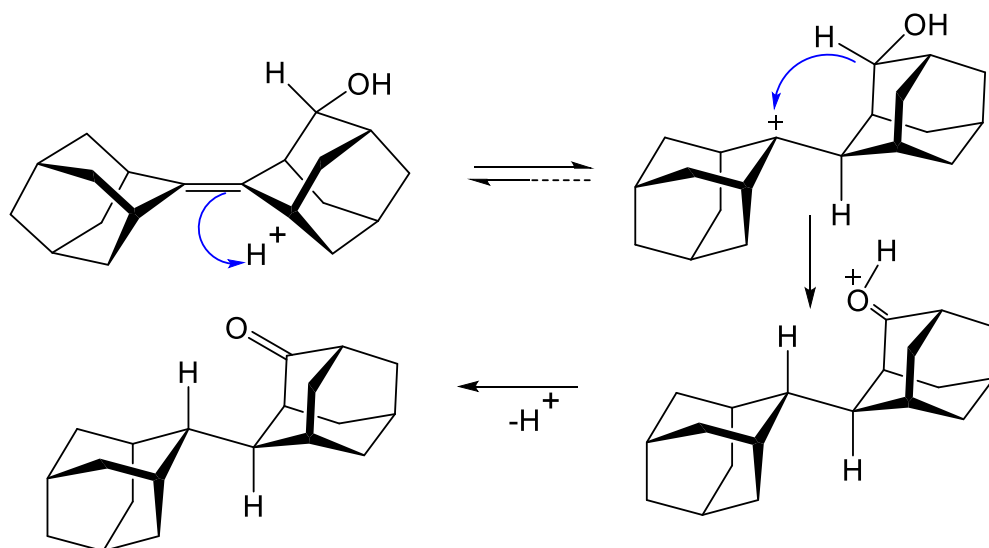
Figure 1.12   Acid-catalyzed 1,4-hydride shift rearrangement mechanism for the formation of ketone *7*.[22]

It is interesting to note that in the isotopic labelling experiment, the authors observed only the formation of ketone **7**, evidence which revealed that the carbenium ion **6-(a)⁺** does not undergo a 1,3-hydride shift to yield an isotopologue of the original carbenium ion (Figure 1.13).[22] That is, cation **6-(a)⁺** is formed reversibly from **6-D** and that on protonation of the double bond to give cation **6-(b)⁺** is followed by the rate determining step (RDS) 1,4-hydride transfer.
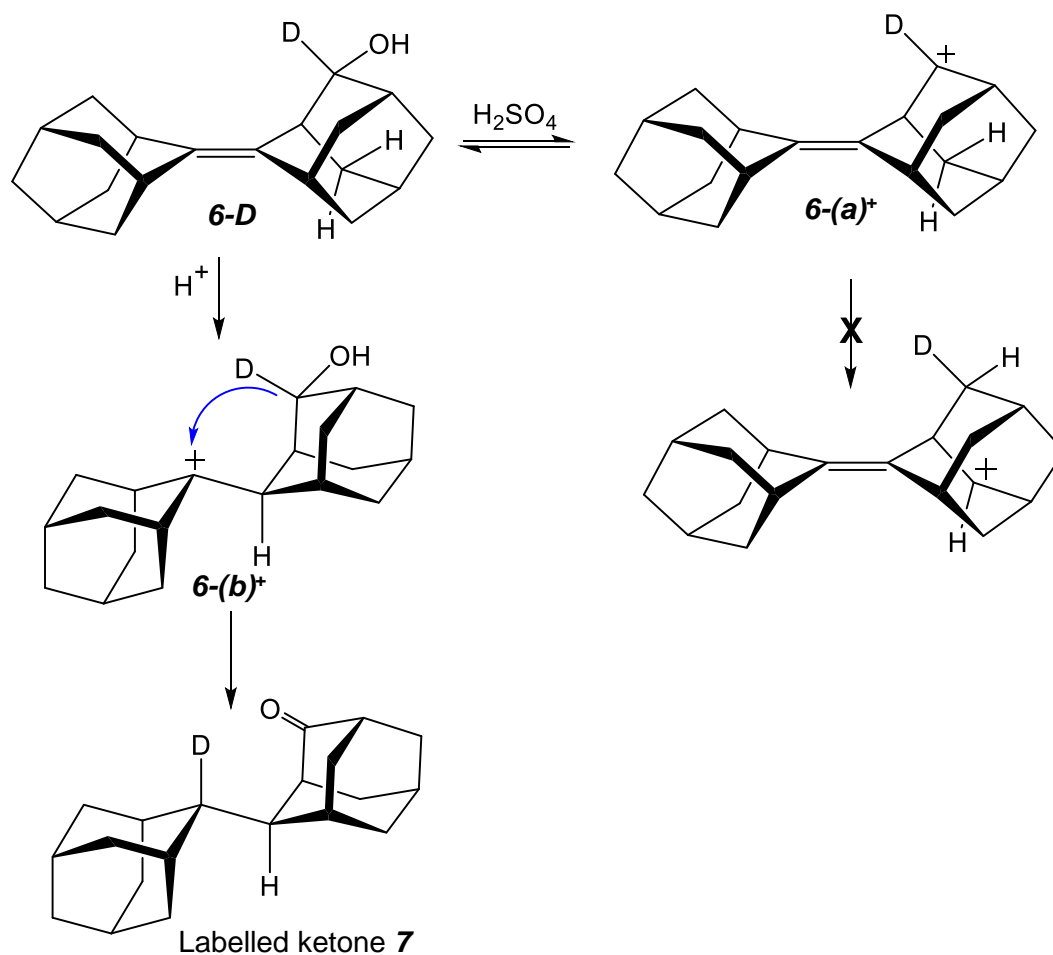
Figure 1.13   Investigation of 1,4-hydride shift isomerization mechanism using isotopically labelled alcohol **6-D**.[22]

Moreover, the presence of the two adamantane rings after treatment under such harsh conditions highlights the intrinsic stability of the adamantane framework.

On another note, several groups reported that the isomer sesquiAdAd (**3**) was unreactive towards bromination.[23] Of note, Brown and coworkers reported the epoxidation of several sterically congested alkenes and sesquihomoadamantene (sesquiAdAd), being one of the most highly strained alkenes used in their study, was shown to also undergo epoxidation with m-CPBA (Figure 1.14).[24]
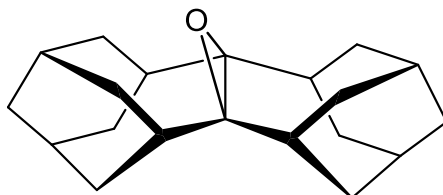
Figure 1.14   Epoxide of sesquihomoadamantene.

Surprisingly, based on unpublished results, the Bennet group observed that [AdAdBr]$^+$[B(Ar$_F$)$_4$]$^-$ was formed when sesquiAdAd was subjected to bromination in presence of NaB(Ar$_F$)$_4$ (Figure 1.15). This initial observation brings forward a key question about the mechanism for the skeletal rearrangement of sesquiAdAd to Ad=Ad, that is, does this rearrangement occur via the high energy intermediate [SesquiAdAdBr]$^+$?
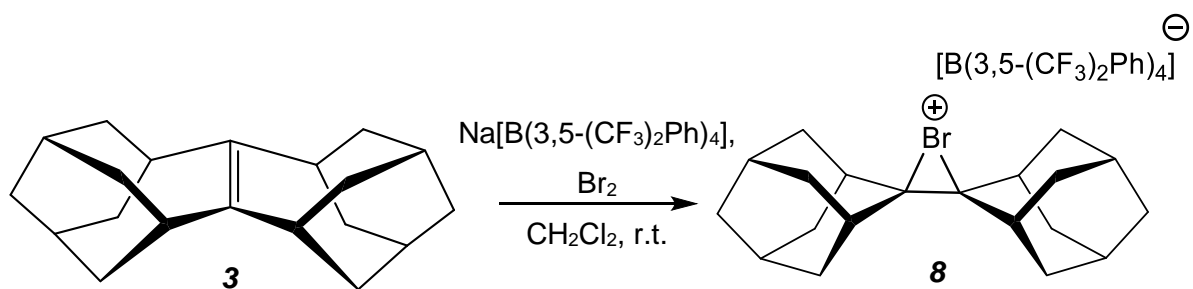
Figure 1.15   Bromination of sesquihomoadamantene in presence of NaB(ArF)4 gives a rearranged bromonium ion.

1.3. Thesis Overview

This thesis consists of three chapters with Chapter One giving a general introduction on adamantane and the adamantylideneadamantane system which are the common carbon skeletons used in Chapters Two and Three.

Chapter Two titled as "Synthesis of Sterically Congested Chiral Ligands based on *Bis*-Adamantane". Work in that Chapter investigates a chiral synthetic pathway to access bulky chiral alcohol and amine ligands based on the Ad=Ad framework that employs some of the chemistry described in the introduction. Furthermore, a racemic synthetic route is also described and is focused on protocol optimization for the synthesis and purification of the sterically congested alcohol and amine. Full characterization of these bulky ligands is also detailed.

Chapter Three titled as "Probing the Bromonium Ion Catalyzed Rearrangement of Sesquihomoadamantene by ^{1}H NMR Spectroscopy". The work in this Chapter addresses a mechanistic question about the rearrangement of sesquihomoadamantene into the more stable isomeric Ad=Ad. This investigation involves a series of kinetic experiments using ^{1}H NMR spectroscopy. The synthesis for the starting materials is also described.

Chapter 2.   Synthesis of Sterically Congested Chiral Ligands based on *Bis*-adamantane

2.1. General Introduction

2.1.1.   Ligands

Ligands have been of great interest as they have an impact over the electronics, structures, reactivities and properties of (transition) metal complexes. Ligands can be neutral molecules or ions, which contain lone pair(s) of electrons that can donate electron density to a metal to form a coordination complex.[25] Ligands can be simple monodentate molecules like ammonia[26] to much more complex macrocyclic structures such as porphyrins[27] (Figure 2.1). Ligands can incorporate numerous features such as charge,[28] chirality,[29] coordinating atom,[30] denticity,[31] hapticity,[32] and steric hindrance.[33] Numerous studies have highlighted the importance of ligands for key applications in bioinorganic,[34] environmental, material, [35, 36] and medicinal chemistry,[37] as well as in homogenous catalysis.[38] Hence, the ability to control the structure-reactivity relationship of a metal complex is often achieved by tuning the different features of a ligand. This project focuses on the design of bulky, hydrophobic, chiral ancillary (i.e. unreactive) ligands.

a) [CoCl₂(NH₃)₄]⁺   **b) Heme B**
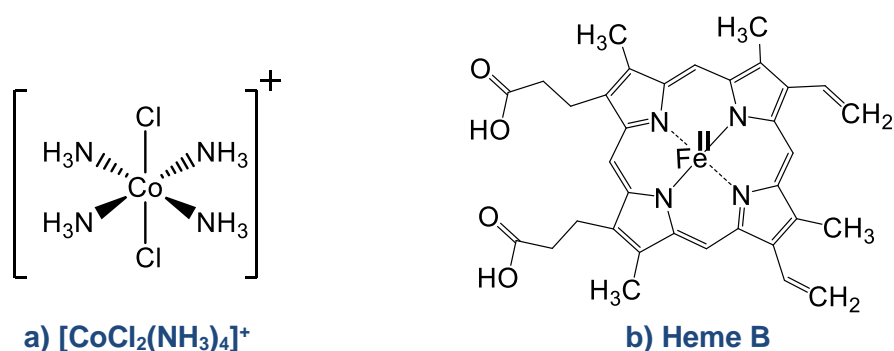
Figure 2.1   Typical metal complexes with a) ammine and b) porphyrin ligands.[26,27]

2.1.2. Chiral Ligands

Many of the chiral ligands, when coordinated to metal centres, generate chiral catalysts that have great potential for use in asymmetric catalysis.[39] The use of asymmetric synthesis is of great importance especially in the pharmaceutical industry where the desired biological activity of the molecule often depends entirely on the enantiomeric configuration.[40]

In 1968, William Standish Knowles developed one of the first asymmetric hydrogenation catalysis (Figure 2.2) by modifying the phosphine ligands that are present in Wilkinson's catalyst.[41] The achiral triphenylphospine ligands were replaced with the (R or S) enantiomers of a trialkylated phosphine (Figure 2.2).[42] In spite of the modest enantiomeric excess (ee) for the asymmetric hydrogenation reaction,[43] the potential use of chiral ligands seemed promising. Since this first report, the field of asymmetric catalysis has flourished and numerous notable advances have resulted.[43] Some of these successes involve asymmetric hydrogenation by William S. Knowles[41] and Ryoji Noyori,[39] and oxidations by K. Barry Sharpless.[44] These reports on asymmetric catalysis were honoured by these three chemists receiving the Chemistry Nobel Prize in 2001.[45]
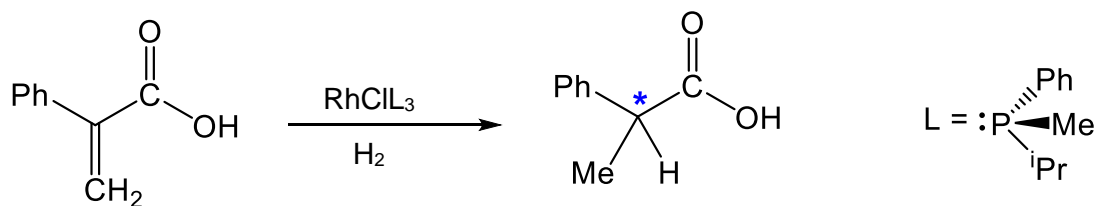
Figure 2.2   The first reported asymmetric hydrogenation used a chiral phosphine ligand.[42]

The use of asymmetric catalysis has rapidly become important in industry because of its high efficiency and selectivity.[46] This chiral technology was applied for the first time in 1972 on an industrial scale at Monsanto company for the production of L-DOPA using the catalyst developed by Knowles and coworkers,[47] and achieved an enantiomeric excess of 95 % with DIPAMP as the chiral ligand (Figure 2.3).[48]

13
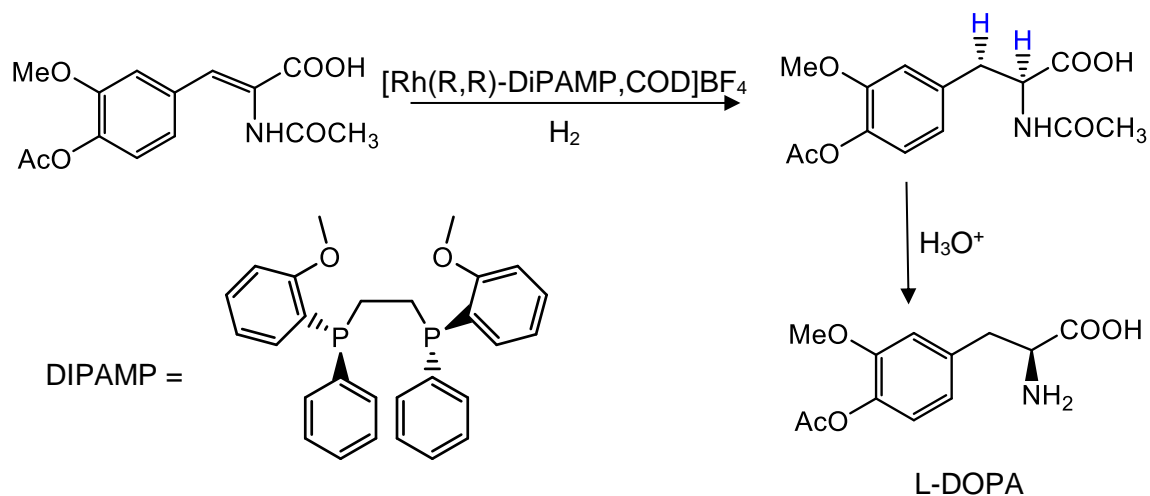
Figure 2.3   Asymmetric hydrogenation for the production of L-DOPA using a DIPAMP ligand.[48]

Some other impressive chiral phosphine ligands (Figure 2.4) that marked history include: 1) the chelating biphosphane ligand DIOP,[49] which was developed by Henri Kagan, with chirality on the carbon backbone rather than on the phosphorus atom, 2) BINAP[39] reported by Noyori and coworkers which possesses axial chirality and has participated in reactions with remarkable stereoselectivity, and 3) DuPhos[50, 51] pioneered by Mark J. Burk at DuPont, which gave a 99.8% ee for asymmetric hydrogenation of enamide esters to yield chiral amino acids.
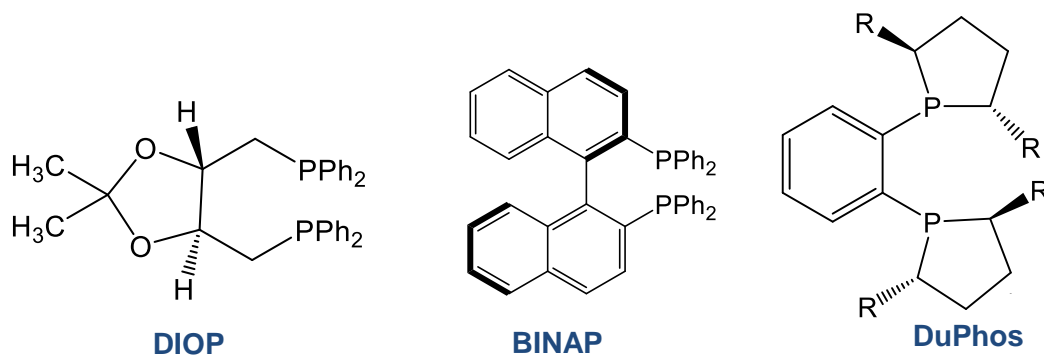
Figure 2.4   Chiral ligands DIOP, BINAP and DuPhos.[49, 39, 50]

14

2.1.3.   Bulky Ligands

Steric hindrance, a term coined by Rudolf Weigsheger,[52] is another factor that greatly influences the chemical and physical properties of a compound. In the late 1880's, Hofmann, Kehrmann and Meyer reported difficulties encountered for the alkylation of trimethylamine,[53] the reactivity of subsquinone[54-56] and the esterification reaction respectively.[57, 58] These observations were justified by the presence of steric hindrance. However, it was not until 1929 that Conant's work on the reactivity of highly branched carbonyl compounds with Grignard reagents, presented the idea that steric effect has an immense impact on reactivities.[59] A few years later, several groups independently investigated the effect of steric factors on reactivity and their work provided a foundation for the influence of steric hindrance on reaction mechanism.[52]

While steric hindrance was a new concept in organic chemistry, it was not until 1950's that Basolo, Pearson and coworkers acknowledged its significant importance in inorganic systems.[60] Pioneering work by Bradley and coworkers showed that monomeric and low coordination number complexes could be achieved when bulky ligands were used. Furthermore, it was reported that the ligands of these complexes stabilize unusual coordination geometries and influenced reactivity.[61] Around the same time, a new dawn in inorganic and organometallic chemistry was witnessed and very quickly, the design and study of sterically congested ligands on metals gained attention especially for catalytic applications. Some of the major sterically congested ligands that were designed and studied are phosphines, alkoxides and amides.

As highlighted above, phosphorus-based ligands are another class of potentially bulky ligand, as the degree of steric encumbrance at the coordinating metal centre can be tuned by varying the substituents on the phosphorus atom, which is typically measured by the Tolman cone angle (θ) (Figure 2.5).[62, 63] The cone angle is the measured angle at the apex of the cone, that is, the metal and the substituents on the phosphorus atom. Studies have shown how the cone angle for $Ni(CO)_3L$ complexes are affected by the steric size of the substituents of the phosphorus ligands with the bulky PPh_3 (θ= 145°) to PEt_3 (θ= 132°) and PMe_3 (θ= 118°).[63]
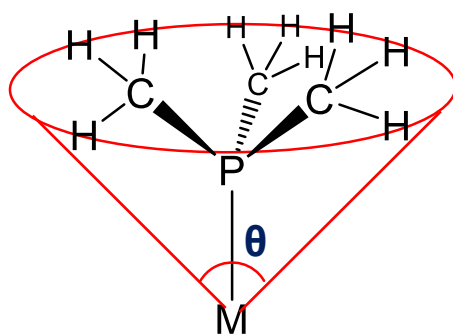
Figure 2.5   Tolman cone angle for PMe$_3$ as ligand.[63]

As a result, low coordinate metal complexes can be accessed by varying the steric size of the substituents of the phosphorus atom. The Pd[PPh(t-Bu)$_2$]$_2$ complex (Figure 2.6) by Otsuka *et al.,* showed a bent linear coordination with a cone angle of 176.6°.[64]
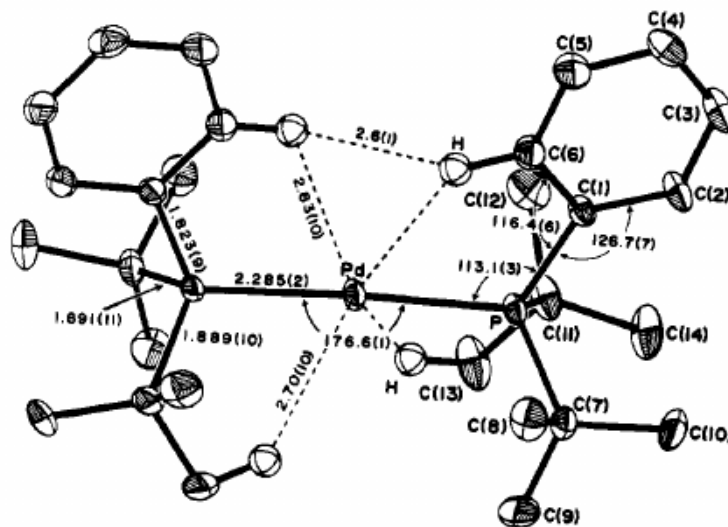
Figure 2.6   Low coordinate palladium(0) complex with PPh(^{t}Bu)$_2$ ligands. Reprinted (adapted) with permission from Otsuka, S.; Yoshida, T.; Matsumoto, M.; Nakatsu, K, "Bis(tertiary phosphine)palladium(0) and -platinum(0) complexes: preparations and crystal and molecular structures" *J. Am. Chem. Soc.,* **1976**, *98* (19), 5850-5858. Copyright 1976 American Chemical Society.

In keeping with the high steric bulk of the adamantyl group, which is the subject of this thesis, Carrow and coworkers reported the synthesis of a phosphine with three adamantyl substituents and measured a very large cone angle of 179° (Figure 2.7).[65]
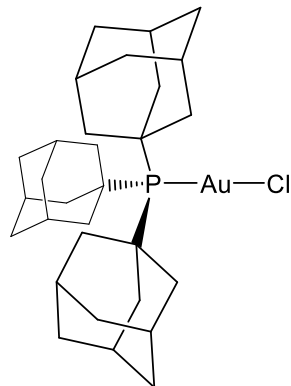
Figure 2.7   Tris(1-adamantyl)phosphine complex with a cone angle (θ) of 179°.[65]

They further investigated the use of this tri(1-adamantyl)phosphine ligand for a Suzuki–Miyaura palladium cross-coupling (Figure 2.8) and obtained 99% yields over 4 hours with high turnover frequency and turnover number. These results showed promising avenues for industrial applications.[65]
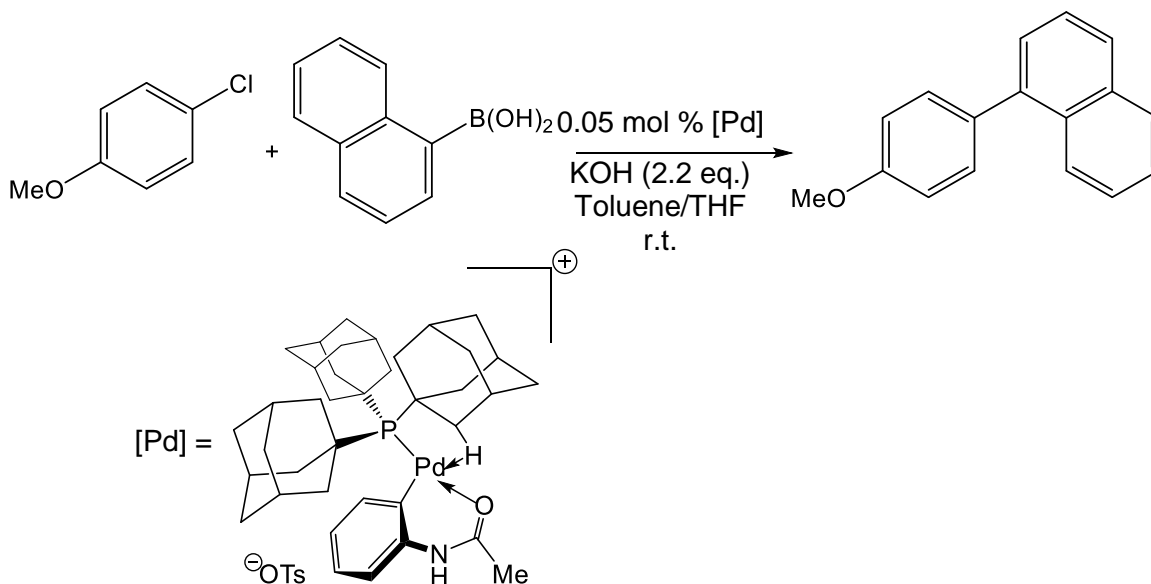
Figure 2.8   Palladium catalyzed Suzuki–Miyaura cross-coupling of chloro(hetero)arenes using a *tris*(1-adamantyl)phosphine ligand.[65]

17

Bulky alkoxide, siloxide and aryloxide ligands such as $-OCBu^t_3$,[66] $-OSiBu^t_3$[67] and C_6H_3-2,6-Bu^t_2[68] gave rise to low coordination number complexes. In 1980, Wilkinson and coworkers isolated Cr^{3+}, Cr^{4+}, Mn^{2+}, Fe^{3+} and Co^{2+} complexes with $-O(1\text{-}Ad)$ and $-O(2\text{-}Ad)$ (Figure 2.9).[69] The adamantane backbone seems appealing as it is chemically inert, thermally stable, offers kinetic stability and gives rise to unusual coordination geometries. Further studies on the formation of high valent complexes of chromium and manganese such as $Cr(1\text{-}AdO)_4$ and $Mn(1\text{-}AdO)_2$ further support the interesting advantages of these adamantane-based ligands.[69] Moreover, Schrock noted the importance of bulky adamantyl-based alkoxides and aryloxides in the effectiveness of Ta, Mo, W and Re metathesis catalysts (Nobel Prize 2005).[70]
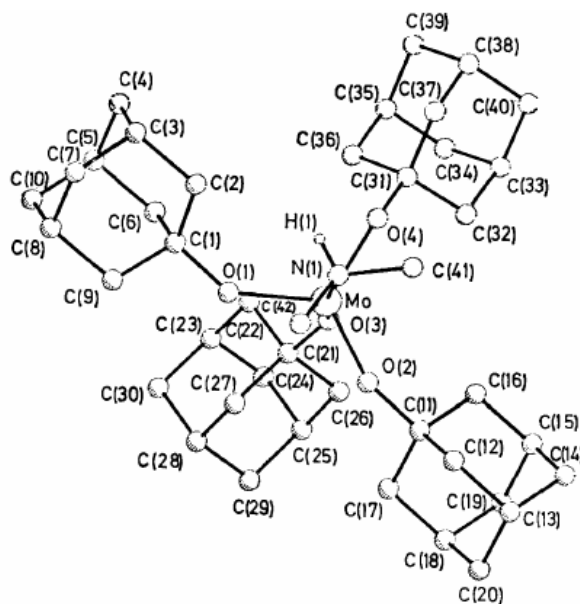
Figure 2.9   Structure of $Mo(1\text{-}ado)_4(NHMe_2)$ using adamantan-1-ol as ligand. Reprinted (adapted) with permission from Bochmann, M.; Wilkinson, G.; Young, G. B.; Hursthouse, M. B.; Malik, K. M. A, "Preparation and properties of 1-adamantoxides, 2-adamantoxides, and 1-adamantylmethoxides of Ti, V, Nb, Nb, Cr, Cr, Mo, Mn, Fe, and Co. The crystal and molecular structure of tetrakis(1-adamantoxo)dimethylaminemolybdenum(IV)" *J. Chem. Soc., Dalton Trans.* **1980**, 901-910. Copyright 1969 Royal Society of Chemistry.

Bulky anionic diorganoamide ligands have also gained attention as the two substituents on the nitrogen can engender it to be more sterically crowded when compared to the corresponding alkoxide. Low coordinate complexes with ligands such as $-NPr^i_2$,[71] $-N(SiMe_3)_2$[72, 33] and $-N(SiMePh_2)_2$[73] (Figure 2.10) further illustrate the impact of steric features on the overall metal complex structure. Cummins and coworkers successfully isolated three coordinate tris-anilide complexes of Mo^{III} with $-N(1-Ad)Ar$ and $-N(2-Ad)Ar$ ligands and X-ray crystallography confirmed their existence as discrete mononuclear complexes.[74] Thus, it is clear that the adamantyl group is an excellent unreactive bulky substituent that can be employed to yield highly steric, low-coordinate complexes, as shown with phosphines, alkoxides and amides.

a)   b)
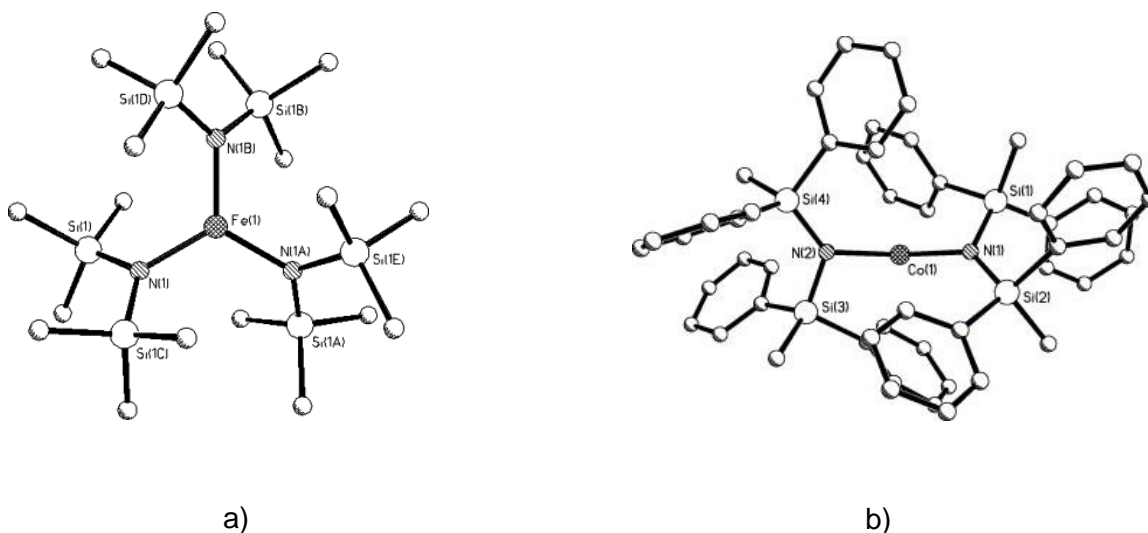
Figure 2.10   a) Three coordinate and b) two coordinate complexes with $\Theta N(SiMe_3)_2$ and $\Theta N(SiMePh_2)_2$ as sterically hindered ligands respectively. a) Reprinted (adapted) with permission from Bartlett, R. A.; Power, P. P, "Two-coordinate, nonlinear, crystalline d6 and d7 complexes: syntheses and structures of M{N(SiMePh2)2}2, M = Fe or Co" *J. Am. Chem. Soc.* **1987**, *109* (24), 7563-7564. Copyright 1987 American Chemical Society. b) Reprinted (adapted) with permission from Cummins, C, "Reductive cleavage and related reactions leading to molybdenum-element multiple bonds: new pathways offered by three-coordinate molybdenum(III)" *Chem. Commun.* **1998**, (17), 1777-1786. Copyright 1969 Royal Society of Chemistry.

2.2. Ligands of Interest

Ligand design has become a crucial component in asymmetric syntheses. The features of the ligand greatly influence the metal complex catalyst, which ultimately has an impact on the rate, reaction and product. Hence, by tuning the properties of a ligand, one should be able to control the desired features of a reaction product. Studies on ligands design have been published at a phenomenal pace during the past couple of decades, especially in the field of catalysis.

We were interested to build on recent (non-asymmetric) catalyst research in the Leznoff group that harnessed diamidoether ligands for hydroamination and alkene and lactide polymerization. Previous work in the Leznoff group have shown that an increase in steric hindrance on amido ligands promotes greater reactivity for hydroamination reaction,[75] and control over polymer tacticity for lactide polymerization could be achieved by using bulky groups on the diamidoether ligand framework.[76] Also, these studies led to an interest in using chiral groups on the diamidoether ligands to target enantioenriched hydroamination products and access highly tactic polymers. The above interests for steric encumbrance and chirality led to this thesis work, which is the design and synthesis of highly sterically encumbered chiral ligands. Previous studies reported in the literature have demonstrated that adamantane-based ligands have valuable applications in the formation, isolation and reactivities of low coordinate complexes by virtue of the steric bulkiness, and so far, no studies on the use of the highly congested *bis*-adamantane based ligands have been explored. As such, this research project explores the *bis*-adamantane framework for the synthesis of an alcohol and amine (Figure 2.11), as this system can offer:

1) Chirality: The presence of two stereogenic centres, which makes the molecule chiral (Appendix A). (Out of the 6 stereogenic centres present in the *bis*-adamantane molecule, four of them are locked by the bridges).

2) Steric bulk: The steric encumbrance of the two adamantane fragments.

3) Chemical inertness: Minimal sites for additional chemical reactivity.

a) Alcohol _10_   **b) Amine _11_**
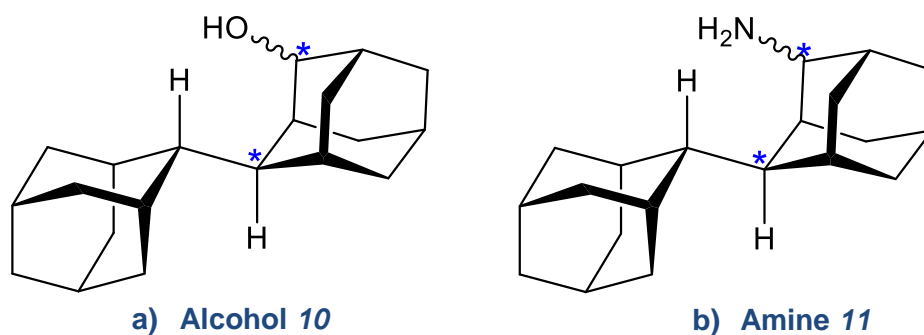
Figure 2.11   The targeted sterically congested a) chiral alcohol and b) amine ligands.

Given the desired design features of high steric profile, chirality and chemical inertness, the _bis_-adamantane framework was identified as an excellent target group to incorporate into ancillary ligands for catalysis. The resulting metal complexes of the diamido ligands with the _bis_-adamantane amine group, and Ti(IV) or Zr(IV) will be used as catalysts for hydroamination,[75] alkene[76] and lactide[77] polymerization. The synthesis of low coordinate complexes of the first row transition metals such as scandium, titanium and vanadium, with the _bis_-adamantane alcohol and amine ligands, is also a subject of interest.

We plan to access these chiral ligands via a chiral ketone intermediate. Based on the isotopic labelling experiment of the stereospecific acid-catalyzed 1,4-hydride shift rearrangement of homoallylic alcohol _6_, Bennet and coworkers have shown that access to ketone _7_ occurs without scrambling.[22] This key observation is at the core of the design of chiral _bis_-adamantane based ligands as access to a chiral _bis_-adamantane ketone would result from rearrangement of a chiral alcohol. This ketone intermediate then could be used to make chiral alcohol _10_ and amine _11_ (Figure 2.11).

The first three steps of the synthetic pathway (Figure 2.12) consists of a McMurry coupling[78] of commercially available 2-adamantone to give Ad=Ad (_2_) which then undergoes a homoallylic chlorination[14] to afford _rac-4_ and this in turn undergoes solvolysis[79] to give the racemic unsaturated alcohol _rac-6_. The following steps include the preparation of the racemic ester _rac-9_, crucial towards the synthesis of the chiral homoallylic alcohol _(±)6_, which involves a stereospecific enzymatic hydrolysis as a key

step, and this in turn undergoes a stereospecific acid-catalyzed 1,4-hydride shift to give the chiral ketone *(±)7*. The final steps to access the chiral alcohol *±10* and amine ligands *±11* would be via reduction and reductive amination reactions respectively.
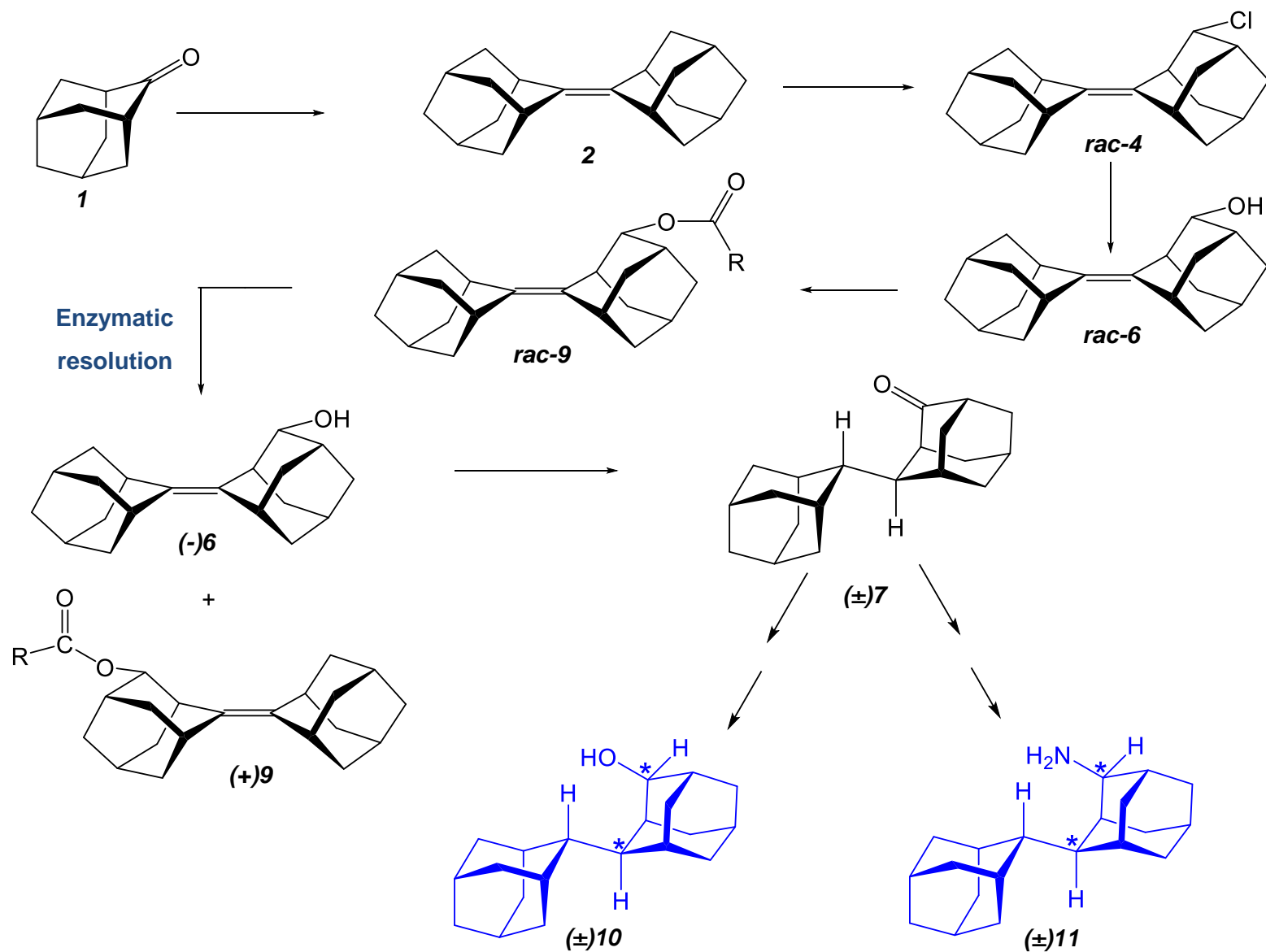
Figure 2.12   Proposed synthetic pathway to access the chiral ketone intermediate, and chiral alcohol and amine ligands.

2.3. Results and Discussion

2.3.1. Optimization of Reduction and Reductive Amination Reactions via the Racemic Ketone Intermediate

A racemic ketone intermediate *rac-7* which can be accessed via a 2-step synthetic pathway (Figure 2.13),[80, 22] was used for the optimization of reduction and reductive amination reactions (without sacrificing valuable chiral materials). Optimization of the purification protocols for the two diastereomers *10* and *11*, formed in the above key reactions was also investigated; these results, which set the stage for the reactions with chiral intermediates, are described below.
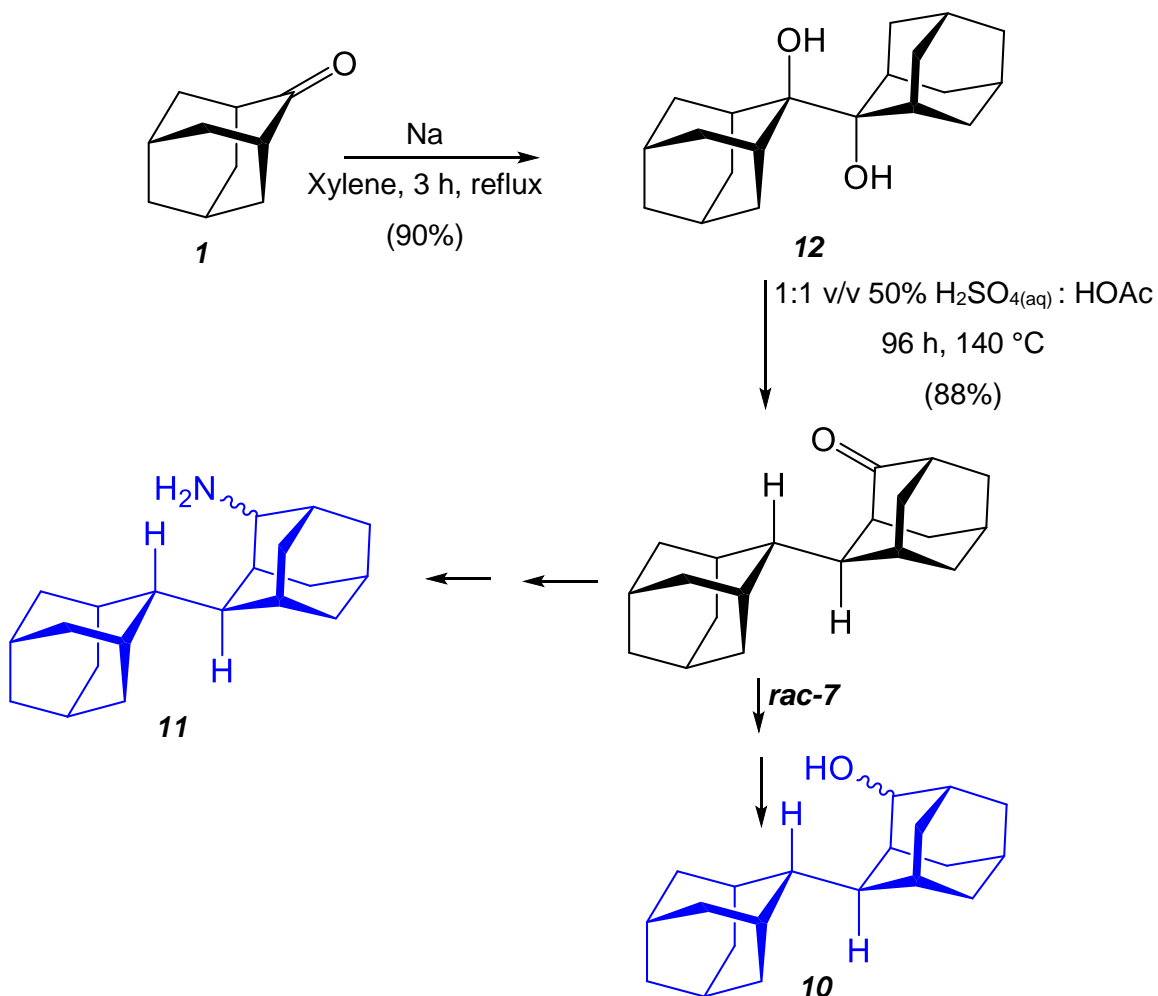
Figure 2.13   Racemic synthetic pathway to access the racemic alcohol and amine ligands

Synthesis of Ketone rac-7

2-Adamantanone was transformed into diol **12** by using a reductive pinacol coupling reaction.[80] Subsequent acid-catalyzed dehydration,[22] which initially generates a mixture of oxiranes **13** and spiroketone **14** that favours the formation of spiroketone,[10, 81] gave the ketone **rac-7** when the reaction was conducted at higher temperatures with longer reaction time (Figure 2.14), as described in the literature.[22]
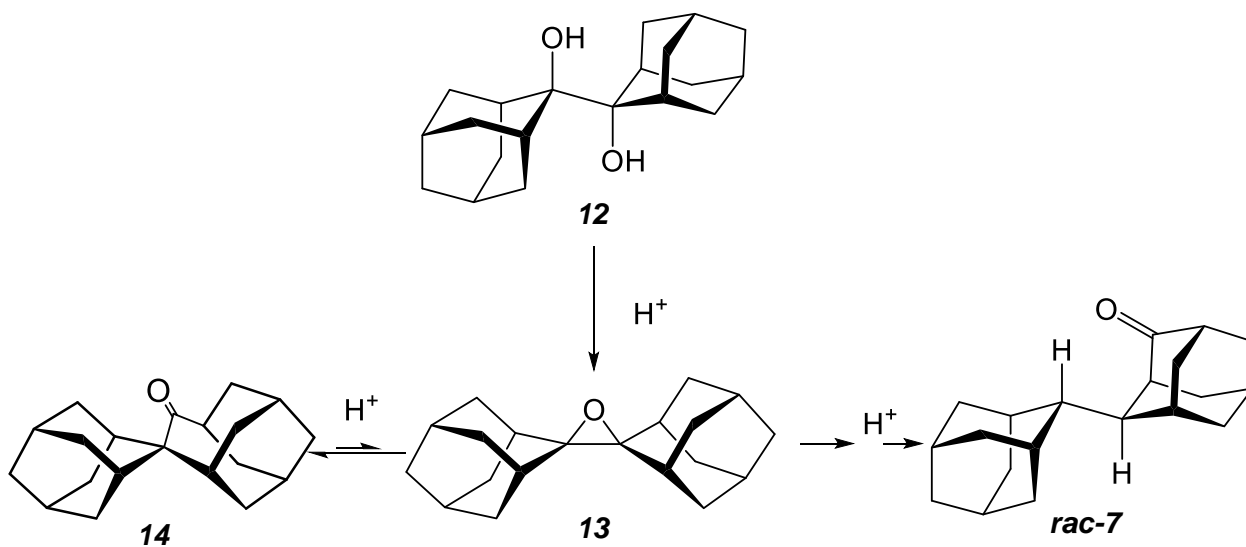
Figure 2.14   Acid-catalyzed hydration of **12** followed by a rearrangement to yield saturated ketone **rac-7**.[22]

Since the racemic ketone **rac-7** (**R-ketone + S-ketone**) is used, two pairs of enantiomers (axial and equatorial) are expected for both reduction and reductive amination reactions (Figure 2.15). Thus, after the above key reactions, a separation of the R,R/S,S pair from the R,S/S,R pair (i.e., diastereomers) is necessary and will yield separate single pairs of enantiomers as the final product.
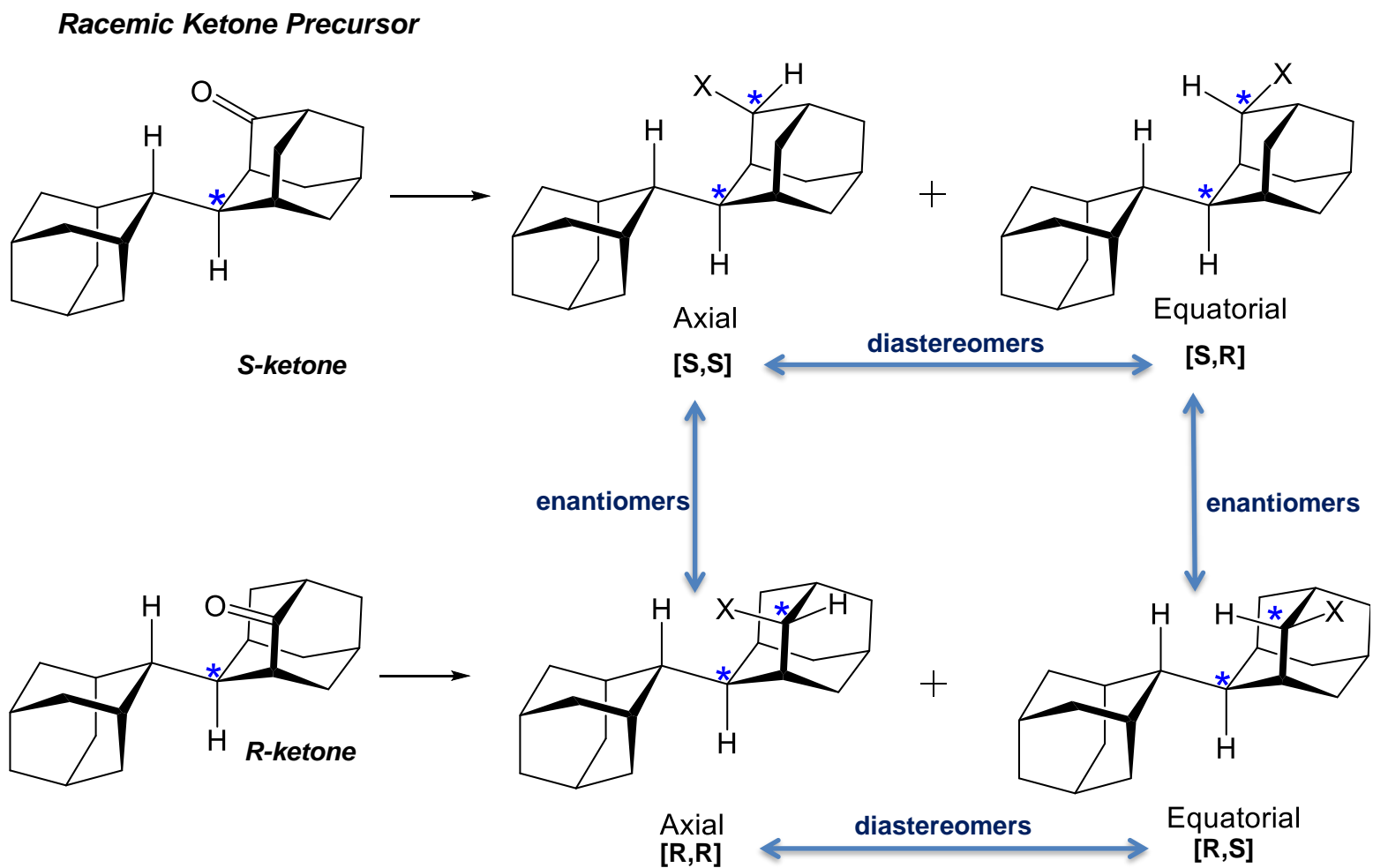
Figure 2.15   Expected formation of two pairs of enantiomers (axial and equatorial) from the reduction and reductive amination of ***rac-7***.

Optimization of the Reduction of rac-7
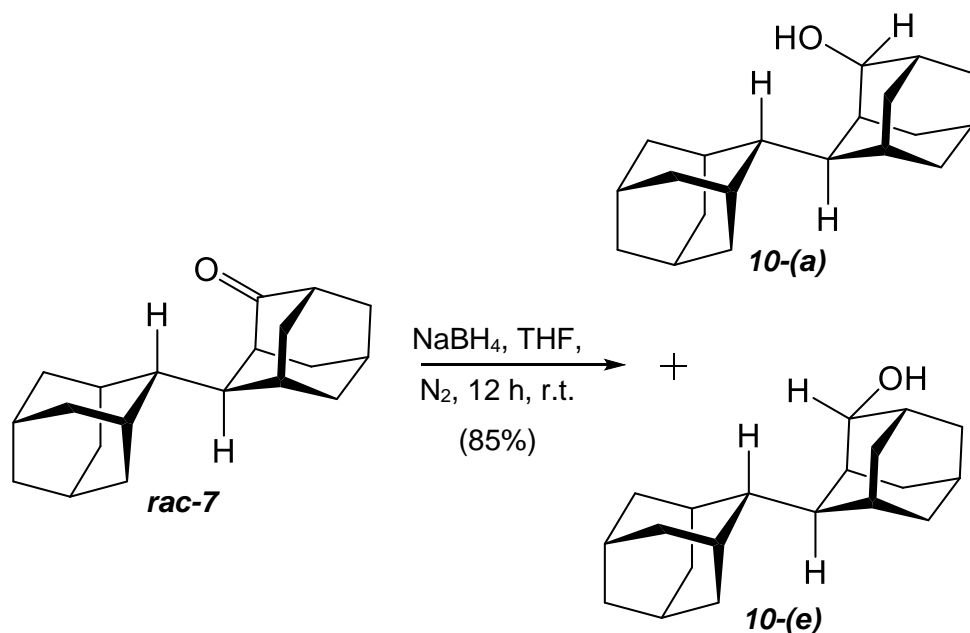
Figure 2.16   Reduction of ketone **rac-7** using sodium cyanoborohydride as the reducing agent.

When **rac-7** was subjected to sodium cyanoborohydride reduction in THF at room temperature (Figure 2.16), a mixture of diastereomers (**10-(a)** and **10-(e)**) were observed, with a diastereomeric ratio of 7:1, determined by ^{1}H NMR spectroscopy (Figure 2.17). We reasoned this high degree of diastereoselectivity occurred due to a preferential equatorial attack of the hydride on the carbonyl carbon that minimizes the steric interactions during the hydride addition caused by the second adamantane fragment (Figure 2.18).
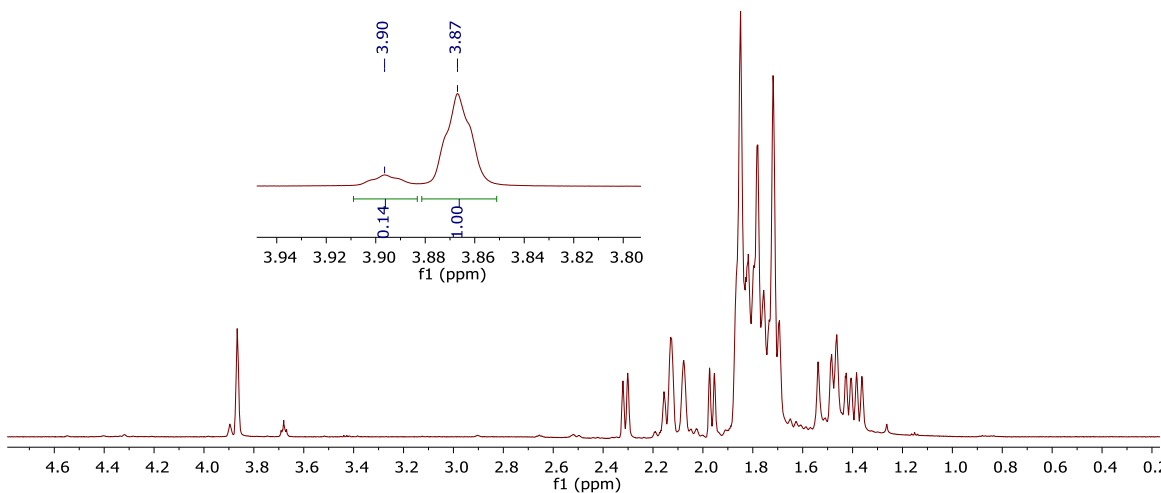
Figure 2.17   ^{1}H NMR spectrum of reaction mixture for reduction of *rac-7* with a diastereomeric ratio of 7:1 for *10-(a)*: *10-(e)* in CD$_2$Cl$_2$.
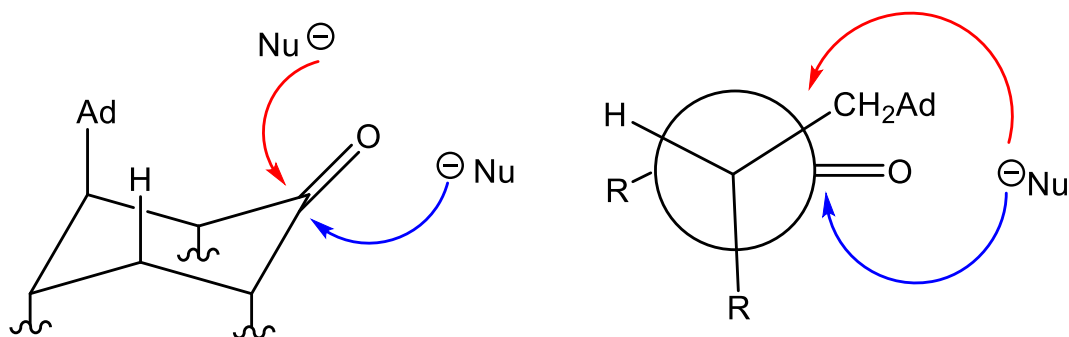
Figure 2.18   Nucleophilic attack of the carbonyl group of *rac-7* that occurs with a high preference for equatorial attack relative to the second adamantyl fragment.

Also, in our attempts to increase the diastereoselectivity, we reduced the ketone under Luche conditions[82] and with L-selectide®. These reactions were monitored by ^{1}H NMR spectroscopy and no significant improvement in diastereoselectivity was observed (Table 2.1).

28

Table 2.1   Conditions and diastereomeric ratio for reduction of ketone *rac-7*.

Entry	Conditions	*10-(a)* : *10-(e)*
1	NaBH₄, THF, r.t.	7:1
2	NaBH₄, CeCl₃, THF/MeOH, r.t.	9:1
3	L-Selectride®, THF, −78 °C	7:1

Purification of the crude mixture was challenging since separation of the diastereomers by HPLC was impractical as we were targeting multigram quantities of material. Consequently, the need to optimize the separation and purification of the diastereomers on a large scale was essential. We addressed this issue by incorporating an aromatic group on the molecule via a benzoyl (Bz) protection (Figure 2.19 and Appendix B) which improved separation and TLC detection significantly using a UV lamp.
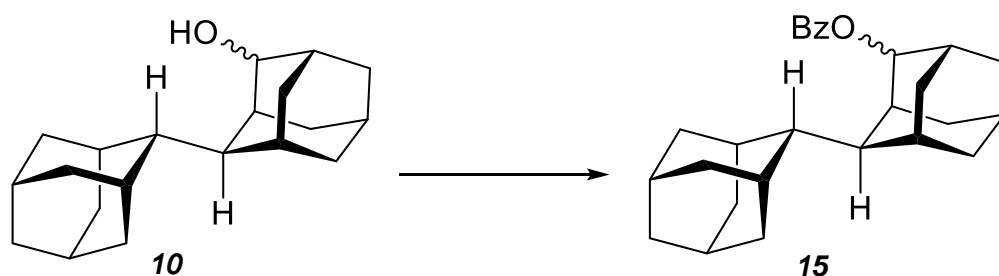
Figure 2.19   Protection of alcohol *10* with a benzoate protecting group.

Purification by flash column chromatography (hexanes : EtOAc, 9:1) followed by precipitation in isopropanol afforded the pure major diastereomer (Figure 2.20).
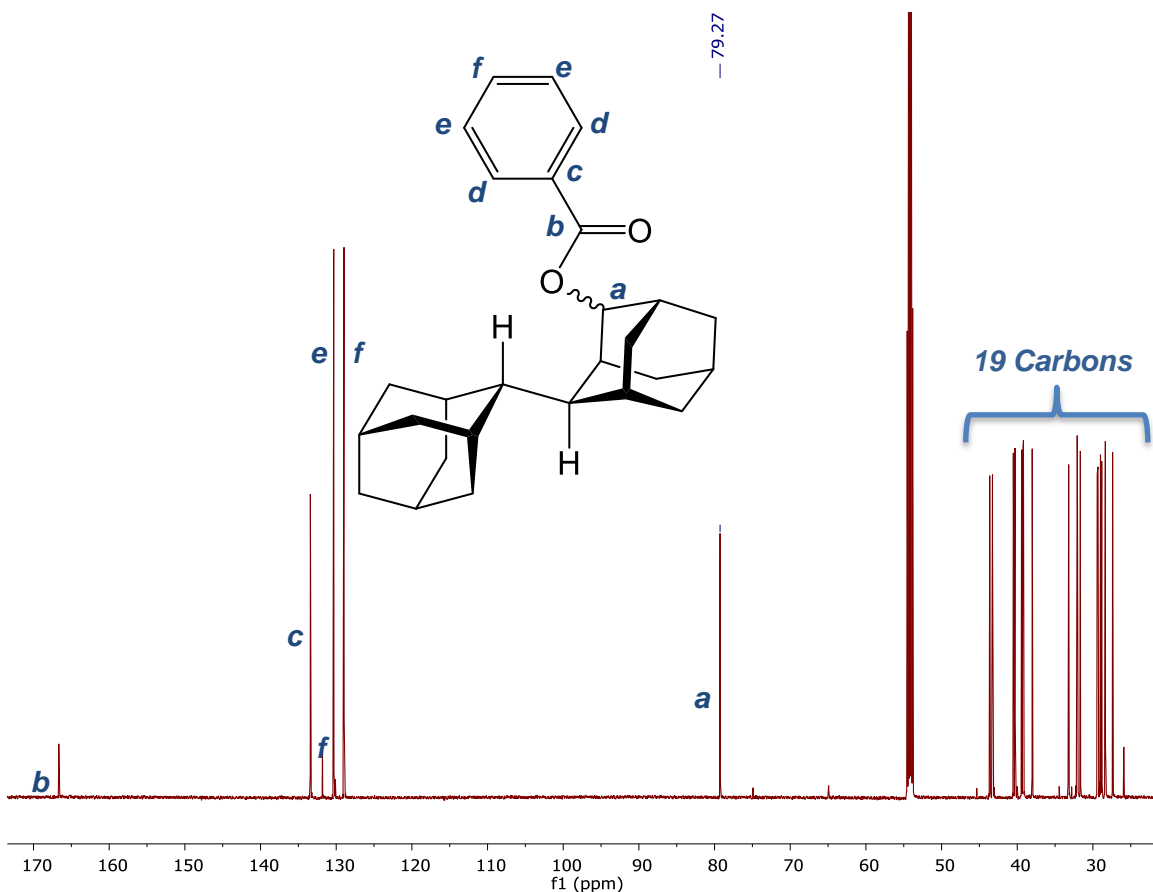
Figure 2.20 ^{13}C NMR spectrum of the purified major diastereomer in CD$_2$Cl$_2$.

The stereochemistry of the major diastereomer was assigned by ^{13}C NMR DEPT 135 spectrum based on an analysis of the γ-gauche effect.[83, 84] The major diastereomer displayed three shielded CH$_2$ groups which is consistent with the structure **15-(a)**, where the –OBz group is in the axial position relative to the second adamantyl ring. For the diastereomer with the –OBz group in the equatorial position (**15-(e)**), five shielded CH$_2$ are expected. The shielded CH$_2$ groups are designated with asterisks on both the structures and ^{13}C DEPT 135 NMR spectrum (Figure 2.21 and 2.22).
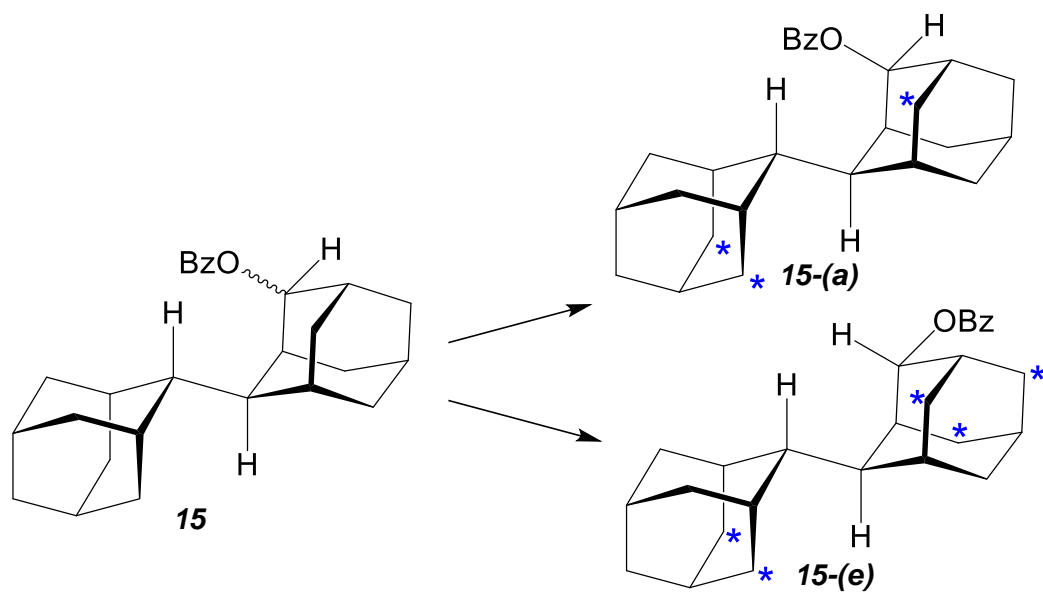
Figure 2.21   Assignment of the stereochemistry of the diastereomer *15* based on the γ-gauche effect.
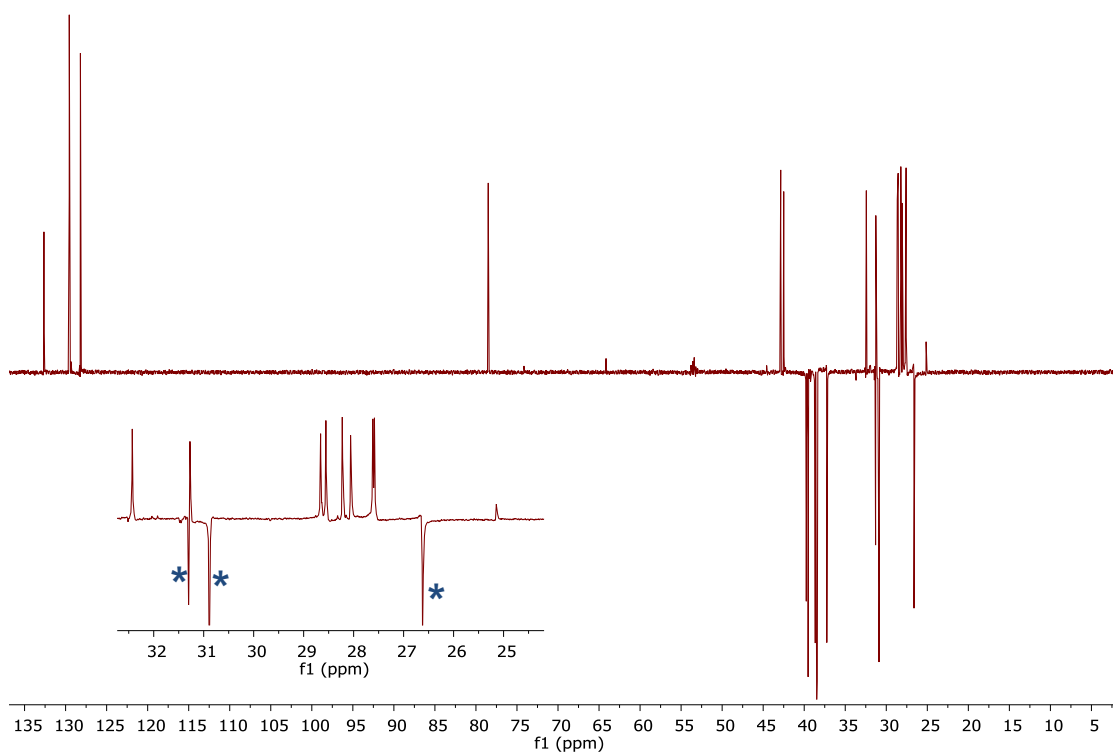
Figure 2.22 ^{13}C DEPT 135 NMR spectrum of the major diastereomer *15-(a)* containing three shielded CH$_2$.

An interesting observation was made during the benzoyl protection of the diastereomers. When the reaction was stopped at 45% of completion and worked up, we observed from ^{1}H NMR spectroscopy that the minor diastereomer **10-(e)** was completely converted into **15-(e)** and some of the major diastereomer **10-(a)** was also protected (Figure 2.23). That is, we had a mixture containing protected minor diastereomer **15-(e)**, major diastereomer **15-(a)** and major diastereomer of alcohol **10-(a)** (assignment of stereochemistry supported by γ-gauche effect using ^{13}C NMR DEPT 135 spectroscopy), which implies that the desired alcohol **10-(a)** can be obtained directly from separation and purification of this partially protected mixture by flash column chromatography.
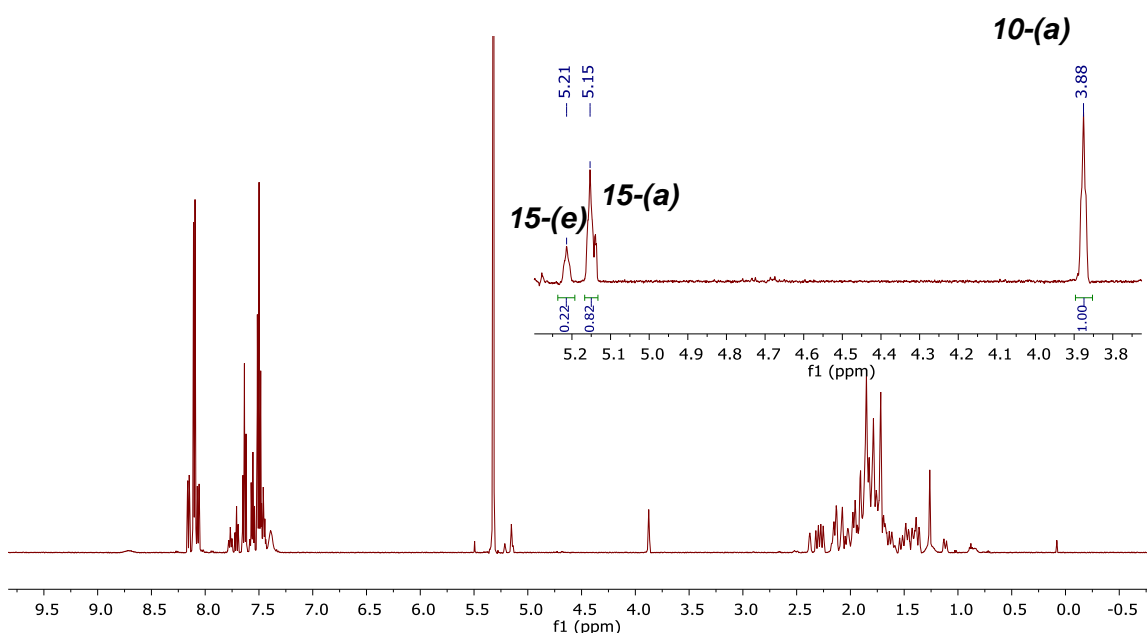
Figure 2.23   ^{1}H NMR spectrum of the benzoyl protection reaction mixture at 45% completion.

We rationalized this observation on the severe steric hindrance from the second adamantane fragment which rendered the esterification reaction with benzoyl chloride at the axial position much slower in comparison to protection of the equatorial diastereomer.

Upon purification of this partially protected crude mixture by flash column chromatography (hexanes: EtOAc, 9:1), the pure major diastereomer of alcohol **10-(a)** was isolated as a white powder. ^{13}C NMR spectroscopy indicated a *C*-OH (77 ppm) peak which

corresponds to the major diastereomer. The stereochemistry of **10-(a)** was confirmed by the presence of three shielded CH_2 in the ^{13}C DEPT 135 NMR spectrum based on the γ-gauche effect analysis (Figure 2.24).
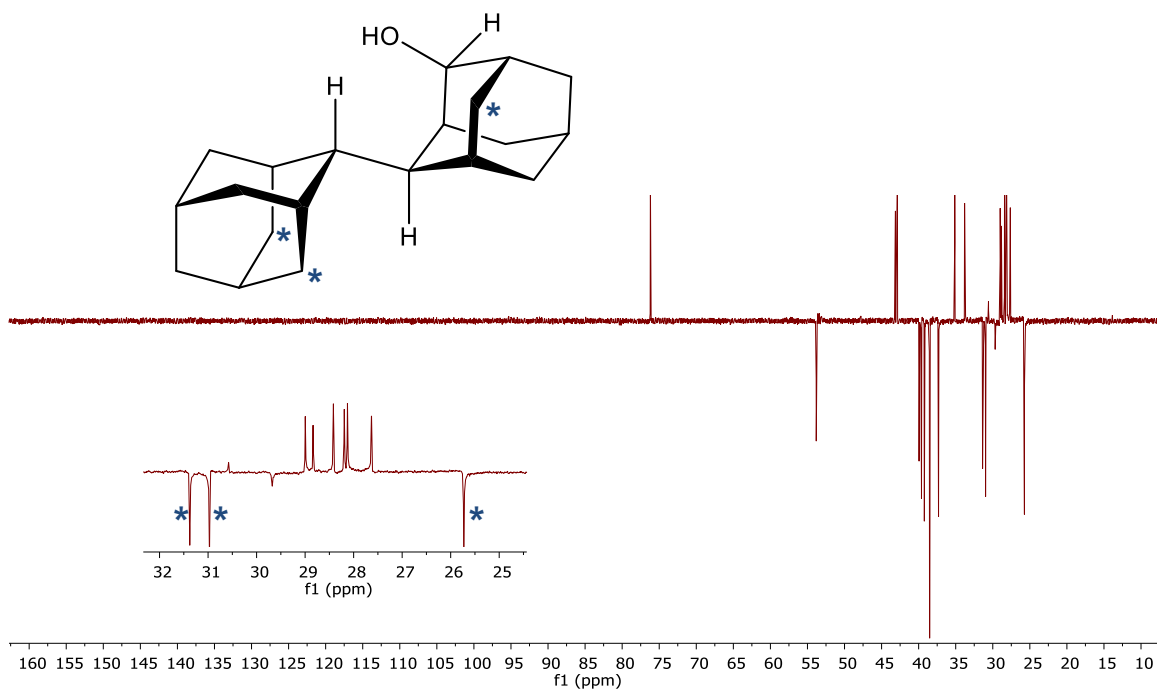
Figure 2.24 ^{13}C DEPT 135 NMR spectrum of the pure major diastereomer alcohol **rac-10-(a)**.

In summary, access to the major pure diastereomer of the saturated *bis*-adamantane alcohol via sodium borohydride reduction followed by partial benzoyl protection, proved to be more efficient as it does not require a deprotection step and also allowed easy separation and purification of the reaction mixture.

Optimization for Reductive Amination

Initially, *rac*-ketone ***rac-7*** was subjected to reductive amination using methanolic ammonia, 4 Å molecular sieves and NaBH$_4$.[85] However, the crude mixture proved to contain mainly the corresponding alcohol ***10*** instead of the amine with the carbon resonance at 77 ppm being consistent with that for an alcohol. Of note, these conditions were used to convert 2-adamantanone ***(1)*** into the corresponding amine (*C*-NH$_2$ resonance at 53 ppm) successfully with these reagents.[85] Hence, we had to change the conditions for imine formation and its subsequent reduction to afford the corresponding amine (Figure 2.25 & 2.26).
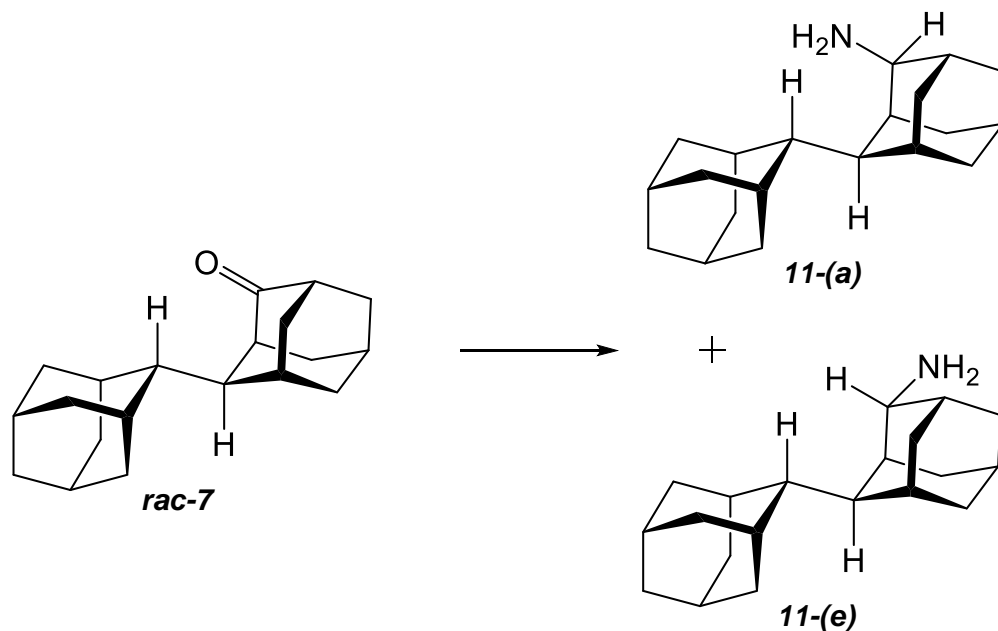
Figure 2.25   Reductive amination of ketone ***rac-7***.

Formation of iminium ion:
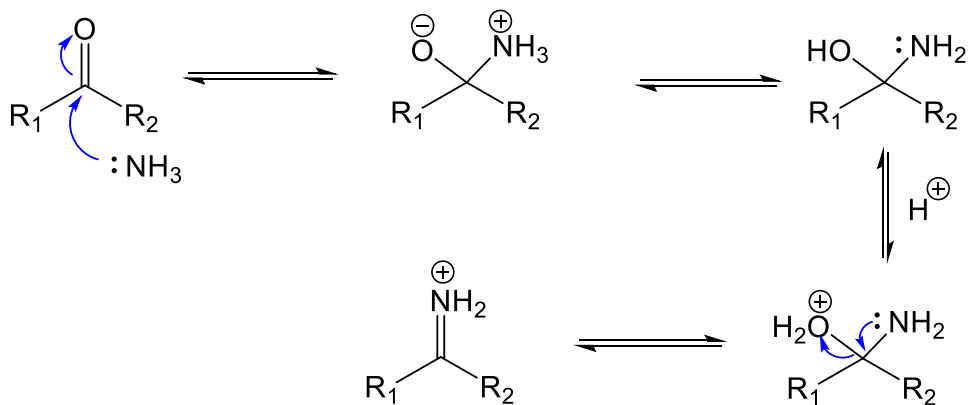
Reduction of iminium ion:
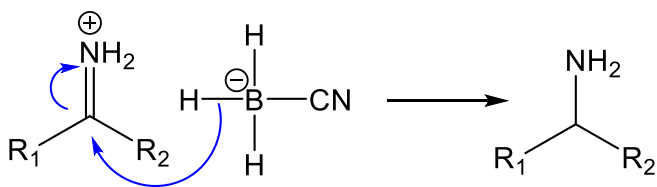
Figure 2.26   Reductive amination mechanism involving two key steps, notably formation of the iminium ion followed by reduction of the ion to form the amine.

Upon switching from molecular sieves to titanium isopropoxide, a sharp C-NH_2 peak at 57 ppm was observed. However, we also detected a minor peak at 77 ppm corresponding to the C-OH. We further screened conditions for both the iminium ion formation and the reduction step (Table 2.2).

Table 2.2   **Optimization of reductive amination reaction conditions and the ratio of the formation of amine:alcohol.**

Entry	Conditions	Amine: Alcohol
	MeOH/NH$_3$	
	4Å molecular sieves	
1	NaBH$_4$	1:7.7
	N$_2$, 12 h, r.t.	
	MeOH/NH$_3$	
	Titanium isopropoxide	
2	NaBH$_4$	1.6:1
	N$_2$, 12 h, r.t.	
	MeOH/NH$_3$	
	Titanium isopropoxide	
3	NaCBH$_3$CN	5:1
	N$_2$, 12 h, r.t.	
	MeOH/NH$_3$	
	Acetic acid	
4	NaBH$_3$CN	20:1
	N$_2$, 24 h, r.t.	

Conditions for reductive amination in entry 4 seemed to be optimal, with minimum alcohol formation. However, when this reaction was conducted on a 1 g scale, a significant amount of alcohol was still detected (amine : alcohol/ 6:1).

At this point, the optimization for the purification of the crude mixture which contained the diastereomers of amine and alcohol was essential for three main reasons. Firstly, issues in controlling the formation of the alcohol *10* side product were critical. Moreover, separation and purification of the diastereomers on a multigram scale cannot

be achieved by analytical HPLC. Furthermore, visualization and separation of the sample (i.e the alcohol and amine) spots on TLC were quite difficult. To address these problems, we incorporated an aromatic group in the form of a benzyl (Bn) protection which improved detection and the separation of the spots on TLC as well as facilitating purification significantly by using flash column chromatography. Thus, we conducted the reductive amination reaction using benzyl amine as the amine source, acetic acid and sodium cyanoborohydride (Figure 2.27).
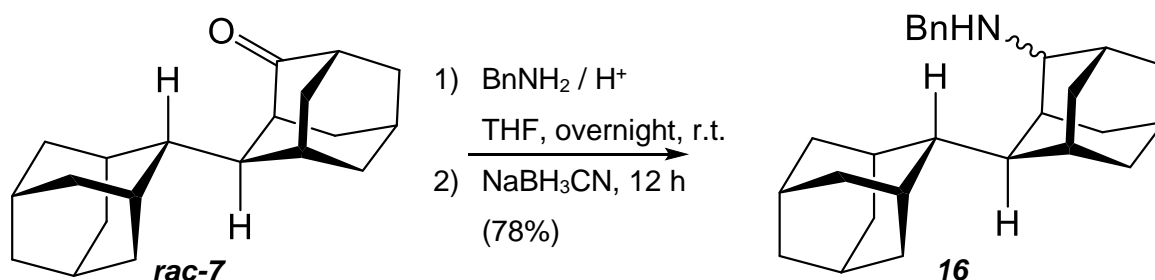
Figure 2.27   Reductive amination of ketone *rac-7* with benzyl amine to access diastereomers *16*.

We also determined a diastereomeric ratio of 1.5:1 from the ^{1}H NMR spectrum (Figure 2.28).
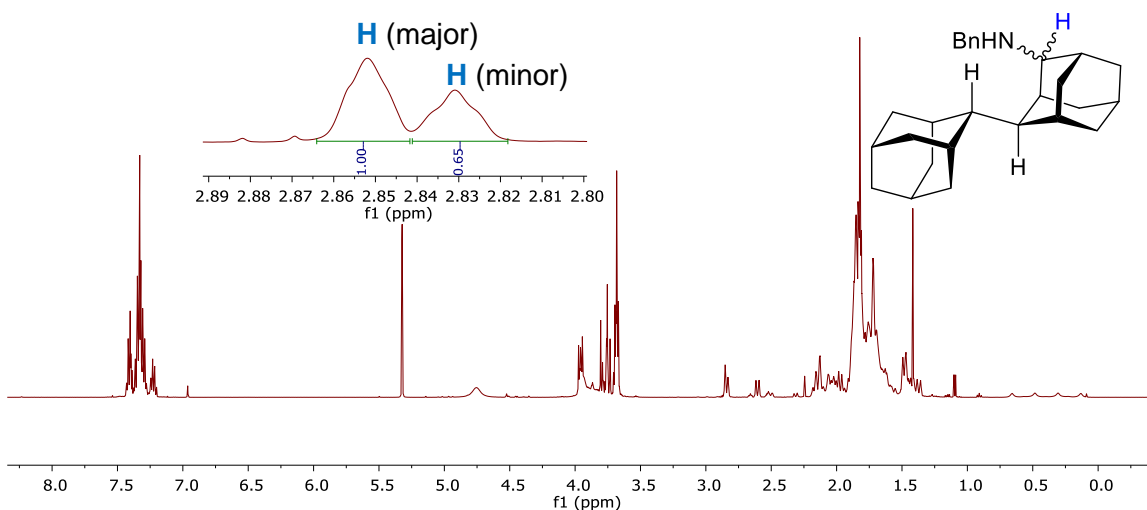
Figure 2.28 ^{1}H NMR spectrum of crude mixture of reductive amination reaction with a diastereomeric ratio of 1.5:1.

37

Purification of the crude mixture by flash column chromatography (hexane:EtOAc, 9:1) and precipitation in methanol afforded pure major diastereomer of the protected amine (48% yield) (Figure 2.29 & 2.30).
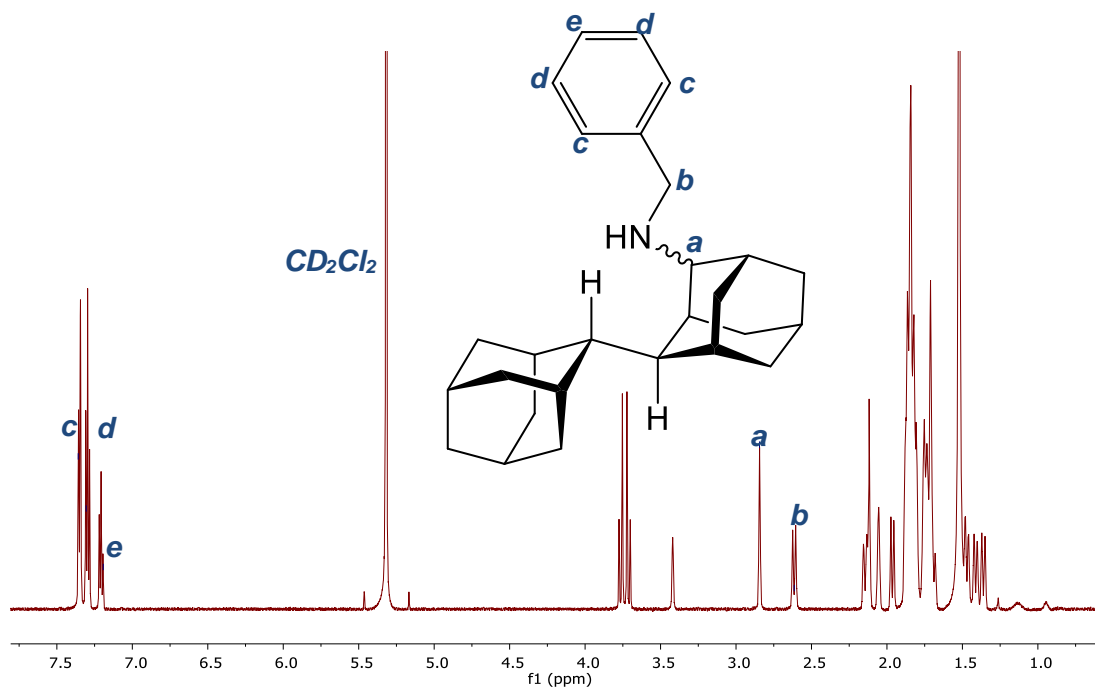
Figure 2.29 ^{1}H NMR spectrum of pure major diastereomer of protected amine *16*.
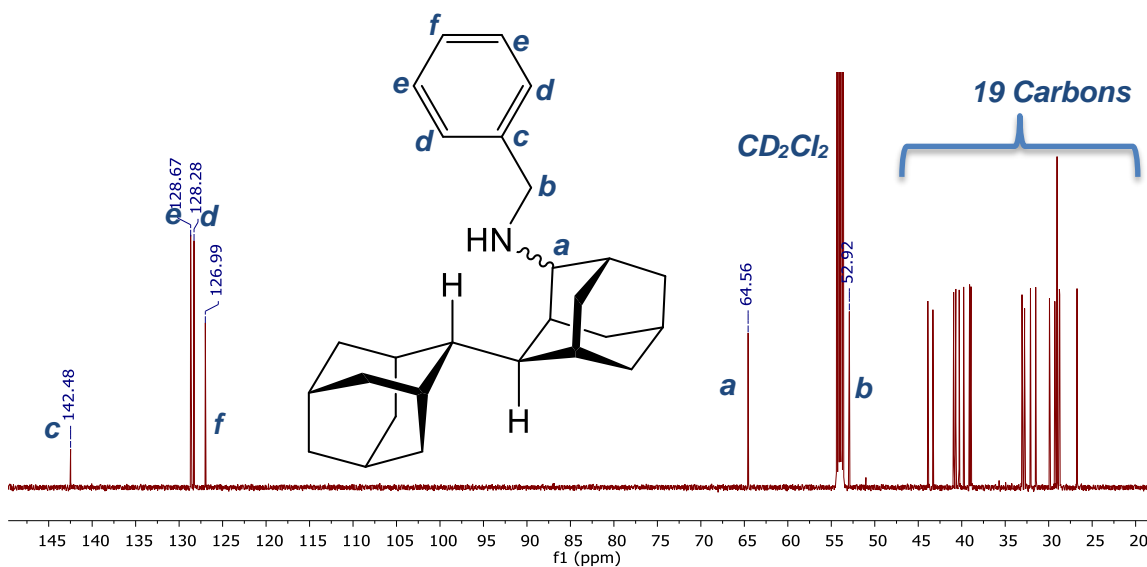
Figure 2.30 ^{13}C NMR spectrum of pure major diastereomer *16*.

The stereochemistry of this compound was assigned using ^{13}C DEPT 135 NMR experiment as compound **16-(a)**, a designation based on the γ-gauche effect.[84] The major diastereomer displayed three shielded CH$_2$ groups which is consistent with the structure **16-(a)**, where the amine group is in an axial position with respect to the second adamantyl group (Figure 2.31).
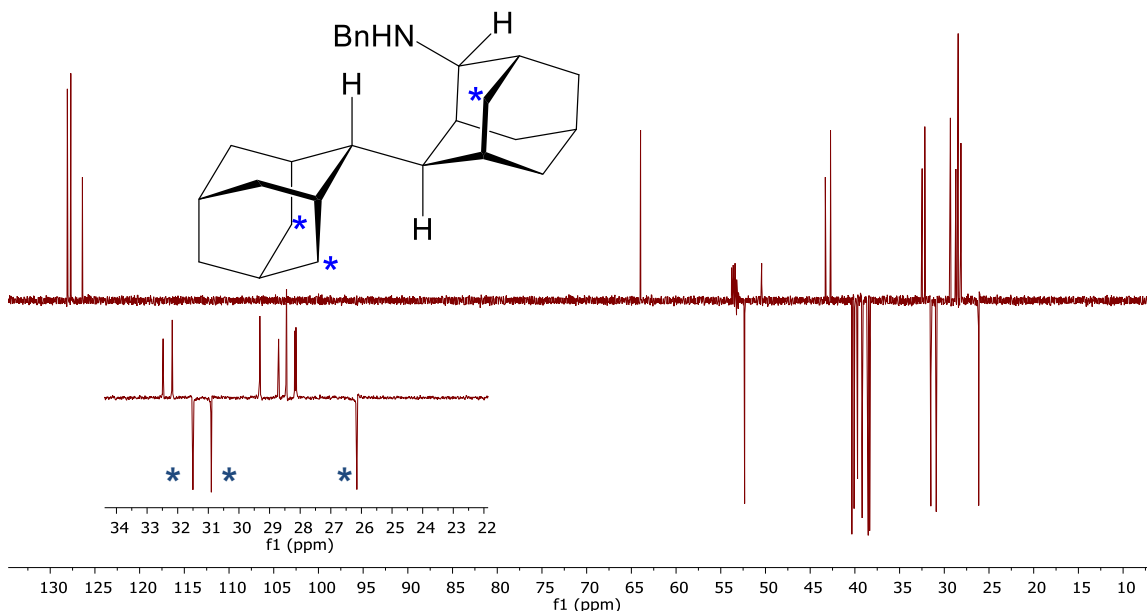
Figure 2.31 ^{13}C DEPT 135 NMR spectrum of pure major diastereomer **16-(a)**.

Deprotection of the Major Diastereomer 16-(a)
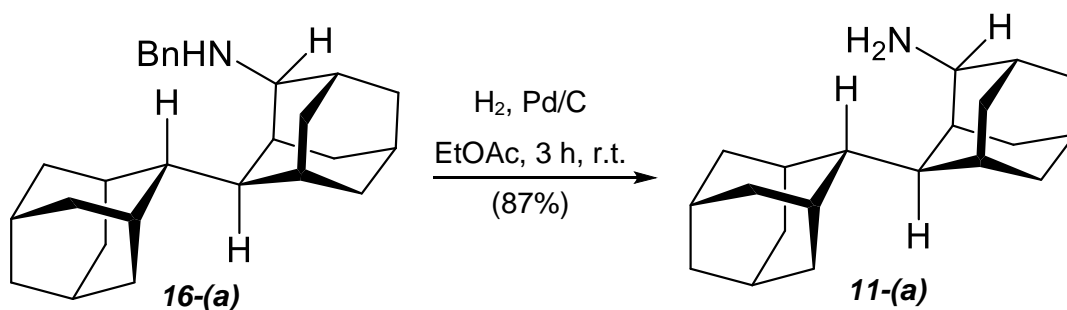
Figure 2.32   Deprotection of **16-(a)** via hydrogenation to yield *rac*-amine **11-(a)**.

Deprotection of *16-(a)* with H_2 and Pd/C in EtOAc afforded the sterically congested racemic *bis*-adamantane based amine *11-(a)* (Figure 2.32). That this reaction did not involve epimerization, was confirmed by the presence of three shielded CH_2 groups in the ^{13}C DEPT 135 NMR spectrum (Figure 2.33).
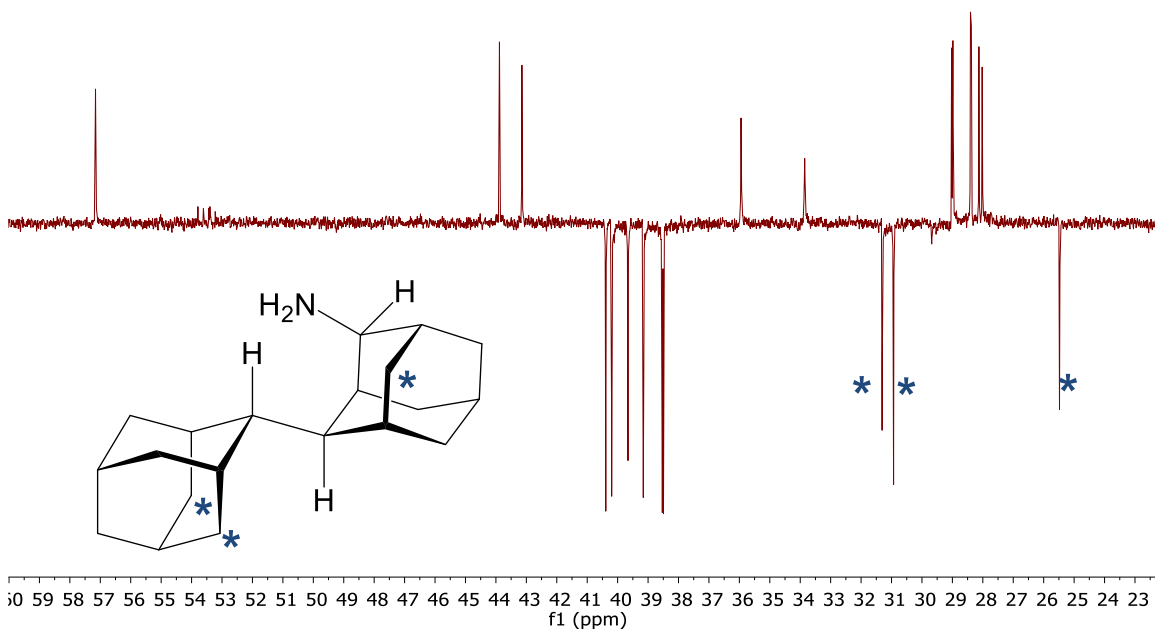
Figure 2.33 ^{13}C DEPT 135 NMR spectrum of *rac*-amine *11-(a)* with retention of stereochemistry after deprotection by hydrogenation.

In addition to this hydrogenation reaction, we attempted deprotection by performing a Birch reduction with $Na/NH_3(l)$ in THF/MeOH, however, we recovered only starting material. We also carried this reaction in ethyl acetate but with no success. One possible reason behind this unsuccessful Birch reduction might be the low solubility of the starting material *16-(a)* at −70 °C in these solvents.

Formation of Amine (11) via Reduction of an Oxime Intermediate

Furthermore, the synthesis of the desired amine via reduction of an oxime intermediate was also investigated as an alternative pathway to avoid the formation of the side product alcohol *10*. (Figure 2.34).
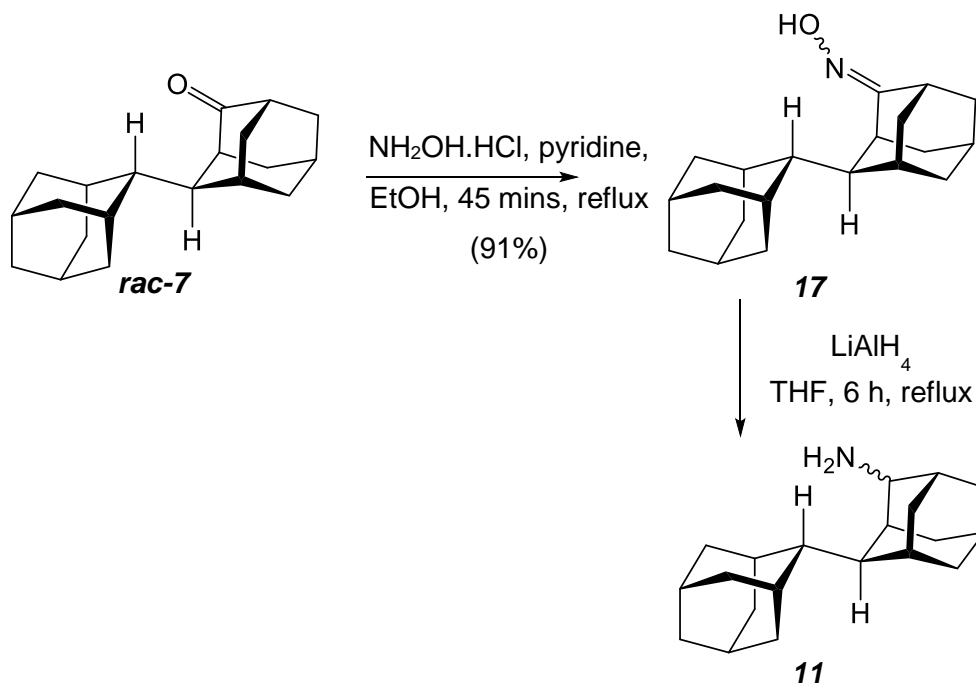
Figure 2.34   Synthesis of amine *11* via LiAlH₄ reduction of the diastereomeric oxime *17* intermediates.

The ketone *rac-7* was converted into a pair of diastereomeric oximes (E and Z) *17* in presence of pyridine and hydroxylamine hydrochloride. Recrystallization in ethanol favored the Z-isomer. A single crystal X-ray structure of this new compound was determined (Figure 2.35 & Table 2.3). The structure of this crystal corresponds to the Z-isomer. Bond lengths of C=N, N–O and O–H present in the oxime functional group are very similar to those reported in literature for other oximes.[86]
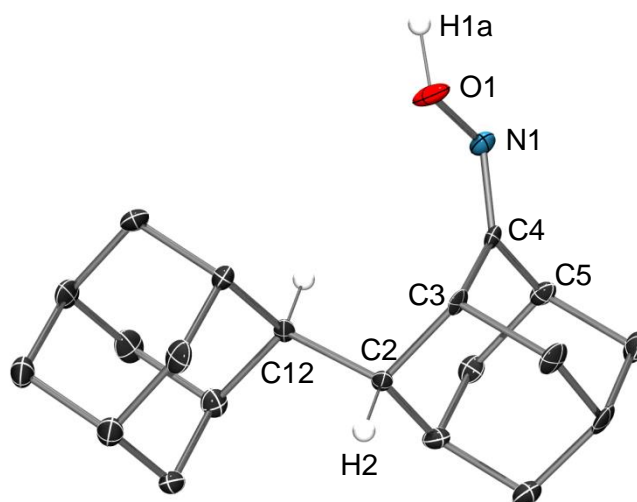
Figure 2.35   The crystal structure of the oxime intermediate **17**.[1] Colour scheme: Carbon, black; Hydrogen, white; Oxygen, red; Nitrogen, steel blue. Most of the hydrogen atoms on the *bis*-adamantane framework have been omitted for clarity.

Table 2.3   Selected bond lengths (Å) and angles (°) for *17*.

Bond length		Bond angle	
C12–C2	1.547(5)	C3–C4–N1	127.8(3)
C4–N1	1.281(4)	C5–C4–N1	118.3(3)
N1–O1	1.415(4)	C4–N1–O1	113.0(3)
O1–H1a	0.98(4)	N1–O1–H1a	109(2)
		C12–C2–H2	107.5

[1] Assignment of atom numbering of the crystal structure is not based on the IUPAC rules for nomenclature.

Reduction of Oxime 17

Reduction of the oxime was carried out using LiAlH$_4$ and the ^{13}C NMR spectrum of the product (Figure 2.36) showed amine peaks (67.63 & 60.80 ppm) with a diastereomeric ratio of 1.4:1 Thus, we did not pursue this route further given the problems of separation and purification of these diastereomers that we encountered earlier (as described on pages 36 and 37).
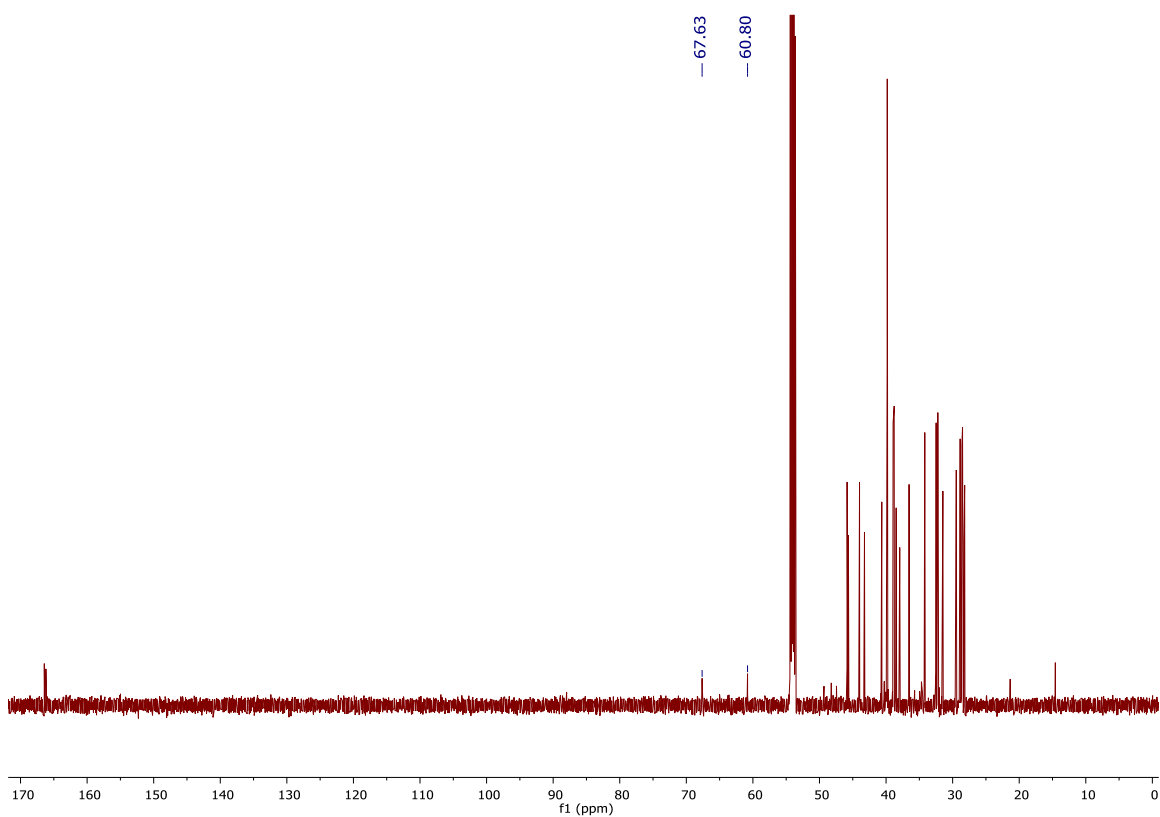
Figure 2.36   ^{13}C NMR spectrum of crude mixture of amine *11* from reduction of oxime *17*.

In summary, two pathways towards the synthesis of the *bis*-adamantane amine notably the reductive amination of *rac*-ketone **rac-7** and reduction of oxime **17**, were investigated. No alcohol side product was observed in the case of the reduction of the oxime intermediate but separation and purification of the amine diastereomers were problematic and this pathway was not further studied. Optimization for the reductive amination was achieved on using acetic acid, benzyl amine as the amine source and NaBH$_3$CN as reducing agent (78% yield for crude mixture) since formation of the side product alcohol was minimal and separation and purification of the amine diastereomers could easily be carried out owing to the presence of the aromatic group of the benzyl amine. The pure major diastereomer of the protected amine (48% yield) was then deprotected by hydrogenation to obtain the pure major diastereomer of the *bis*-adamantane amine (87%).

2.3.2. Synthesis of Targeted Ligands through the Chiral Synthetic Pathway

In the previous section, we carried out the optimization protocols for the synthesis and purifications of the racemic saturated alcohol and amine from the racemic ketone intermediate. With this knowledge in hand, we proceeded to the synthesis of the chiral ketone intermediate via the proposed synthetic scheme (Figure 2.12) to access the chiral saturated alcohol and amine ligands.

Synthesis of Compound 2

Commercially available 2-adamantanone (**1**) was subjected to a McMurry coupling reaction to obtain Ad=Ad (**2**) (Figure 2.37).[78]
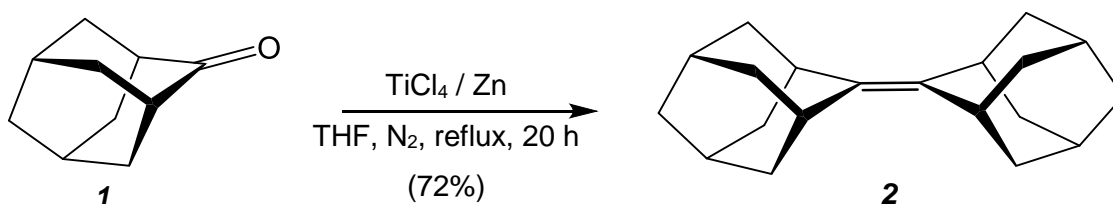
Figure 2.37   McMurry coupling reaction of 2-adamantanone to form Ad=Ad.

Synthesis of Compound rac-4

When compound **2** is reacted with *N*-chlorosuccinimide (NCS), a single monochlorinated product **rac-4** was observed (Figure 2.38), as reported by Huang *et al.*[14] These authors also conducted a mechanistic study for this homoallylic chlorination reaction and showed that it occurs via an anti-stereospecific transition state.
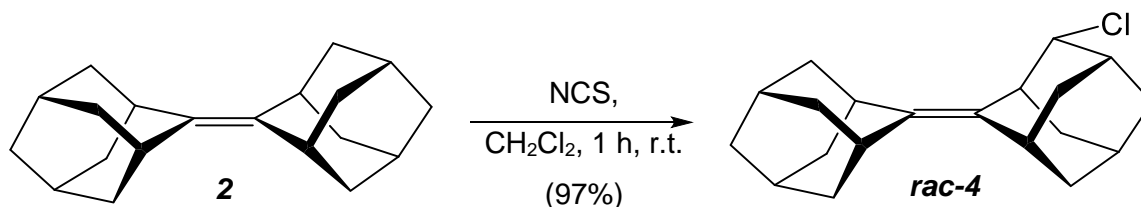
Figure 2.38   Homoallylic chlorination of compound **2** with NCS.

Synthesis of Compound rac-6

Rac-4 was then converted into the alcohol **rac-6** in the presence of Ag₂O and H₂O (Figure 2.39). Huang *et al.,* reported that the solvolysis occurs via a carbenium ion **4.1⁺** (Figure 2.40) intermediate with retention of the stereochemistry at the reaction centre.[79, 87, 88]
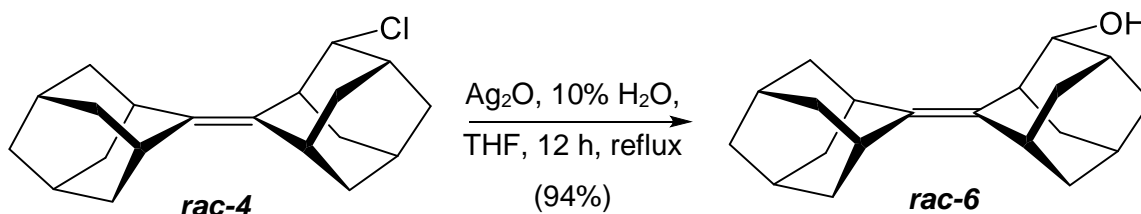
Figure 2.39   Solvolysis of compound **rac-4** with retention of stereochemistry.

They further probed the participation of the double bond, which contributes to stabilization of the carbenium ion, during the solvolysis of the corresponding tosylate where reaction occurs with retention of stereochemistry. [14, 79, 88]
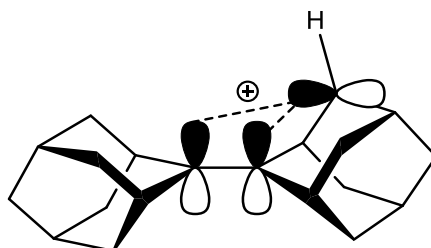
Figure 2.40   Stabilization of carbenium ion **4.1⁺** by the p-orbitals of the double bond which leads to retention of stereochemistry during solvolysis.

Synthesis of Compound rac-9

At this point, it was critical to separate the enantiomers of **rac-6** in order to access chiral ketone **7.** Separation by chiral analytical HPLC was ruled out as we wanted to perform the separation on a multigram scale. Based on some unpublished results from the Bennet group, it had been observed that separation via selective enzymatic hydrolysis of the racemic ester of the *bis*-adamantane afforded chiral alcohol **6** and importantly, was

feasible on a large scale. Hence, in order to perform the enzymatic resolution of the ester, *rac-6* was converted into *rac-9* (Figure 2.41).
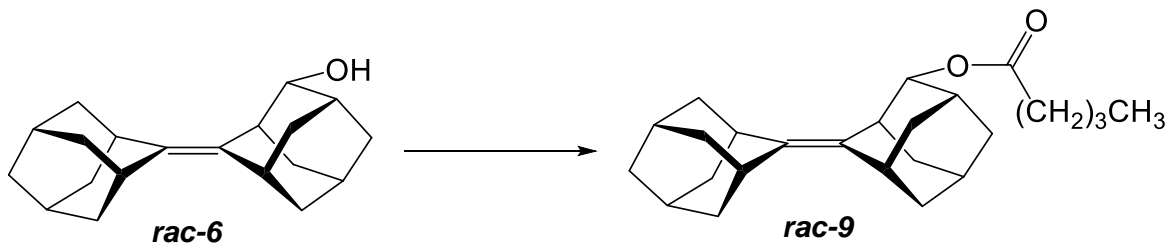
rac-6

Figure 2.41   Esterification reaction of *rac-6* with pentanoyl chloride.

Optimization for the esterification reaction was achieved using pentanoyl chloride (3 eq.), pyridine (4 eq.) and heating under reflux for 3 hours (78%) (Appendix B). Purification by column chromatography (hexane:EtOAc, 11:3) afforded an oil of pure ester *rac-9* (Figure 2.42).
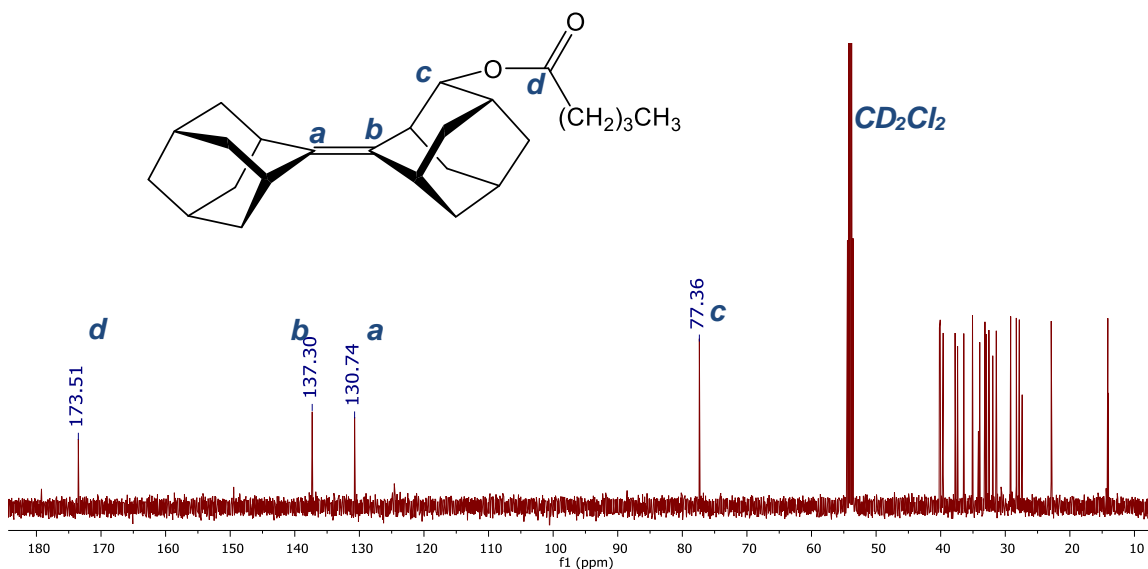
Figure 2.42 ^{13}C NMR spectrum of the purified ester *rac-9*.

Synthesis of Unsaturated Chiral Alcohol (-)6
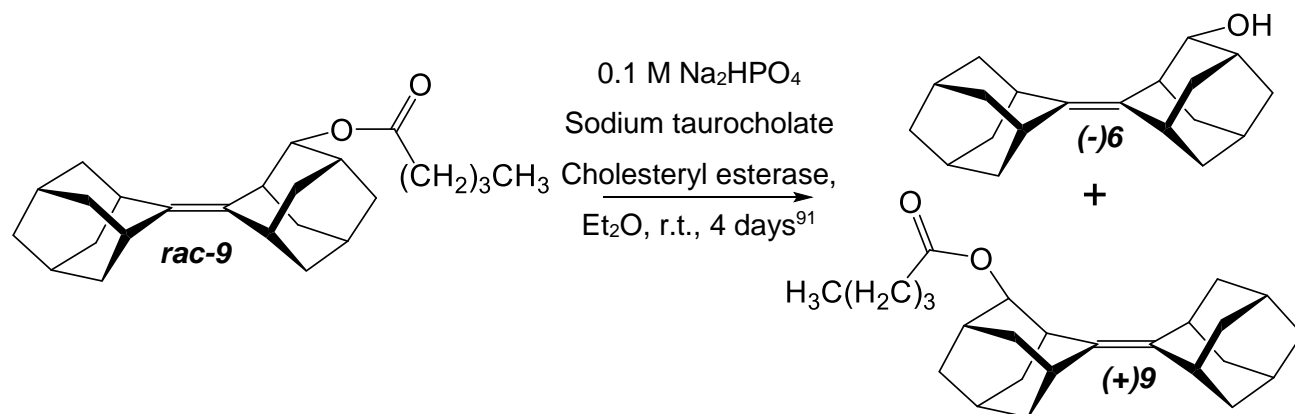
Figure 2.43   Enzymatic resolution of ester **rac-9** using cholesterol esterase to obtain chiral unsaturated alcohol **(-)6**.

This enzymatic resolution involves the use of an esterase, which hydrolyzes the ester in one of the two enantiomers, and thus results in generation of chiral alcohol (Figure 2.43). For our study, we used the enzyme cholesterol esterase which has the standard catalytic triad, consisting of serine, histidine and aspartate residues. [89, 90]

We adopted the reported procedure for the resolution of 1,1'-bi-2-naphthol[91] for separation of enantiomers. So, our starting material, the ester **rac-9** was dissolved in diethyl ether and the enzyme, purified cholesterol esterase, was dissolved in 0.1 M Na_2HPO_4 buffer of pH 7.3. Since this enzyme reacts at a water-organic liquid interface, it was necessary to perform the reaction in an emulsion. Thus, the addition of bile salt such as sodium taurocholate was important for the success of the hydrolysis.

However, after 1 hour of stirring, a clear brown solution was observed rather than an emulsion. At first, we attributed this observation to poor stirring and hence attempted to create the emulsion via sonication and mechanical stirring but with no success. Upon vigorous shaking followed by an extremely fast stirring with the mechanical stirrer, a mediocre emulsion was observed but it very rapidly coalesced into a cloudy solution. This solution was left to stir overnight and a portion of this mixture was then worked up and analyzed by ^1H NMR spectroscopy where only a 5% conversion to the chiral alcohol was

detected. The remaining mixture was allowed to stir overnight and no further hydrolysis was observed.

Since the emulsion was crucial for the hydrolysis to occur, we further screened for solvents and use of surfactant sodium dodecyl sulphate (SDS) (Table 2.4). A laboratory blender was also acquired to perform the initial mixing. However, none of these optimization attempts yielded any substantial amount of alcohol.

Table 2.3   Optimization of enzymatic resolution with purified cholesterol esterase enzyme.

Entry	Et$_2$O	THF	SDS	Blender	Observation	% Alcohol (^{1}H NMR)
1	✓			X	Cloudy solution	5
2	✓		✓	X	Brown solution	x
4	✓			✓	Brown solution	x
3		✓			Cloudy solution	2
4		✓		✓	Cloudy solution	3

Surprisingly, upon switching from purified to crude enzyme preparation, an off-white emulsion was observed instantaneously and the alcohol peak was detected using ^{1}H NMR spectrum (Figure 2.44) with 17% conversion after 36 hours. This yield can be improved with further optimization of reaction time and work up methodology. Of note, an ideal resolution can yield a maximum of 50% conversion.
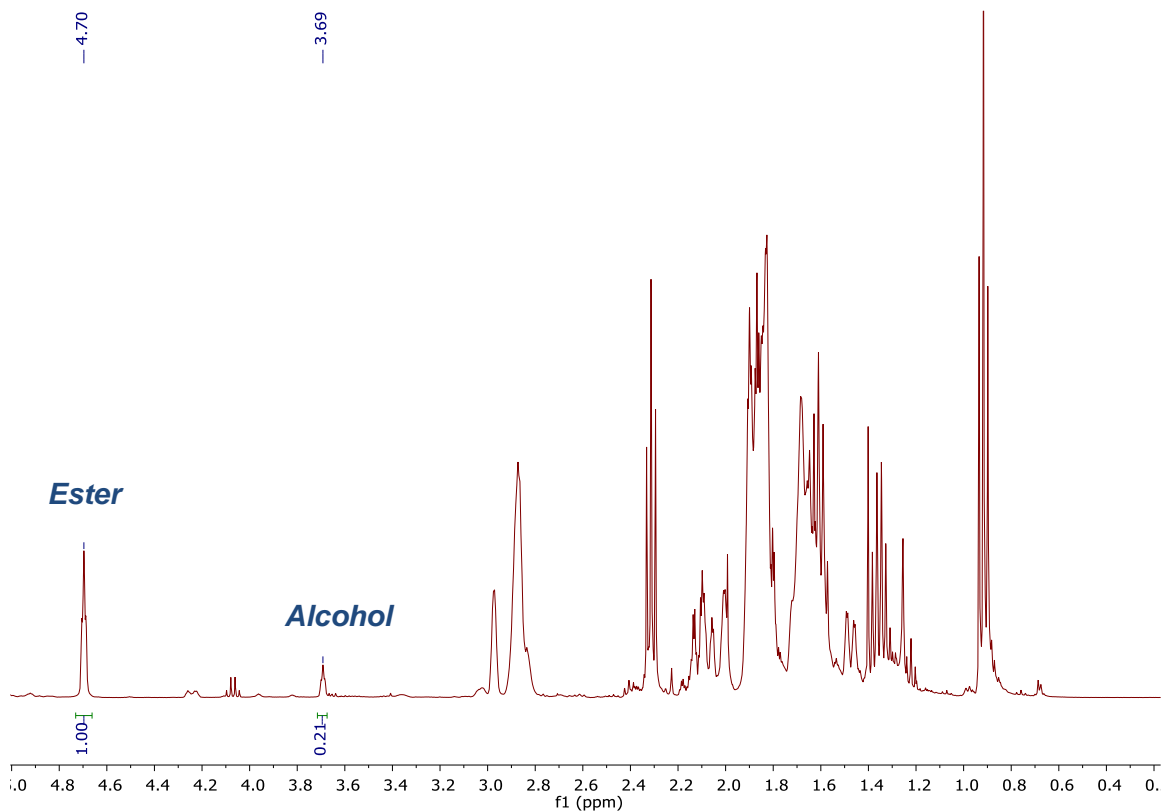
Figure 2.44   ¹H NMR spectrum of the crude mixture from enzymatic hydrolysis after 36 hours using crude enzyme.

The 2.57 g scale reaction was stopped at 17% conversion, worked up and purified by column chromatography (hexanes: EtOAc, 11:3) followed by recrystallization to afford 0.186 g of pure white solid of unsaturated alcohol **6** (Figure 2.45 and Table 2.5) which has a specific rotation of $[\alpha]_{589}^{20}$ -12.9 (c = 1.33, CH$_2$Cl$_2$). A single crystal X-ray structure of this chiral unsaturated alcohol was acquired and it was shown to be in a chiral space group of P2$_1$2$_1$2. The bond lengths C(1)-O(1) and O(1)-H(5) of the alcohol functional group correspond to typical values reported in literature.[92]
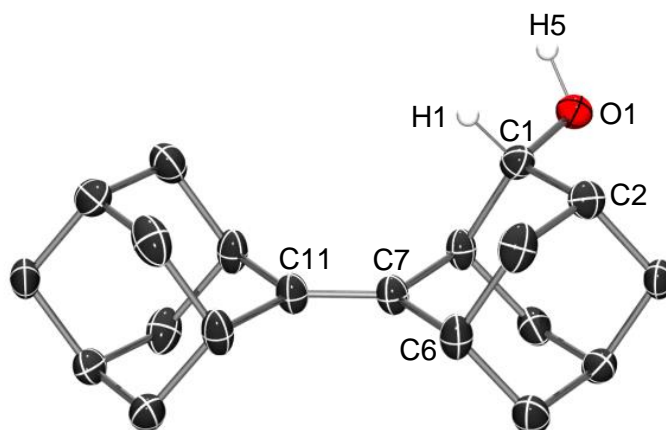
Figure 2.45   The crystal structure of chiral unsaturated alcohol *(-)6* with a $P2_12_12$ space group. Colour scheme: Carbon, black; Hydrogen, white; Oxygen, red. Hydrogen atoms on the *bis*-adamantane framework have been omitted for clarity.

Table 2.4   **Selected bond lengths (Å) and angles (°) for *(-)6.***

Bond length		Bond angle	
C11–C7	1.331(4)	C1–O1–H5	106(3)
C1–H1	0.981	H1–C1–O1	108.6
C1–O1	1.444(5)	C2–C1–O1	110.6(3)
O1–H5	0.93(5)	C6–C7–C11	125.5(3)

A closer look at the crystal lattice packing when viewed in the ab plane (Figure 2.46) revealed the formation of tetramers held by hydrogen bonding. Viewed down the c-axis, these tetramers generate columns of materials supported by extensive hydrogen bonding. This array of hydrogen bonding can rationalize the high melting point range 197-204 °C of the chiral alcohol.
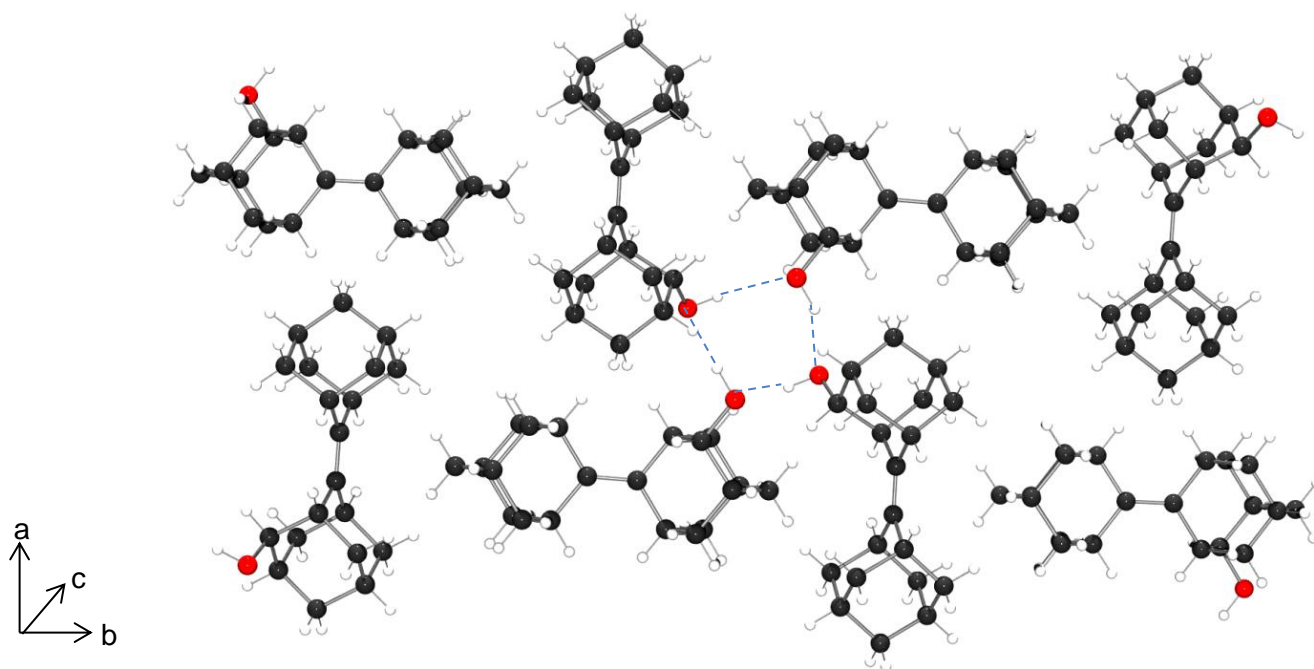
a) Formation of tetramers held by hydrogen bonding.
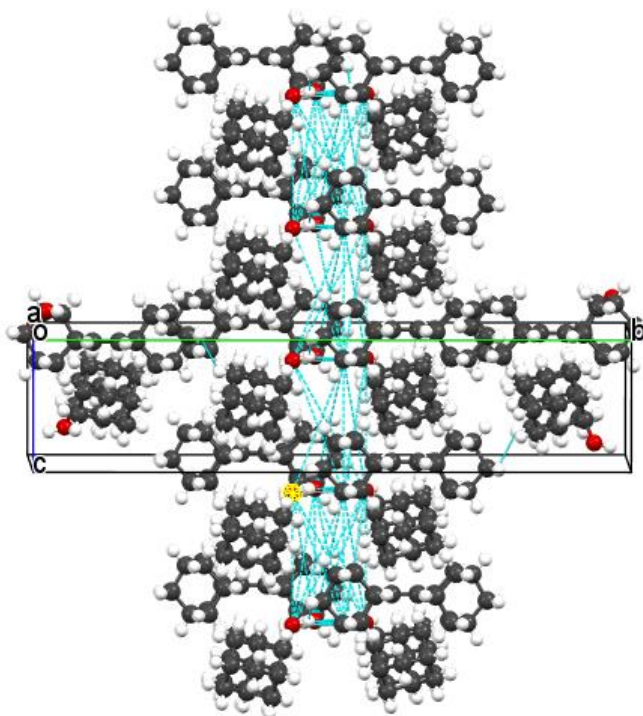
b) Column of hydrogen bonding between stacked tetramers along the c-axis.

Figure 2.46   Crystal packing of the unsaturated chiral alcohol *(-)6* forming a) tetramers linked by hydrogen bonding and b) a column of hydrogen bonding between the stacked tetramers. Blue dotted lines represent hydrogen bonds.

Using the racemic alcohol **6**, as a standard, the enantiomeric excess of chiral compound **(-)6** was determined by chiral HPLC. The chromatogram below (Figure 2.47) shows an enantiomeric excess of 97.7% of the unsaturated chiral alcohol.
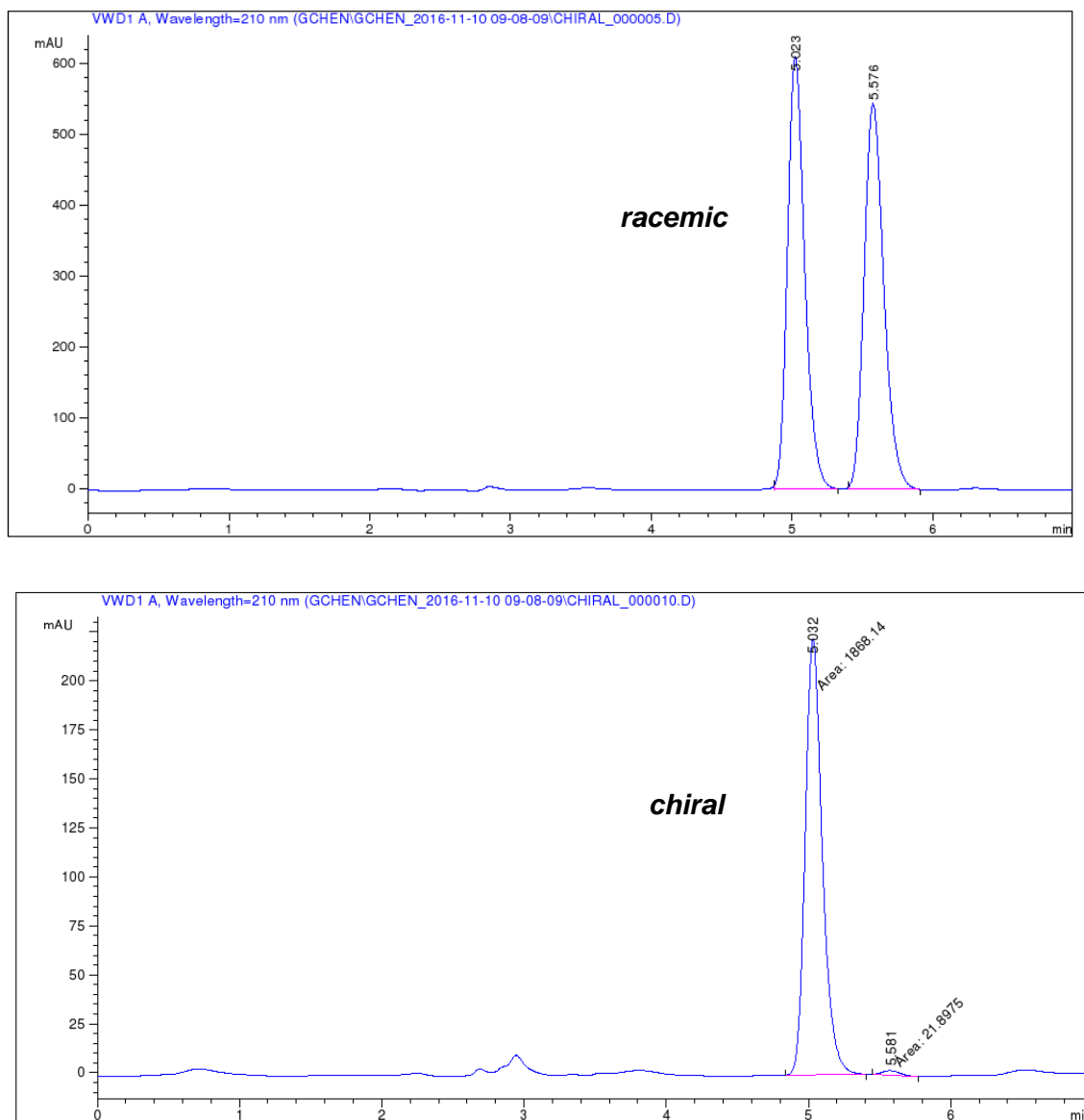
Figure 2.47   Chiral HPLC traces of alcohols **rac-6** and **(-)6**.

Synthesis of Chiral Ketone *(+)7*

50% v/v $H_2SO_{4(aq)}$, CH_3COOH

3 h, 110 °C[22]

(81%)
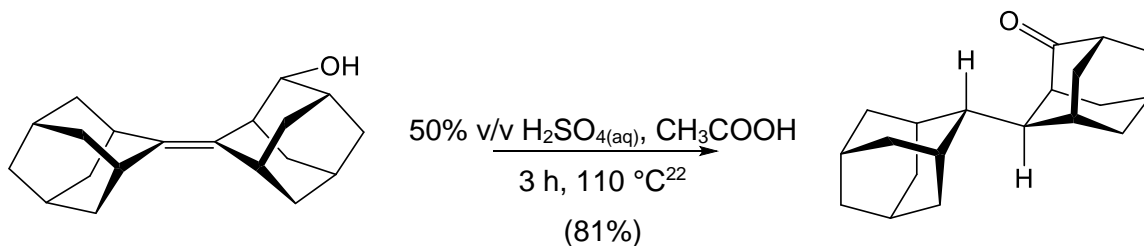
Figure 2.48   Synthesis of chiral ketone *(+)7* by the acid-catalyzed 1,4-Hydride shift rearrangement of compound *(-)6*.

Chiral alcohol *(-)6* was then transformed into the targeted saturated chiral ketone (Figure 2.48) by an acid-catalyzed 1,4-hydride shift.[22] The crude product was recrystallized in methanol to obtain pure *(+)7* with a specific rotation $[\alpha]_{589}^{20}$ 19.6 (c = 0.29, C_6D_6). A single crystal X-ray structure of this new compound (Figure 2.49 and Table 2.6) was also acquired, however the quality of the crystal and the associated diffraction data is poor. The C(10)-O(1) bond length of the ketone functional group is similar to typical literature values.[22]
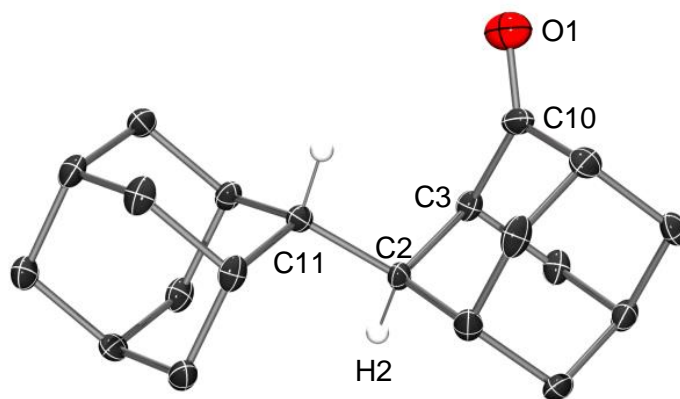
Figure 2.49   The crystal structure of the targeted chiral ketone *(+)7* intermediate in a chiral P2₁ space group. Colour scheme: Carbon, black; Hydrogen, white; Oxygen, red. Hydrogen atoms of the *bis*-adamantane framework have been omitted for clarity.

Table 2.5   Selected bond length (Å) and bond angle (°) for *(+)7*.

Bond length		Bond angle	
C11–C2	1.536(6)	O1–C10–C3	123.0(4)
C2–H2	0.980	H2–C2–C11	107.2
C10–O1	1.207(6)		

The large melting point difference of about 130 °C between the chiral (m.p: 55-58 °C) and racemic (m.p: 185-188 °C) ketone and the difficulty encountered when recrystallizing the chiral ketone under the same conditions used for the racemic ketone drew our attention, and since we had the crystal structure for both the chiral and racemic (we inadvertently re-solved the previously published[22] crystal structure of the racemic ketone) molecules, we decided to compare their crystal lattice packing. We compared the packing densities, which surprisingly has a low difference of only 0.026 g/cm^3. Furthermore, we also examined the close contact bond lengths of the oxygen and hydrogen atoms but there were no significant differences which could be attributed to intermolecular interactions and the packing. The other difference that was observed was molecular orientation (Figure 2.50), which presently lead us to regard the latter as the main factor influencing the crystal packing. The above observations are subjects of interest for future studies.

.
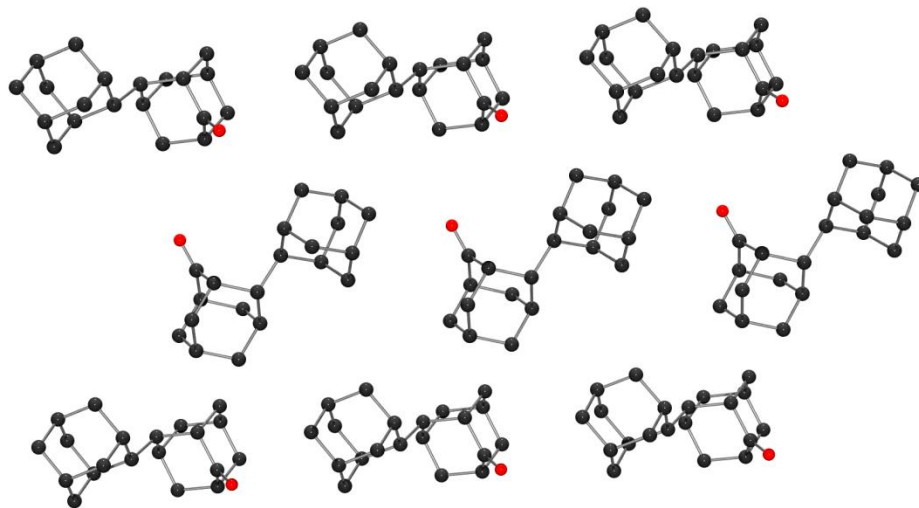
a)   Crystal lattice packing of the chiral ketone with a space group of $P2_1$ and packing density of 1.252 gcm^{-3}.
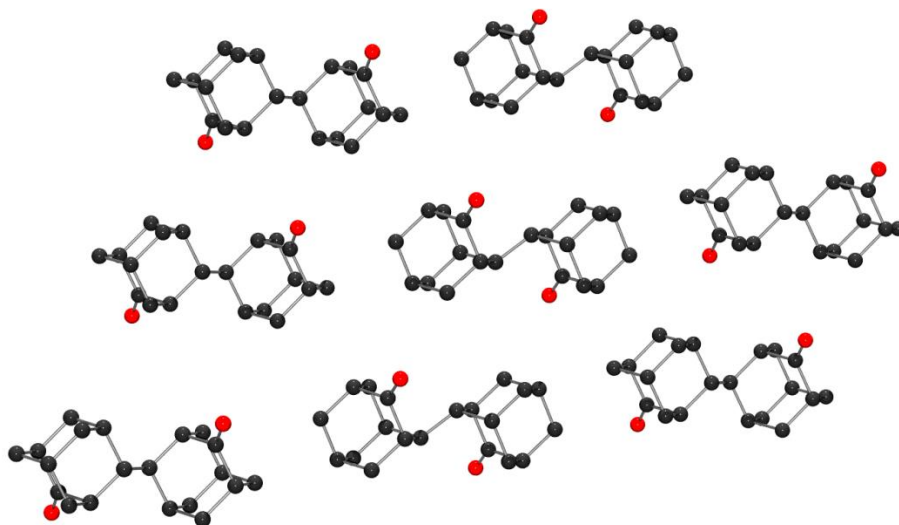
b)   Crystal lattice packing of the racemic ketone with a space group of C2/c and packing density of 1.226 gcm^{-3}.

Figure 2.50   Crystal lattice packing of the a) chiral and b) racemic ketone.

This intermediate ketone *(+)7* was then used for reduction and reductive amination reactions to access the targeted ligands, using the optimized syntheses and purification of these two key reactions which were already carried out on the racemic ketone *rac-7* (addressed in section *2.3.1*).

At this point, since the chiral ketone intermediate is used, only two diastereomers are expected for the reduction and reductive amination reactions (Figure 2.51) and thus separation of the two diastereomers should lead to single enantiopure alcohol and amine products. The absolute configuration of the chiral ketone has not been determined yet and the chiral ketone, the axial and the equatorial diastereomers used in figure 2.51 are only for illustration.
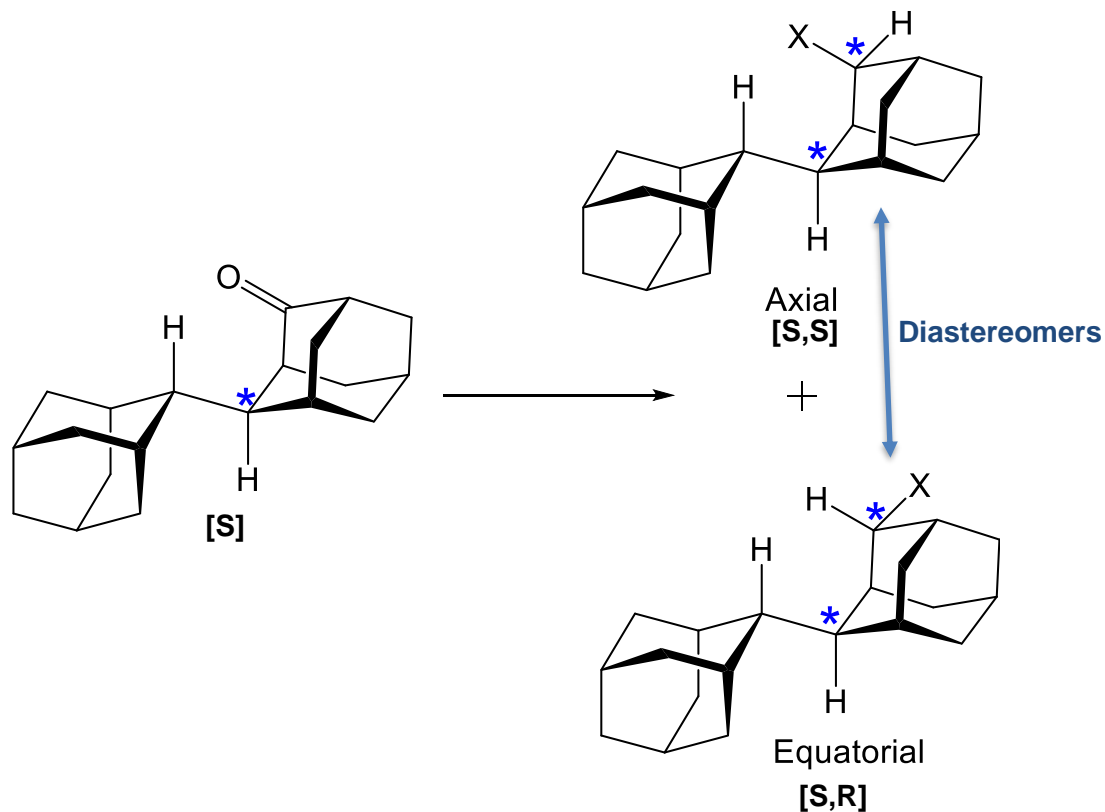
Figure 2.51   Expected formation of the two diastereomers from the reduction and reductive amination reactions of the chiral ketone.

Reduction of Chiral Ketone (+)7

Compound *(+)7* was thus subjected to sodium borohydride reduction to obtain the two diastereomers of the chiral alcohol.

Purification of Alcohol 10

The crude alcohol mixture was then transformed into the benzoyl derivatives for the separation and purification of the diastereomers by flash column chromatography followed by precipitation in ^{i}PrOH with a few drops of H_2O to afford the major diastereomer of the protected alcohol *(+)15-(a)* with a specific rotation $[\alpha]_{589}^{20}$ 33.28 (c = 0.19, CH_2Cl_2). Due to insufficient quantities of *(+)15-(a)*, we could not proceed to the final step to access the pure chiral alcohol *(±)10-(a)*. Unfortunately, the observation of pure major diastereomer of alcohol *10-(a)* from the partial protection of the alcohol *10* (from the racemic pathway *section 3.2.1*), was made after we protected the alcohols from the reduction of chiral ketone *(+)7*.

Reductive Amination of Chiral Ketone

Compound *(+)7* was also used for reductive amination in the presence of benzyl amine, acetic acid and $NaBH_3CN$. The crude mixture was then purified by flash column chromatography and precipitated in methanol to afford pure chiral *(+)16-a* with a specific rotation $[\alpha]_{589}^{20}$ 5.25 (c = 0.4, CH_2Cl_2). Due to insufficient materials of chiral *16-(a)*, we were unable to proceed to the final step to isolate the targeted chiral *bis*-adamantane based amine *11-(a)*, however, the proof of principle synthetic procedure optimized for the racemic version indicates that the final chiral amine *11-(a)* should be accessible.

2.4. Conclusion and Future Work

In conclusion, two synthetic pathways have been investigated towards the synthesis of congested *bis*-adamantane based alcohol and amine ligands. The first pathway involved a two-step route to access the racemic ketone (*rac-7*) intermediate; this was used to conduct all optimization protocols for the synthesis and purification of compounds *10* and *11*, the *bis*-adamantane alcohol and amine respectively. Access to multigram quantities of the ligands was also taken into consideration during the optimization.

For the synthesis of the saturated alcohol, a diastereomic ratio of 7:1 was obtained when *rac-7* was reduced with NaBH$_4$ and no significant improvement in the diastereoselectivity was observed when selective reducing conditions such as Luche reduction and L-selectride® reagent were used. Purification of the alcohol diastereomers were performed by incorporating an aromatic group in the form of benzoyl protecting group which were then separated by flash column chromatography followed by recrystallization in isopropanol. An interesting observation was made during the benzoyl protection of the alcohol, where at 45% reaction completion, we noted full conversion of minor alcohol diastereomer to its corresponding protected alcohol and partial protection of the major diastereomer. Separation by flash column chromatography afforded the major diastereomer of the *bis*-adamantane alcohol. Some more studies would need to be conducted to determine the optimal conditions for this partial benzoyl protection. The synthesis of the *bis*-adamantane amine was carried out via the reductive amination reaction of ketone *rac-7*. NaCNBH$_3$, acetic acid and benzyl amine were found to be the most favorable conditions. We had some challenges in controlling the formation of the alcohol side product when reductive amination reaction was performed on a large scale and at this point, purification was crucial. Again, the presence of the aromatic group of the benzyl amine aided in the separation and purification of the crude mixture by flash column chromatography. Precipitation from methanol afforded the pure major diastereomer of the protected amine. Compound *16-(a)* was then deprotected by hydrogenation to give the *bis*-adamatane amine *11-(a)*. The isolation of the targeted sterically congested racemic alcohol and amine ligands was successful. Formation of amine *11* via the reduction of the oxime intermediate *17* was also investigated as a potential pathway to minimize the

formation of the side product but due to purification difficulties, this route was not further inspected.

The second synthetic route was explored to access the chiral ketone intermediate *(+)7* where optimization of one of the key steps –the enzymatic resolution– crucial to the formation of the chiral ketone, was also performed. An enantiomeric excess of 97.7% for this reaction was achieved. However, due to insufficient amount of the penultimate chiral intermediates *15-(a)* and *16-(a)*, we could not proceed to the final step to access the chiral ligands. Nonetheless, we have demonstrated that we could access the chiral ketone intermediate and have successfully isolated the racemic ligands. With this knowledge and skills acquired on the *bis*-adamantane ligand framework, the stage has been set to access the sterically encumbered chiral alcohol and amine, which should now be readily obtainable in multigram quantities.

Future work will include the assignment of the absolute configuration for the chiral compounds *(-)6*, *10-(a)* and *11-(a)* as well as the full characterization of the final saturated chiral alcohol and amine. Moreover, it would be worthwhile to test these sterically congested chiral ligands for asymmetric deprotonation and its use as monomeric anionic ligands in metal coordination. The eventual incorporation of the chiral amine as an amido-R group of a multidentate ligand framework for alkene and lactide polymerization and asymmetric hydroamination will be the exciting subject of future studies.

The synthesis and use of several adamantane-based ligands have been reported with its steric feature highly acknowledged for the formation of low-coordinate complexes and its use in catalysis but till now, to our knowledge, no *bis*-adamantane based ligands have been synthesized and studied. As such, the adamantane-chemistry remains rich even after four decades.

2.5. Experimental

2.5.1. General Remarks

All chemical reagents were analytical grade and were purchased from Sigma-Aldrich unless stated otherwise, and used without further purification. Solvents used for anhydrous reactions were dried and distilled prior to use. Et_2O and THF were freshly distilled over sodium/benzophenone and CH_2Cl_2 was dried over CaH_2. For anhydrous reactions, all glassware was dried overnight at 100-150 °C in an oven prior to use and reactions were performed under an atmosphere of dry nitrogen. Thin layer chromatography (TLC) was carried out on aluminium sheet TLC plates backed with silica gel 60 plate (E. Merck, $F_{554,}$ thickness 0.25 mm). Flash column chromatography was performed using Fischer Scientific silica gel 60 (230-400 mesh). Melting points were measured on an Optimelt melting point apparatus and were not corrected. Optical rotations were determined using a Perkin-Elmer 341 polarimeter and units are reported in deg cm^2 g^{-1} (concentration reported in units of g per 100 mL). ^1H NMR, ^{13}C NMR and DEPT-135 NMR were acquired on either a Bruker Avance III 400 spectrometer (400 MHz), Bruker Avance III 500 spectrometer (500 MHz), Bruker Avance II 600 spectrometer equipped with a QNP or TCI cryoprobe (600 MHz). Deuterated chloroform ($CDCl_3$), dichloromethane (CD_2Cl_2) and benzene (C_6D_6) were used as solvent and internal reference. High resolution mass spectra were acquired using a Bruker maXis Impact spectrometer. The IR spectra were recorded on a Thermo Nexus 670 FT-IR spectrometer equipped with a Pike MIRacle attenuated total reflection (ATR) sampling accessory (4000-700 cm^{-1}). Elemental analyses (C, H, N) were performed on a Carlo Erba 1110 CHN elemental analyzer. High performance liquid chromatography (HPLC) were performed on an Agilent 1100 series equipped with a variable wavelength monitoring detector (λ = 210 nm) and Daicel Chemical Industries Ltd. Chiralpak® AD column (4.6 x 250mm).

2.5.2.   Preparation and Experimental Data

Preparation of compound *12*
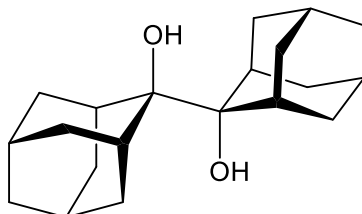
Sodium (14.0 g, 609 mmol) was added to refluxing xylene (500 mL) followed by dropwise addition of a solution of 2-adamantanone *(1)* (50.0 g, 333 mmol) in xylene (250 mL). After 3 hours, the reaction was cooled to room temperature and quenched with isopropanol (20 mL) and H_2O (100 mL). The mixture was then acidified with 2 N H_2SO_4 (200 mL) to form a white precipitate. This precipitate was filtered and the residue was washed with H_2O, MeOH and pentane and dried to obtain compound *12*, a white solid (45.3 g, 90%).

^{1}H NMR (400 MHz, CDCl$_3$) δ: 2.51 (d, *J* = 11 Hz, 4H), 2.22 (m, 4 H), 2.12 (bs, 4H), 1.86-1.56 (m, 18H).

^{13}C NMR (400 MHz, CDCl$_3$) δ: 80.12, 39.92, 35.72, 35.35, 34.98, 27.37, 27.10.

HRMS: *m/z* calcd. for $C_{20}H_{30}O_2Na$ (M + Na)$^+$: 325.2098; found: 325.2138.

IR: 3668, 3621, 2893, 2862, 1457, 1350, 1037, 997 cm^{-1}.

m.p: 260-266 °C (lit.[1] 267-269 °C).

Preparation of compound *rac-7*
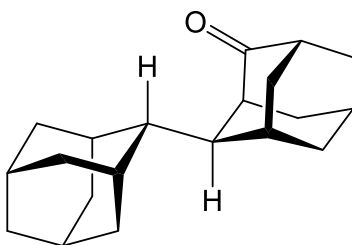
To a mixture of 50% v/v aqueous H_2SO_4 (500 mL) and acetic acid (500 mL), was added compound *12* (10.0 g, 33.1 mmol). After heating at 140 °C for 5 days, the reaction

mixture was cooled and poured onto ice water and extracted with CH_2Cl_2 (3 x 300 mL). The combined organic fractions were washed with $NaHCO_3$ (300 mL), brine (300 mL) and dried over Na_2SO_4, filtered and evaporated. The crude product was recrystallized in MeOH to give pure white crystals of **rac-7** (8.26 g, 88%).

^1H NMR (500 MHz, C_6D_6) δ: 2.66 (bs, 1H), 2.44 (bs, 1H), 2.11 (bd, J= 2.41 Hz, 1H), 2.06 (bs, 1H), 1.88 (m, 1H), 1.55-1.88 (m, 19H), 1.47-1.54 (m, 2H), 1.40-1.45 (m, 1H), 1.35-1.39 (m, 1H).

^{13}C NMR (126 MHz, C_6D_6) δ: 215.03, 48.81, 47.73, 46.95, 43.68, 40.02, 39.54, 39.34, 38.54, 38.39, 34.11, 31.92, 31.75, 28.38, 28.32, 28.20, 27.93, 27.88, 27.74.

HRMS: m/z calcd. for $C_{20}H_{28}OH$ $(M + H)^+$: 285.2218; found: 285.2215.

IR: 2900, 2849, 1719, 1450, 1058 cm^{-1}.

m.p: 185-188 °C (lit.[22] 186.5-187.5 °C).

Preparation of compound *10*
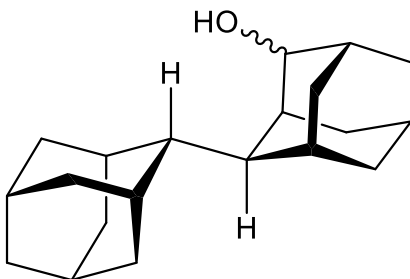
NaBH$_4$ (0.640 g, 16.9 mmol) was added to a solution of **rac-7** (2.40 g, 8.44 mmol) in dried THF (200 mL) and was stirred under nitrogen at room temperature overnight. The reaction was quenched by MeOH (30 mL) followed by H_2O (30 mL) and extracted with CH_2Cl_2 (3 x 50 mL). The combined organic layer was acidified with 1 N HCl and dried over Na_2SO_4, filtered and evaporated to give a crude mixture of compound *10* (2.05 g, 85 %).

Preparation of compound *15-(a)*
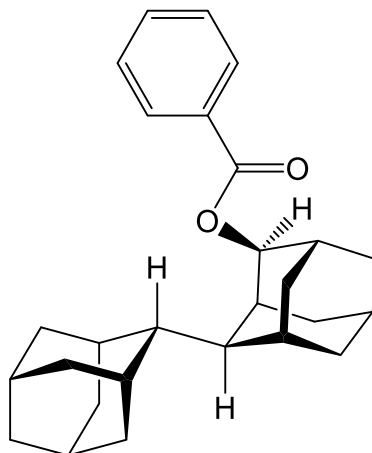
The crude mixture of compound **10** (200 mg, 0.699 mmol) was dissolved in dried CH_2Cl_2 (20 mL) and pyridine (0.25 mL, 2.80 mmol) was added to the solution. Benzoyl chloride (0.35 mL, 1.04 mmol) was then added and the reaction was stirred at room temperature under nitrogen for 24 hours. The reaction mixture was poured onto ice water (5 mL) and washed with cold 1 M H_2SO_4 (5 mL). The organic layer was extracted with CH_2Cl_2 (3 x 5 mL), washed with brine (7 mL), dried over Na_2SO_4 and concentrated under reduced pressure. The crude mixture (213 mg, 78%) was purified by flash column chromatography (hexanes:EtOAc, 9:1) and precipitated in methanol to afford a white solid of the pure major diastereomer *15-(a)* (75 mg, 27%).

^1H NMR (500 MHz, CD_2Cl_2) δ: 8.07 (d, 2H), 7.57 (t, 1H), 7.46 (t, 2H), 5.16 (bs, 1H), 2.38 (s, 1H), 2.27 (d, 2H), 2.07-1.12 (m, 25H).

^{13}C NMR (151 MHz, CD_2Cl_2) δ: 166.48, 133.23, 131.63, 130.15 (2C), 128.72(2C), 79.09, 43.46, 43.09, 40.34, 40.12, 39.25, 39.08, 39.01, 37.83, 33.02, 31.90, 31.87, 31.48, 29.26, 29.15, 28.82, 28.66, 28.21, 28.18, 27.22.

HRMS: *m/z* calcd. for $C_{27}H_{34}O_2Na$ (M + Na)$^+$: 413.2457; found: 413.2466.

IR: 3333, 2980, 2893, 1728, 1615, 1453, 1279, 1132, 949, 709 cm^{-1}.

m.p: 113-124 °C.

Preparation of compound *10-(a)*
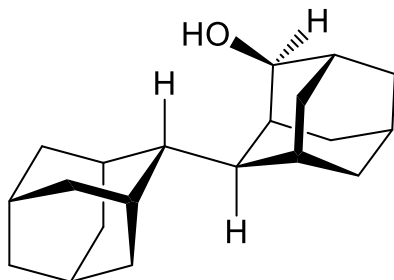
Compound ***10*** (100 mg, 0.350 mmol) was dissolved in dried CH_2Cl_2 (10 mL) and pyridine (0.10 mL, 1.24 mmol) was added to the solution. Benzoyl chloride (0.15 mL, 1.29 mmol) was then added and the reaction was stirred at room temperature under nitrogen for 9 hours. The reaction mixture was poured onto ice water (3 mL) and washed with cold 1 M H_2SO_4 (2 mL). The organic layer was extracted with CH_2Cl_2 (3 x 5 mL), washed with brine (5 mL), dried over Na_2SO_4 and concentrated under reduced pressure. The crude product was purified by flash column chromatography (hexanes:EtOAc, 9:1) to obtain a white solid of the pure major diastereomer ***10-(a)*** (30 mg, 35%).

^{1}H NMR (600 MHz, CD_2Cl_2) δ: 3.86 (bs, 1H), 2.30 (d, J = 11.6 Hz, 1H), 2.14-2.07 (m, 4H), 1.95 (d, 1H), 1.84-1.35 (m, 23 H).

^{13}C NMR (151 MHz, CD_2Cl_2) δ: 76.78, 43.72, 43.45, 40.53, 40.20, 39.82, 39.11, 37.91, 35.72, 34.39, 31.97 (2C), 31.56, 29.59, 29.43, 29.01, 28.78, 28.72, 28.22, 26.32.

HRMS: *m/z* calcd. for $C_{20}H_{30}OH$ (M + H)[+]: 287.2369; found (M − H_2O)[+]: 269.2257.

IR: 3343, 2908, 2840, 1709, 1449, 1320, 1293, 1042, 922 cm^{-1}.

m.p: 154-161 °C.

Preparation of compound *16-(a)*
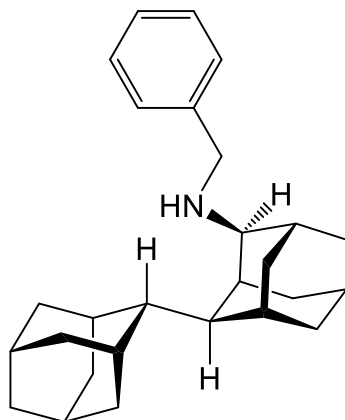
Benzylamine (1.75 mL, 15.9 mmol) was added to a solution of ***rac-7*** (3.03 g, 10.7 mmol) in dried THF (100 mL). A few drops of acetic acid were added to the mixture, which was then stirred overnight at room temperature under nitrogen. NaBH$_3$CN (1.00 g, 16.0 mmol) was added to the reaction mixture and it was stirred for 6 hours. The reaction was quenched with MeOH (5 mL) and H$_2$O (10 mL) and extracted with EtOAc (3 x 30 mL). The combined organic layers were then dried over Na$_2$SO$_4$ and evaporated. The crude mixture (3.13 mg, 78%) was purified by flash column chromatography (hexanes: EtOAc, 9:1) and precipitation in MeOH gave the pure major diastereomer ***16-(a)*** (1.17 g, 48%).

^{1}H NMR (600 MHz, CD$_2$Cl$_2$) δ: 7.35 (d, 2H), 7.30 (t, 2H), 7.21(t, 1H), 3.78-3.70 (dd, 2H), 2.85 (bs, 1H), 2.62 (d, 1H), 2.16-2.12 (m, 2H), 2.06 (s, 1H), 1.97 (d, 1H), 1.90-1.34 (m, 25H).

^{13}C NMR (151 MHz, CD$_2$Cl$_2$) δ: 142.47, 128.67 (2C), 128.28 (2C), 126.98, 64.56, 52.92, 43.89, 43.31, 40.92, 40.67, 40.29, 39.77, 39.09, 38.93, 33.06, 32.76, 32.09, 31.48, 29.90, 29.29, 29.03 (2C), 28.76, 28.72, 26.73.

HRMS: *m/z* calcd. for C$_{27}$H$_{37}$NH (M + H)$^+$: 376.3004; found: 376.3000.

IR: 3347, 2903, 2849,1603, 1453, 1342, 1132, 1091, 927, 810, 730 cm^{-1}.

m.p: 84-89 °C.

Preparation of compound *11-(a)*
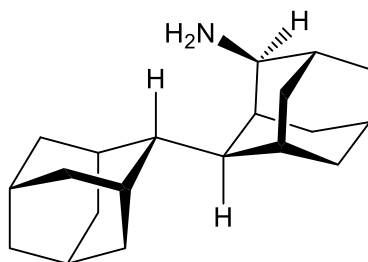
To a solution of compound ***16-(a)*** (100 mg, 0.266 mmol) in EtOAc (4 mL), was added Pd/C (10% Pd, 28.3 mg, 0.266 mmol) and the resulting mixture was hydrogenated for three hours under atmospheric pressure at room temperature. The solution was then filtered through a pad of celite and washed with MeOH (3 mL). Tosic acid (0.051 g, 0.266 mmol) was added to the filtrate and the resulted salt was extracted with H_2O. The aqueous layer was then washed with $NaHCO_3$ (2 mL) and extracted with CH_2Cl_2. The organic layer was then dried over Na_2SO_4 and concentrated under reduced pressure to give compound ***11-(a)*** (66.0 mg, 87%).

To a solution of compound ***16-(a)*** (100 mg, 0.266 mmol) in EtOAc (4 mL), was added Pd/C (10% Pd, 28.3 mg, 0.266 mmol) and the resulting mixture was hydrogenated for three hours under atmospheric pressure at room temperature. The solution was then filtered through a pad of celite and washed with MeOH. Tosic acid (0.051 g, 0.266 mmol) was added to the filtrate and the resulted salt was extracted with H_2O. The aqueous layer was then washed with $NaHCO_3$ and extracted with CH_2Cl_2. The organic layer was then dried over Na_2SO_4 and concentrated under reduced pressure to give compound ***11-(a)*** (66.0 mg, 87%).

^{1}H NMR (600 MHz, CD_2Cl_2) δ: 3.03 (bs,1H), 2.25-1.36 (m, 30H).
^{13}C NMR (151 MHz, CD_2Cl_2) δ: 57.76, 44.48, 43.75, 40.99, 40.26, 39.75, 39.13, 39.09, 36.58, 34.47, 31.91, 31.53, 29.62, 29.58, 29.01, 28.97, 28.73, 28.62, 26.08.
HRMS: *m/z* calcd. for $C_{20}H_{31}NH$ (M + H)$^+$: 286.2535; found: 286.2538.
IR: 3420, 3125, 2898, 2850, 1594, 1507, 1449, 1347, 1112, 1091, 756 cm^{-1}.
m.p: 117-129 °C.

Preparation of compound *17*
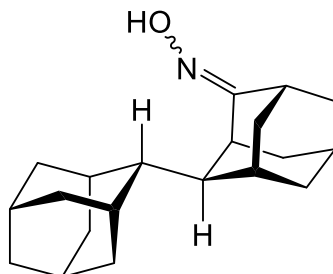
Compound ***rac-7*** (1.50 g, 5.28 mmol), hydroxylamine hydrochloride (0.55 g, 7.92 mmol) and pyridine (1.50 mL) were added to the reaction flask containing ethanol (15 mL). The mixture was refluxed on a water bath for 45 mins. The ethanol solvent was removed by distillation and water (15 mL) was added to the cooled residue. The mixture was further cooled in an ice bath until the formation of crystals, which were filtered off and washed with minimal water (3 mL) and dried. Recrystallization from ethanol afforded pure white crystals of compound ***17*** (1.43 g, 91 %).

^{1}H NMR (600 MHz, CD$_2$Cl$_2$) δ: 7.28 (s, 1H), 7.11 (s, 2H), 3.56 (bs, 2H), 3.44 (bs, 1H), 2.51(s, 1H), 2.42 (s, 2H), 2.18-1.44 (m, 78H).

^{13}C NMR (151 MHz, CD$_2$Cl$_2$) δ: 166.36, 166.12, 45.88, 45.67, 43.98, 43.23, 40.62, 39.83(3C), 39.8(3C), 38.94, 38.89, 38.87, 38.82, 38.79, 38.46, 37.99, 36.57, 34.18, 32.52, 32.47, 32.27, 32.22, 32.17, 31.51, 29.45, 28.87, 28.85, 28.84, 28.61, 28.58, 28.51, 28.50, 28.46, 28.43, 28.28, 28.19.

HRMS: *m/z* calcd. for C$_{20}$H$_{29}$NOH (M + H)$^+$: 300.2327; found: 300.2329.

IR: 3205, 3101, 2903, 2846, 1665, 1450, 1356, 1215, 1087, 960, 950, 839, 792 cm^{-1}.

m.p: 194-196 °C.

Preparation of compound *2*
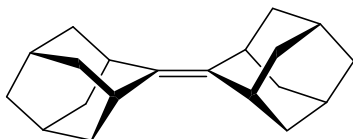
TiCl₄ (5.90 mL, 54.7 mmol) was added to dried THF (140 mL) at 0 °C. To this yellow mixture, Zn dust (7.20 g, 110 mmol) was added portion wise and a black precipitate was observed. A solution of 2-adamantanone (7.50 g, 49.9 mmol) in dried THF (75 mL) was added dropwise and the mixture was heated under reflux for 20 hours under nitrogen. The reaction was cooled to room temperature and a 10% aqueous solution of K_2CO_3 (45 mL) was added. The mixture was filtered and extracted with CH_2Cl_2 (3 x 150 mL). The combined organic layers were washed with H_2O (2 x 100 mL), dried over Na_2SO_4 and concentrated under reduced pressure. The crude product was purified by column chromatography (hexane) to give compound *2* as a white solid (4.82 g, 72%).

^1H NMR (400 MHz, CDCl₃) δ: 2.90 (s, 4 H), 1.92 (s, 4 H), 1.83-1.86 (m, 12 H), 1.67-1.69 (m, 8 H).

^{13}C NMR (101 MHz, CDCl₃) δ: 133.46, 39.8, 37.54, 32.08, 28.74.

Anal. Calcd for $C_{20}H_{28}$: C: 89.49%; H: 10.51%. Found: C: 89.46%; H: 9.96%.

IR: 2902, 2889, 1600, 1450, 1205, 1094 cm⁻¹.

m.p: 184.5-186.2 °C (Lit.[15] 181-182 °C).

Preparation of compound *rac-4*
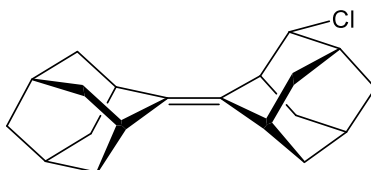
To a solution of compound *2* (18.0 g, 67.1 mmol) in CH_2Cl_2 (225 mL) was added *N*-chlorosuccinimide (9.40 g, 70.4 mmol). After stirring for 1 hour at room temperature,

CH$_2$Cl$_2$ (100 mL) was added and the organic layer was washed with water (2 x 150 mL). The organic layer was dried over Na$_2$SO$_4$ and the solvent was removed under reduced pressure to obtain compound **rac-4**, as a white solid (19.7 g, 97%).

^{1}H NMR (400 MHz, CDCl$_3$) δ: 4.26 (bs, 1H), 3.06 (bs, 1H), 2.88 (bs, 3H), 1.47-2.41 (m, 22H).

^{13}C NMR (101 MHz, CDCl$_3$) δ: 137.31, 131.07, 68.73, 39.84, 39.77, 39.71, 39.66, 39.65, 39.46, 39.07, 37.27, 35.91, 32.70, 32.67, 32.37, 30.73, 30.63, 28.54, 28.50, 27.83.

Anal. Calcd for C$_{20}$H$_{27}$Cl: C79.31%; H: 8.99%. Found: C: 78.98%; H: 8.65%

IR: 2902, 2842, 1691, 1440, 1218, 1084, 795 cm^{-1}.

Mp: 136-143 °C (Lit.[93] 144-145°C).

Preparation of compound *rac-6*
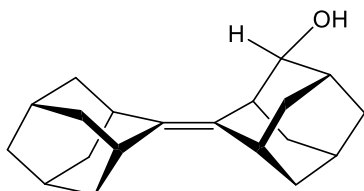
Compound **rac-4** (12.4 g, 40.9 mmol) was added to a mixture of THF (400 mL) and H$_2$O (100 mL) followed by Ag$_2$O (16.8 g, 72.4 mmol). After heating under reflux for 6 hours, the precipitate was filtered on a celite pad and the filtrate was evaporated under reduced pressure. The product was extracted with EtOAc (2 x 200 mL) and the organic layer was dried over Na$_2$SO$_4$, filtered and concentrated under reduced pressure. The crude product was purified by recrystallization from MeOH to afford **rac-6** as a white solid (10.9 g, 94%).

^{1}H NMR (400 MHz, CDCl$_3$) δ: 3.47 (t, 1H), 2.88 (bs, 3H), 2.84 (t, 1H), 2.09-2.20 (m, 2H), 1.76-1.96 (m, 11H), 1.52-1.63 (m, 8H), 1.43-1.47 (m, 1H).

^{13}C NMR (126 MHz, CD$_2$Cl$_2$) δ: 136.09, 131.04, 74.05, 39.87, 39.79, 39.75, 39.72, 39.37, 38.71, 37.37, 37.11, 34.63, 32.68, 32.56, 32.29, 30.78, 30.74, 28.61 (2C), 21.91.

HRMS: *m/z* calcd. for C$_{10}$H$_{28}$OH (M + H)$^+$: 285.221; found (M – H$_2$O)$^+$: 267.2110.

IR: 3356, 2920, 2896, 1606, 1447, 1200, 1061, 1013, 967 cm^{-1}.

m.p: 206-214 °C (Lit.[93] 214-215 °C).

Preparation of compound *rac-9*
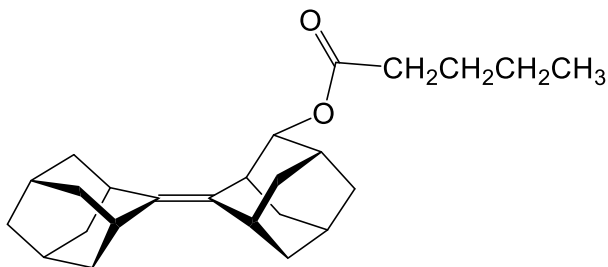
Compound ***rac-6*** (4.25 g, 14.9 mmol) was dissolved in dried THF (400 mL). Absolute pyridine (4.80 mL, 59.8 mmol) was added to the solution and it was stirred for 15 minutes under nitrogen. Pentanoyl chloride (5.40 mL, 44.9 mmol) was added and the resulting mixture was heated under reflux for 3 hours under nitrogen. The reaction mixture was quenched by pouring the mixture onto ice-cold water (100 mL) and brought to pH 7 by addition of 1 M H_2SO_4. This solution was then extracted with hexane (2 x 150 mL), washed with methanol (150 mL), dried over Na_2SO_4 and concentrated in vacuo. The crude compound (4.29 g, 78%) was purified by column chromatography (hexanes: EtOAc, 11:3) to obtain an orange oil of compound ***rac-9*** (3.90 g, 71%).

^{1}H NMR (400 MHz, CDCl$_3$) δ: 4.74 (bs, 1H), 3.00 (bs, 1H), 2.88 (m, 3H), 2.34 (t, 2 H), 2.089-1.37 (m, 26 H), 0.93 (t, 3 H).

^{13}C NMR (126 MHz, CD$_2$Cl$_2$) δ: 173.51, 137.30, 130.74, 77.36, 40.20, 40.15, 40.10, 40.07, 39.61, 37.77, 37.68, 36.42, 35.07, 33.95, 33.14, 32.93, 32.53, 31.94, 31.39, 29.21, 29.17, 28.29, 27.83, 22.92, 14.14.

HRMS: *m/z* calcd. for $C_{25}H_{36}O_2Na$ (M + Na)$^+$: 391.2613; found: 391.2602.

IR: 2900, 2845, 1729, 1600, 1443, 1252, 1168, 1084, 964 cm^{-1}.

Preparation of compound *(-)6*

For this reaction, the crude enzyme Cholesterol Esterase from Porcine pancreas (activity 44 U/mg) was purchased from Lee Biosolutions, Inc.

Compound ***rac-9*** (1.50 g, 4.07 mmol) dissolved in Et_2O (200 mL) was placed in a laboratory blender followed by the addition of crude enzyme cholesterol esterase (44 units) dissolved in 0.1 M Na_2HPO_4 (200 mL) buffer pH 7.3. Sodium taurocholate (30 mg, 0.056 mmol) was added and the mixture was blended at high speed for 5 minutes before being transferred to a 1L round bottom flask. The reaction was then stirred using a mechanical stirrer for 36 hours. The reaction was quenched by the addition of MeOH (300 mL), which resulted in the formation of two layers. The top layer containing the organic phase was collected, washed with brine (150 mL), dried over Na_2SO_4 and concentrated under reduced pressure. The crude mixture was purified by column chromatography (hexanes:EtOAc, 11:3) and recrystallization from MeOH to afford chiral unsaturated alcohol ***(-)6*** (0.124 g, 21%).

^{1}H NMR (400 MHz, $CDCl_3$) δ: 3.47 (t, 1H), 2.88 (bs, 3H), 2.84 (t, 1H), 2.09-2.20 (m, 2H), 1.76-1.96 (m, 11H), 1.52-1.63 (m, 8H), 1.43-1.47 (m, 1H).
^{13}C NMR (151 MHz, CD_2Cl_2) δ: 136.09, 131.04, 74.05, 39.87, 39.79, 39.75, 39.72, 39.37, 38.71, 37.37, 37.11, 34.63, 32.68, 32.56, 32.29, 30.78, 30.74, 28.61 (2C), 21.91.
HRMS: *m/z* calcd. for $C_{10}H_{28}OH$ (M + H)$^+$: 285.221; found (M – H_2O)$^+$: 267.2109.
IR: 3348, 2923, 2888, 1600, 1445, 1200, 1065, 1010, 969 cm^{-1}.
m.p: 197-204 °C.
$[α]_{589}^{20}$ -12.9 (*c* = 1.33, CH_2Cl_2).

Chiral HPLC Traces:

VWD1 A, Wavelength=210 nm (GCHEN\GCHEN_2016-11-10 09-08-09\CHIRAL_000010.D)
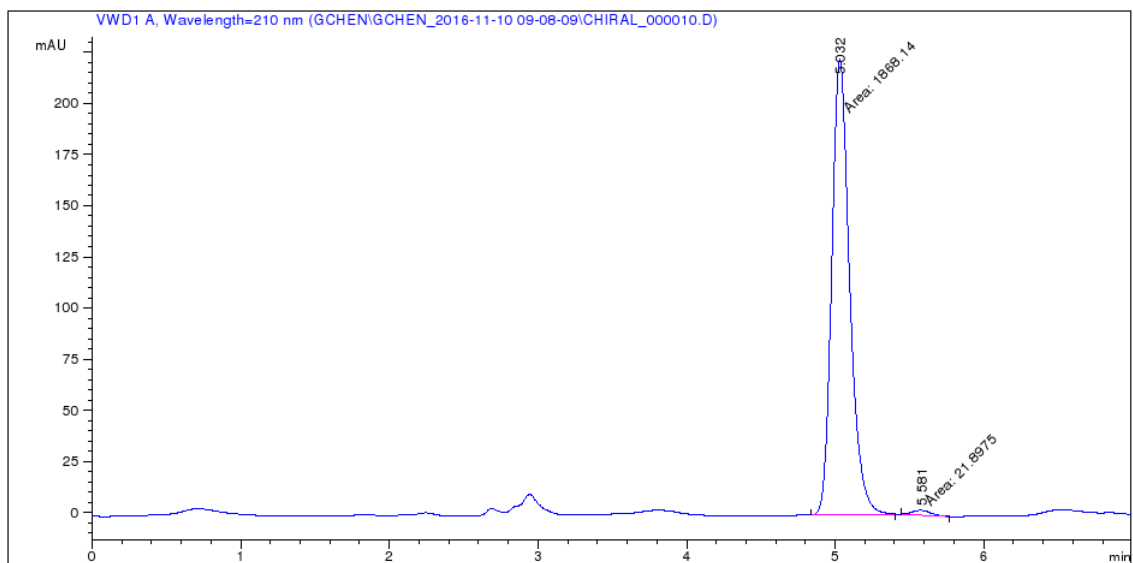
```
========================================================================
                         Area Percent Report
========================================================================


Sorted By            :        Signal
Multiplier           :        1.0000
Dilution             :        1.0000
Use Multiplier & Dilution Factor with ISTDs



Signal 1: VWD1 A, Wavelength=210 nm

Peak RetTime Type  Width      Area        Height      Area
  #    [min]       [min]  mAU    *s    [mAU    ]       %
----|-------|----|-------|----------|----------|--------|
   1   5.032 MM   0.1391 1868.14490  223.85916  98.8414
   2   5.581 MM   0.1499   21.89753    2.43400   1.1586

Totals :                  1890.04242  226.29316
```

Preparation of compound *(+)7*

To a mixture of 50% v/v aqueous H_2SO_4 (15 mL) and acetic acid (25 mL), was added compound *(-)6* (77.0 mg, 0.271 mmol). After heating at 140 °C for 3 hours, the reaction mixture was cooled and poured onto ice water (10 mL) and extracted with CH_2Cl_2

(3 x 15 mL). The combined organic fractions were washed with $NaHCO_3$ (20 mL), brine (20 mL) and dried over Na_2SO_4, filtered and evaporated. The crude product was recrystallized in MeOH to give pure white crystals of *(+)7* (62.0 mg, 81%).

^1H NMR (600 MHz, C_6D_6) δ: 2.66 (bs, 1H), 2.h44 (bs, 1H), 2.11 (bd, 1H), 2.06 (bs, 1H), 1.88 (m,1H), 1.55-1.88 (m, 19H), 1.47-1.54 (m, 2H), 1.40-1.45 (m, 1H), 1.35-1.39 (m, 1H). ^{13}C NMR (151 MHz, C_6D_6) δ: 215.03, 48.81, 47.73, 46.95, 43.68, 40.02, 39.54, 39.34, 38.54, 38.39, 34.11, 31.92, 31.75, 28.38, 28.32, 28.20, 27.93, 27.88, 27.74.
HRMS: *m/z* calcd. for $C_{20}H_{28}OH$ $(M + H)^+$: 285.2218; found: 285.2208.
IR: 2918, 2850, 1710, 1468, 1298, 1075 cm^{-1}.
m.p: 55-58 °C.
$[α]_{589}^{20}$ 19.6 (*c* = 0.29, C_6D_6).

The syntheses of compound *10* from the reduction of ketone *(+)7*, compound *(+)15-(a)* and compound *(+)16-(a)* are the same as for the racemic version *rac 7*, *15-(a)* and *16-(a)*.

Compound *(+)15-(a)*

(12.0 mg, 64% crude mixture, 19% pure compound).

m.p: 52-60 °C.
$[α]_{589}^{20}$ 33.28 (c = 0.19, CH_2Cl_2).

Compound *(+)16-(a)*

(6 mg, 60% crude mixture, 13% pure compound).

$[α]_{589}^{20}$ 5.25 (c = 0.4, CH_2Cl_2).

2.5.3.　X-ray Crystallography

Crystals were covered with Paratone oil, mounted on a MiTe-Gen sample holder, and placed in the cold stream (150 K) of the diffractometer. The temperature was regulated using an Oxford Cryosystems Cryostream Device; compound *17* was collected at 150 K while compounds *(-)6* and *(+)7* were collected at 293 K. All data was collected using a Bruker SMART equipped with an APEX II CCD area detector. The X-ray sources were graphite monochromated Mo Kα (λ = 0.71073 Å) for *(+)7* and Cu Kα (λ = 1.54178 Å) for compounds *(-)6* and *17* radiations. All diffraction data were processed with the Bruker Apex II software suite. All structures were solved with intrinsic phasing method and subsequent refinements were performed using ShelXle. Diagrams were prepared using ORTEP-3[94] and rendered using POV-Ray.[95] The electron density peaks (Q-peaks) for the hydrogen atoms were found and refined. Additional crystallographic information can be found in Appendix D.

Chapter 3.   Probing the Bromonium Ion Catalyzed Rearrangement of Sesquihomoadamantene by ^{1}H NMR Spectroscopy.

3.1. Introduction

The synthetic chemistry of the *bis*-adamantane system was examined in the last chapter, and in this chapter, a kinetic study on a unique reaction with the bromonium ions of Ad=Ad was investigated.

3.1.1.   Bromine Transfer by Bromonium Ions

In 1969, Wynberg and coworkers reported the world's first isolable three membered ring bromonium ion in the form of [AdAdBr]$^+$Br$_3^-$. This bromonium tribromide salt provided valuable information about key mechanistic questions concerning electrophilic addition of bromine such as the possibility that bromine addition to the alkene is reversible and the reactivity of the cationic intermediates.[17, 96, 97] In addition to this, Bennet et *al.,* reported an unprecedented and fast degenerate transfer of bromonium ions between alkenes, i.e. bromine transfer from [AdAdBr]$^+$OTf$^-$ to Ad=Ad (Figure 3.1).[18]
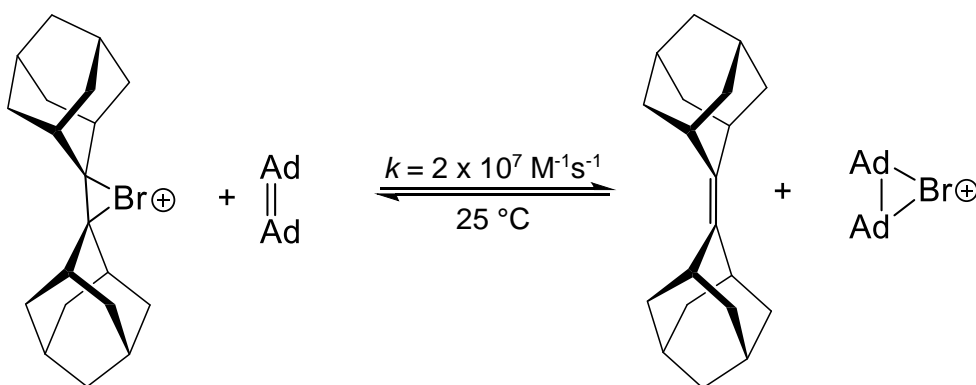
Figure 3.1   Transfer of bromine from a bromonium ion to an acceptor olefin.

Further mechanistic investigations for this transfer of positive halogen ions to acceptor alkenes were carried out by Brown and coworkers.[16] High-level *ab initio* studies were also conducted on an ethene model to probe the "Br⁺" transfer mechanism. A transfer that occurs through an unsymmetrical 1:1 halonium ion:alkene charge transfer complex (CTC) intermediate with a symmetrical D_{2d} transition state (TS) was the lowest energy pathway located by computation (Figure 3.2).[98]
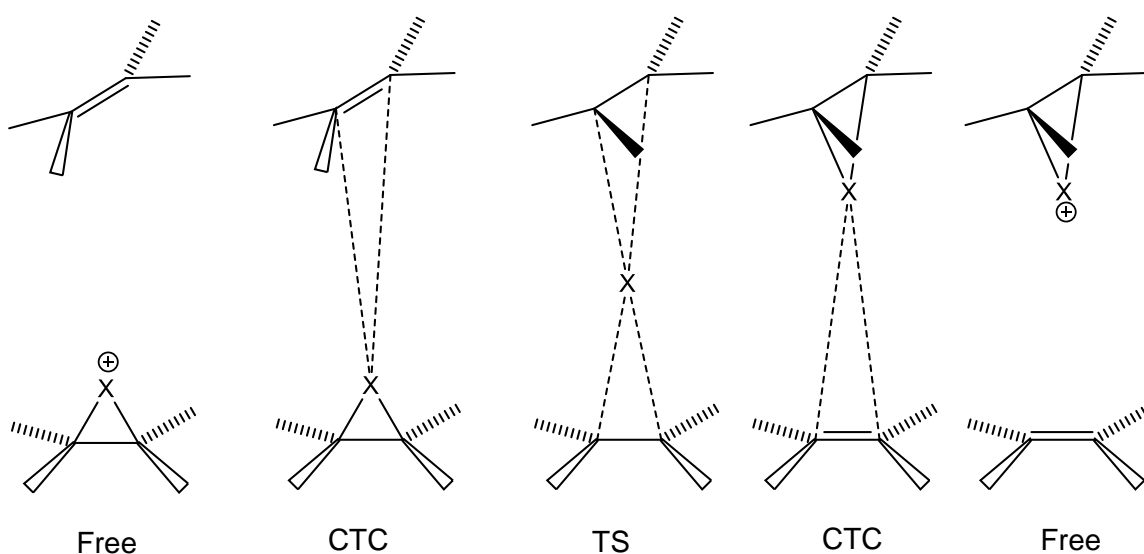
Figure 3.2   Transfer of positive halonium ion "X⁺" to an alkene via a charge transfer complex (CTC).

This "Br⁺" transfer to olefin phenomenon was further confirmed by the work of Rodebaugh and Fraser-Reid on the exchange of bromonium ions formed from a 4-penten-1-yl (*18*) or 5-hexen-1-yl (*19*) glucosides (Figure 3.4).[99] In this investigation, equimolar amounts of the two olefins were reacted with one equivalent of the Br⁺ reagent *N*-bromosuccinimide (NBS). Most of the 5-hexen-1-yl starting material was recovered unchanged while the 4-penten-1-yl material had reacted completely. Importantly, it was noted that separate reactions containing either compound *18* or *19* with NBS reacted at

77

similar rates to give compound **20** or **21**, respectively (Figure 3.3). The authors rationalized these observations by suggesting that bromonium ion transfer between intermediates **18-Br⁺** or **19-Br⁺** and olefins are rapid relative to cyclization and so the products are formed by exclusive channelling of intermediates via the bromonium ion that cyclizes fastest (Figure 3.4). The rate-limiting step for these reactions is transfer of Br⁺ to the olefin, but that subsequent steps are rapid relative to cyclization.[100]
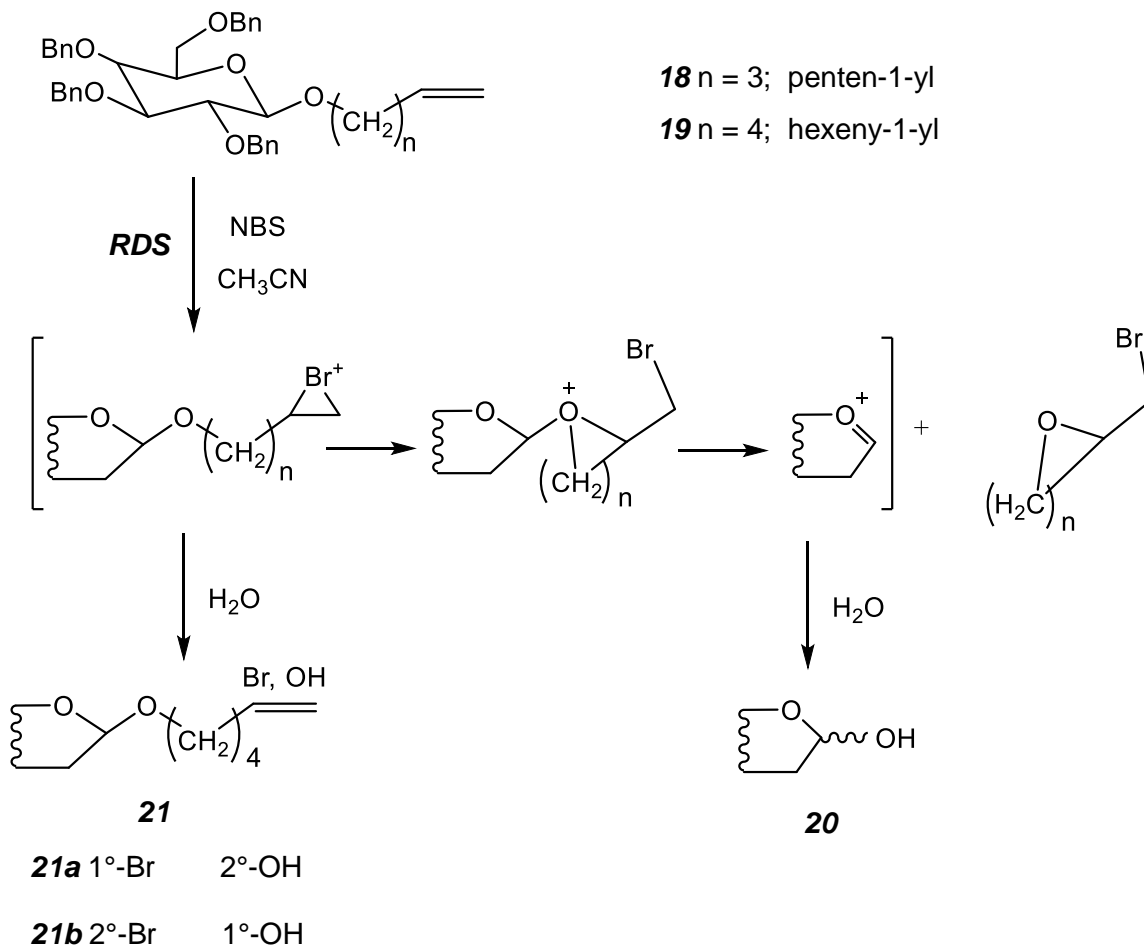
Figure 3.3   Reaction of 4-penten-1-yl (**18**) and 5-hexen-1-yl (**19**) with NBS.
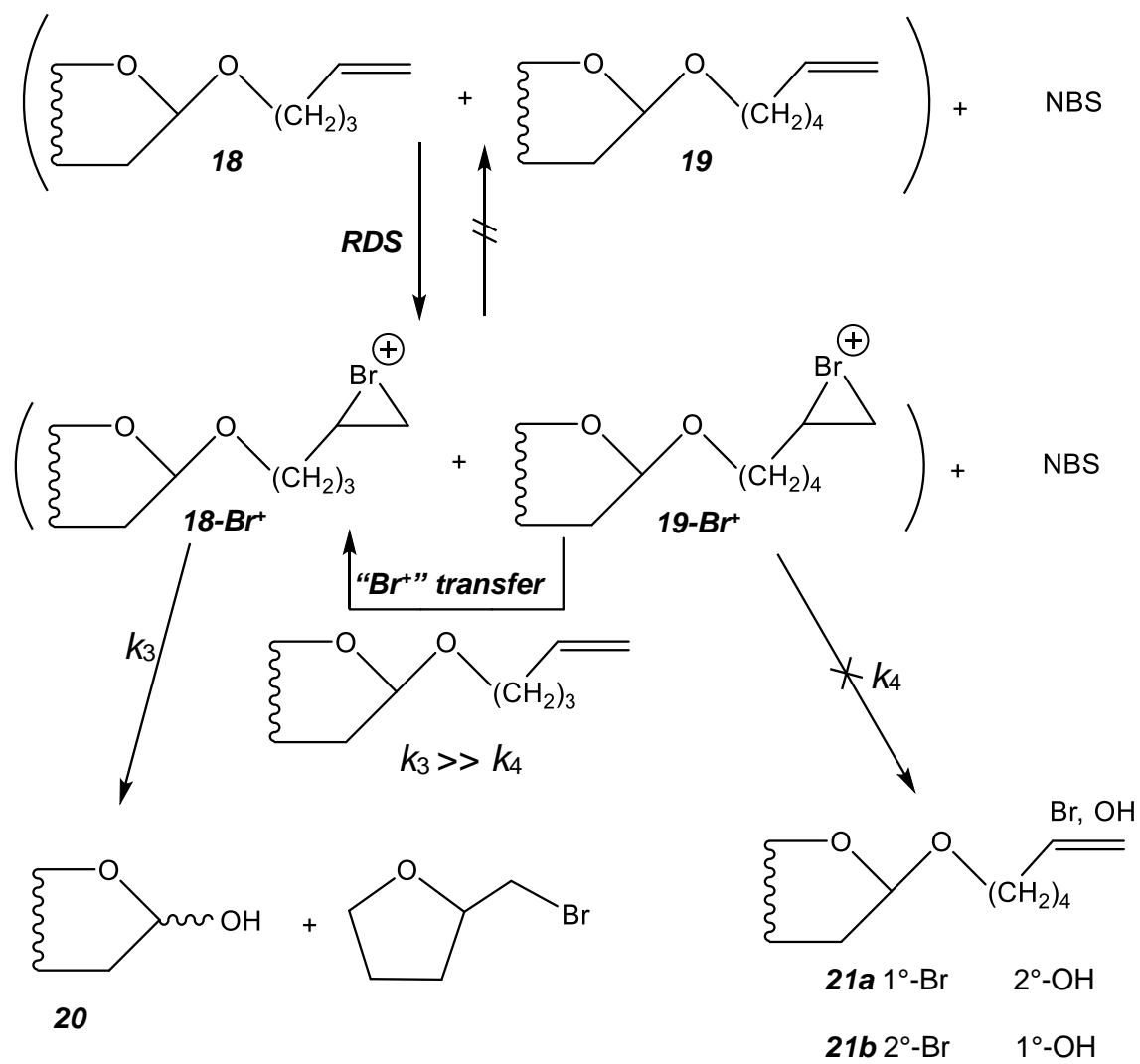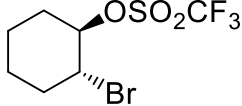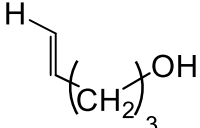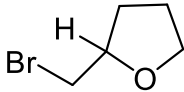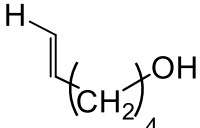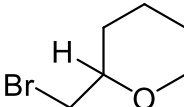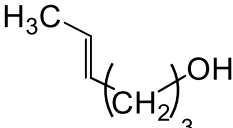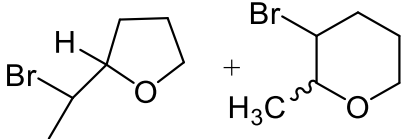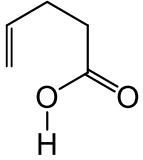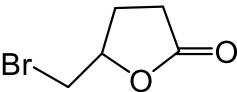
Figure 3.4   Schematic representation of "Br⁺" transfer from the bromonium ion of 5-hexen-1-yl glucoside (**19-Br⁺**) to 5-penten-1-yl glucoside (**18**).

At the same time, Brown *et al.,* showed that halocyclization could also be performed using these halonium ions. They reported the use of [AdAdBr+]CF$_3$SO$_3^-$ as a "Br+" transfer agent with reactive alkenes (Table 3.1) and the bromocyclization of ω-alkene-1-ol was supported with extensive kinetics analysis that provided valuable insights into the above reaction mechanisms (Figure 3.5).[101]

Table 3.1 **Olefins and their corresponding reaction products from reaction with equimolar [AdAdBr]+CF$_3$SO$_3^-$.**

Olefin	Products
22	
23	
24	
25	
26	

Figure 3.5   Postulated pathways for "Br$^+$" transfer and halocyclization.[101]

The above scheme accommodates observations reported by Brown, and coworkers, that is, the product formation can occur via:

a) direct collapse of complex **27** (k_3),

b) dissociation of complex **27** (k_1) into free AdAd and **28** that spontaneously cyclizes (k_2)

c) similar dissociation of complex **27** (k_1) followed by cyclization of **28** that is promoted by a second molecule of olefin (k'_2[ol]).[101]

The critical observations are:

1) For compound **23** as [AdAd] concentration is increased, the reaction rate decreased as Ad=Ad intercepts **28** to reform starting materials via **27**. Further kinetics analysis

demonstrated a dependence on a second molecule of alkene. They further reported the ratio of k_2'/k_{-1} = 0.57 which ruled out the spontaneous break down of **28** (k_2). Hence, formation of product occurs by dissociation of **28** in presence of a second molecule of olefin **23** (k'_2[ol]), which acts as a general base to deprotonate **28** during cyclization.[101]

2) For compound **24**, **25** and cyclohexene (**22**), it was observed with a high concentration of Ad=Ad, the reaction is not fully suppressed such that now K_{eq} and k_3 is of kinetic significance with a direct cyclization from complex **27** (k_3).[101]

Based on the above observations, the authors concluded that rate of "Br+" transfer k_{-1}, from **28** to Ad=Ad, should be as fast or faster than the "Br+" transfer from [AdAdBr]+ to Ad=Ad.[101] Consequently, the rapid step k_{-1} competes and also assists in the kinetic diagnostic of the fast cyclization and deprotonation steps of **28**.[101]

3.1.2.   Sesquihomoadamantene and its Reactivity

Sesquihomoadamantene (SesquiAdAd) is a white crystalline solid, consisting of a tetrasubstituted double bond with rigid cyclic substituents including two seven-membered rings (Figure 3.6).[9] SesquiAdAd (**3**) was first prepared in 1970 by Wynberg *et al.,* via the Lewis acid catalyzed rearrangement of spiro[adamantane-2,4'-homoadamantan-5'-ol], which occurred simultaneously with formation of the isomeric Ad=Ad.[9, 10]

3
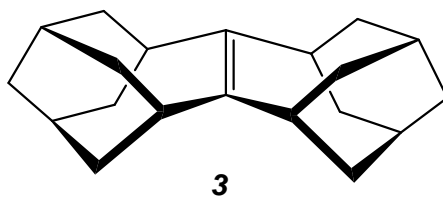
Figure 3.6   Structure of Sesquihomoadamantene (SesquiAdAd).

The reactivity of the highly strained SesquiAdAd towards epoxidation and electrophilic addition reactions was investigated. This constitutional isomer of Ad=Ad was shown to be inert to singlet oxygen ($^1O_2$) epoxidation[102] but reacted, albeit slowly, with m-chloroperbenzoic acid (mCPBA) to give the corresponding epoxide (**29**) (Figure 3.7).[24, 102]
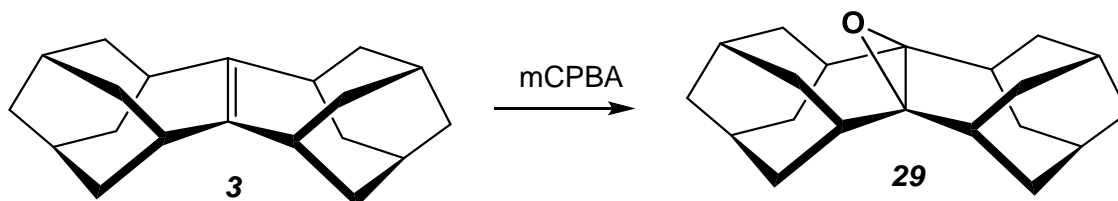
Figure 3.7   Epoxidation of SesquiAdAd with mCPBA.

Furthermore, studies by Gills *et al*, revealed that no reaction was observed when SesquiAdAd was exposed to Br_2 in CCl_4.[10] However, Rathore and coworkers reported that this alkene was reactive towards only three electrophilic agents, notably Brønsted acids, the nitrosonium cation and dichlorine.[23]

In the case of Brønsted acids, it was observed that upon exposure to strong acids in CH_2Cl_2 at −78 °C, SesquiAdAd undergoes a rapid isomerization to give Ad=Ad. These authors further reported that this isomerization takes place in weak acids at room temperature. The authors rationalized that the facile acid-catalyzed rearrangement of SesquiAdAd to Ad=Ad is driven by the relief of strain present in the seven-membered rings.[23]

In addition to this, it was found that SesquiAdAd reacted with nitrosonium ion via an electron transfer process to form the cation radical of SesquiAdAd (SA[+]) (**30**) and the latter was inert to prolonged exposure to dioxygen (Figure 3.8).[23]
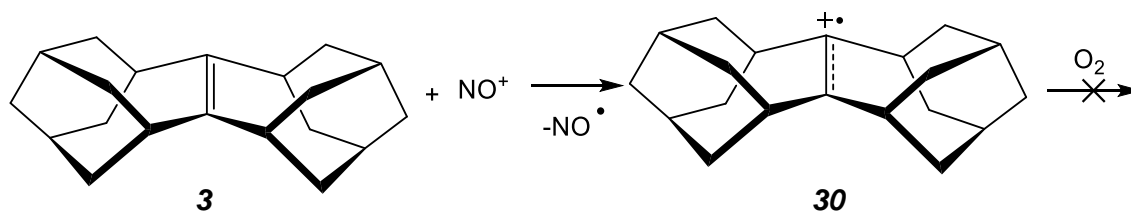
Figure 3.8   Formation of a cation radical of SesquiAdAd and its inertness to dioxygen.[23]

The authors also investigated the chlorination of SesquiAdAd and found that despite prolonged exposure to either antimony pentachloride or sulphuryl chloride at high temperatures, no reaction occurred. However, they found out that when SesquiAdAd was allowed to react with Cl_2 at –78 °C, selective homoallylic chlorinations was detected similar to the reactivity profile of Ad=Ad with electrophilic chlorine reagents (Figure 3.9).[23]
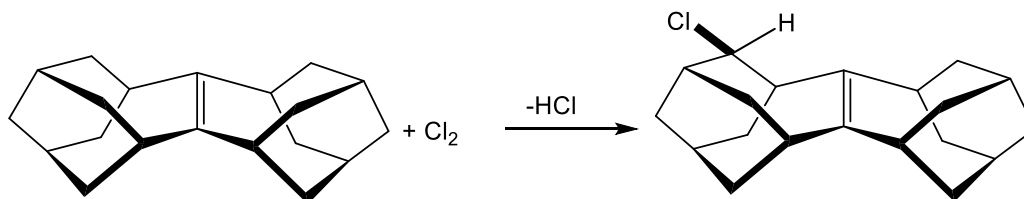
Figure 3.9   Homoallylic chlorination of SesquiAdAd.[23]

Initial Observation

Based on some unpublished results in the Bennet group, the bromonium ion of AdAd (**8**) was unexpectedly formed (Figure 3.10) when SesquiAdAd was reacted with bromine in the presence of Na[B(3,5-$(CF_3)_2$Ph)$_4$].
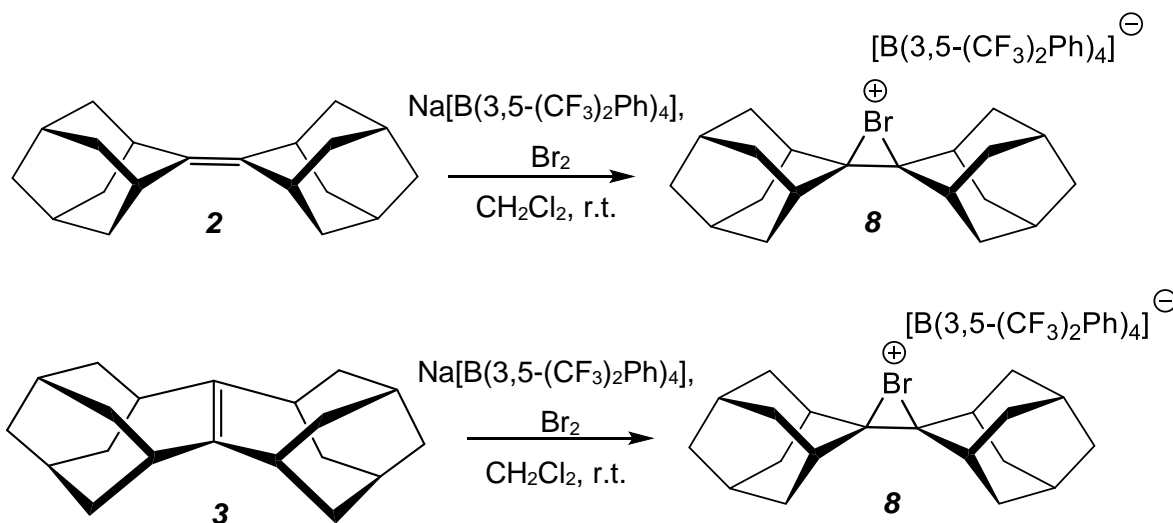
Figure 3.10   Formation of [AdAdBr$^+$][BAr$_F$] from SesquiAdAd.

Given the extensive aforementioned background, this remarkable observation raised several questions about the potential formation of a high energy intermediate of bromonium ion of SesquiAdAd and the rate at which the skeletal rearrangement occurs to give the isomeric bromonium ion.

3.1.3. Objective

The observation made in the Bennet group led to the design of this research project with the aim to probe the mechanistic rearrangement of SesquiAdAd into Ad=Ad catalyzed by [AdAdBr⁺][BArF]⁻. For this purpose, kinetic studies are important and were performed by using ^{1}H NMR spectroscopy. Figure 3.11 represents the proposed mechanism and rate law for this bromonium ion catalyzed rearrangement.

Of note, given that I had access to compound **12**, one of the intermediates required in the course of the preparation of the molecules in chapter two (Figure 2.13), and the skills set acquired on the *bis*-adamantane system, addressing this mechanistic question was an attractive target.

$$k_{obs} = \frac{k_1 k_2 [AB]}{k_{-1}[A] + k_2}$$
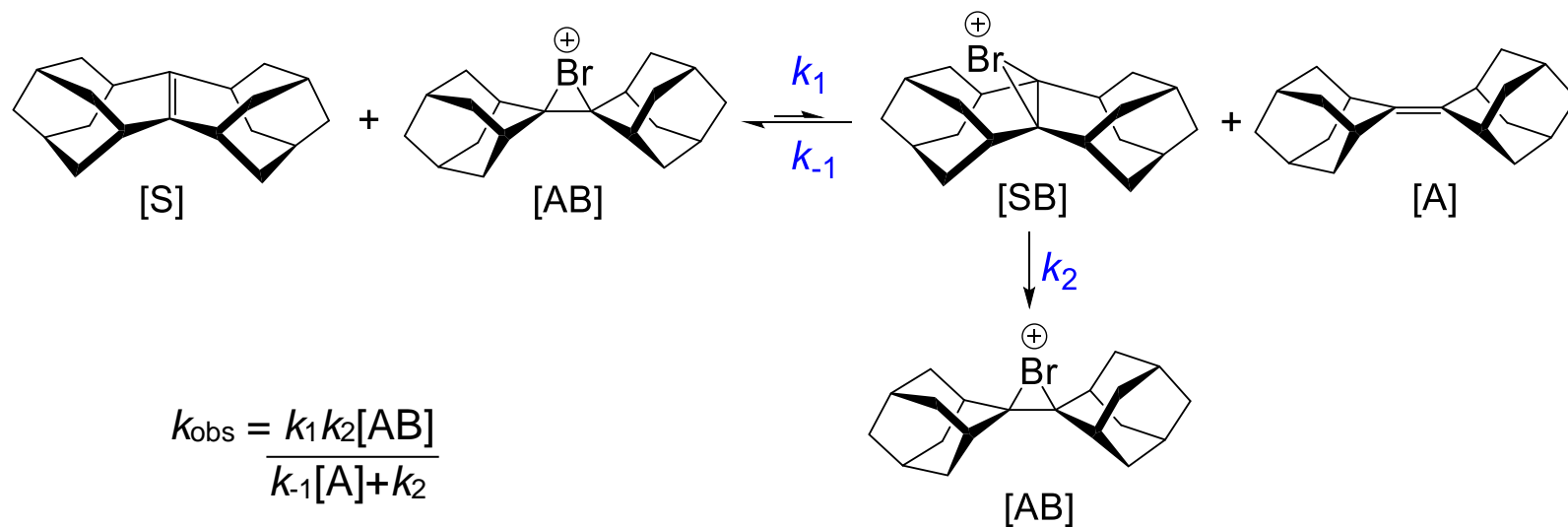
Figure 3.11   Proposed mechanism and rate law for the rearrangement of Sesquihomoadamentene [S] catalyzed by bromonium ion [AB].

Key:

Adamantylideneadamantane: Ad=Ad or A or **2**

Sesquihomoadamantene: SesquiAdAd or S or **3**

Bromonium ion of Ad=Ad: [AdAdBr⁺] or AB

Bromonium ion of SesquiAdAd: [SesquiAdAdBr⁺] or [SB]

3.2. Results and Discussion

3.2.1.   Preparation of Starting Materials

Adamantylideneadamantane (**2**), Sesquihomoadamantene (**3**) and [AdAdBr]⁺Br₃⁻ (**5**) were synthesized according to literature procedures (Figure 3.12).[80, 103] Compound **3** was then transformed to give [AdAdBr]⁺[B(C₆F₅)₄]⁻ (**8**).

The [B(C₆F₅)₄]⁻ anion was used rather than B(3,5-(CF₃)₂Ph)₄⁻[103, 104] as studies have shown that the former anion is more resistant to oxidation.[20, 104, 105] Of note, these bromonium ions are strong oxidising agents and are able to oxidize many metal centres.[20]

Compound **1** was subjected to a pinacol coupling reaction to afford **12**, which was subsequently treated with strong acids to give the rearranged pinacolone product **14**. Upon reduction with LiAlH₄, compound **14** was transformed into alcohol **31**. Treatment of compound **31** with an acidic dehydrating agent such as P₂O₅/H₃PO₄ led to a 3:1 mixture of Ad=Ad (**2**):SesquiAdAd (**3**). The separation of these alkene isomers was effected on basis of their reactivity towards bromine. Ad=Ad reacted readily with Br₂ to form an orange precipitate of [AdAdBr]⁺Br₃⁻ (**5**) and upon filtration sesquiAdAd (**3**) was isolated. Compound **5** was then subjected to anion replacement by the addition of KB(Ar_F)₄ (Ar_F= C₆F₅⁻) to afford [AdAdBr]⁺[B(C₆F₅)₄]⁻ (**8**), a reaction that is driven by the precipitation of KBr.
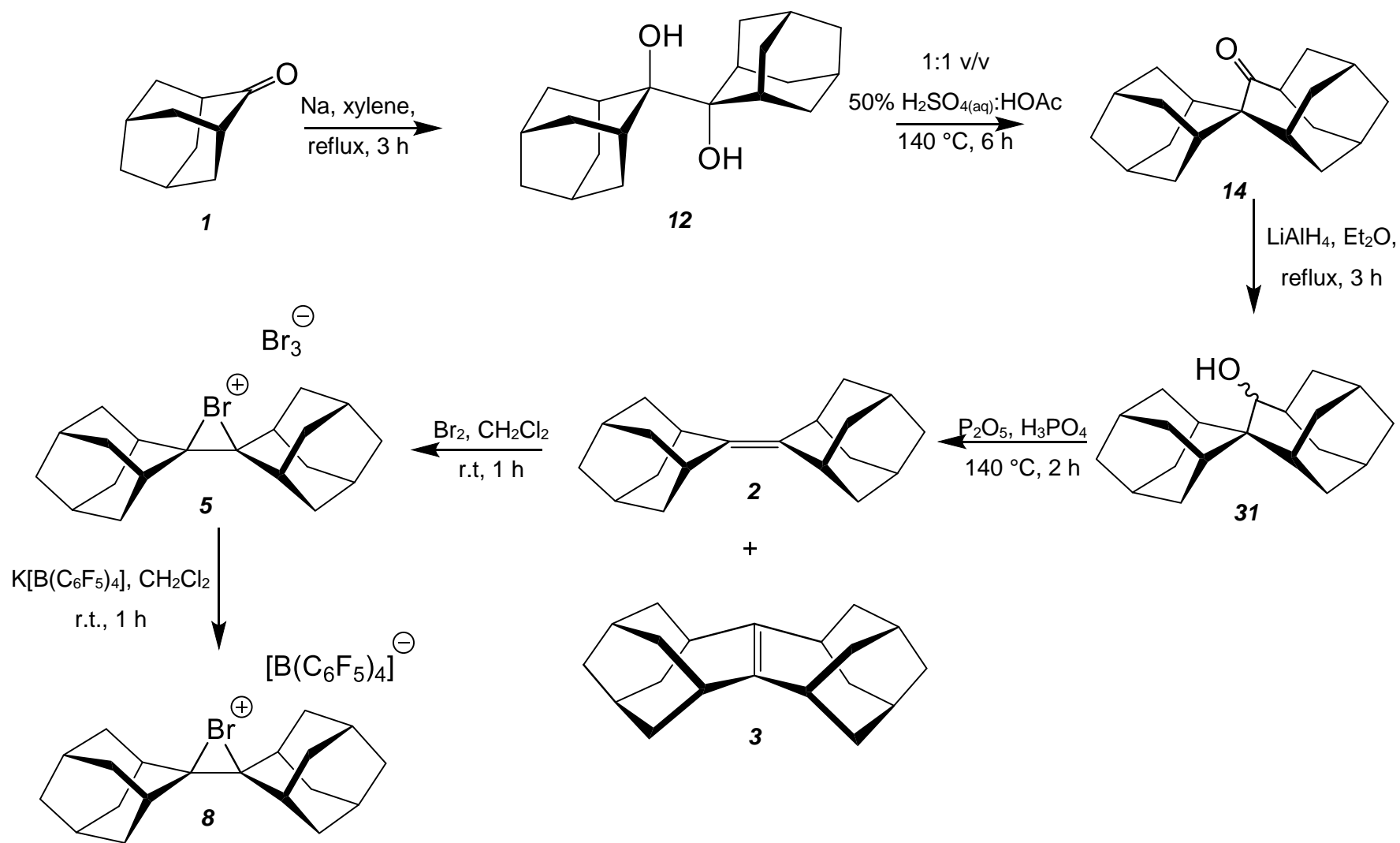
Figure 3.12   Synthetic route for SesquiAdAd, Ad=Ad, [AdAdBr]⁺[BАrF4]⁻.

3.2.2. Kinetics Experiment Protocol

Acquisition of ^{1}H NMR Spectra

All ^{1}H NMR spectra were acquired on a Bruker AVANCE II spectrometer equipped with a 5 mm TCI cryoprobe and operating at 600 MHz. The reactions were conducted in a standard NMR tube at 298 K. CD_2Cl_2 was used as NMR solvent for spectral field locking. Manual shimming was carried out to obtain peaks fitting closely to a Lorentzian curve with good signal to noise ratio.

In a typical experiment, Ad=Ad dissolved in CD_2Cl_2 (300 µL) and $[AdAdBr]^+[BAr_F]^-$ in CD_2Cl_2 (200 µL) were placed in a standard NMR tube followed by the addition of 1,2-dichloroethane (0.2 µL) as the internal standard (IS). Prior to the addition of sesquiAdAd, manual shimming was performed to obtain optimal Lorentzian peaks and great signal to noise ratio. After the acquisition of one ^{1}H NMR spectrum, the sample was removed from the NMR magnet and sesquiAdAd dissolved in CD_2Cl_2 (70 µL) was added and shaken before placing the tube back into the magnet. Re-shimming of the magnetic probe and re-tuning of the probe were performed. More than 50 quantitative proton decoupled NMR spectra were acquired consecutively.

Analysis of the ^{1}H NMR Spectra

The reaction was monitored by the disappearance of the peak at 2.14 ppm, which is assigned to SesquiAdAd (Figure 3.13 & 3.14). However, a minor impurity that exhibited a singlet was observed at 2.12 ppm which partially overlapped with the SesquiAdAd peak (Figure 3.14). We attributed this impurity peak to acetone but it was surprisingly challenging to minimize acetone contamination, given that it appears that SesquiAdAd retains acetone even at very low levels.
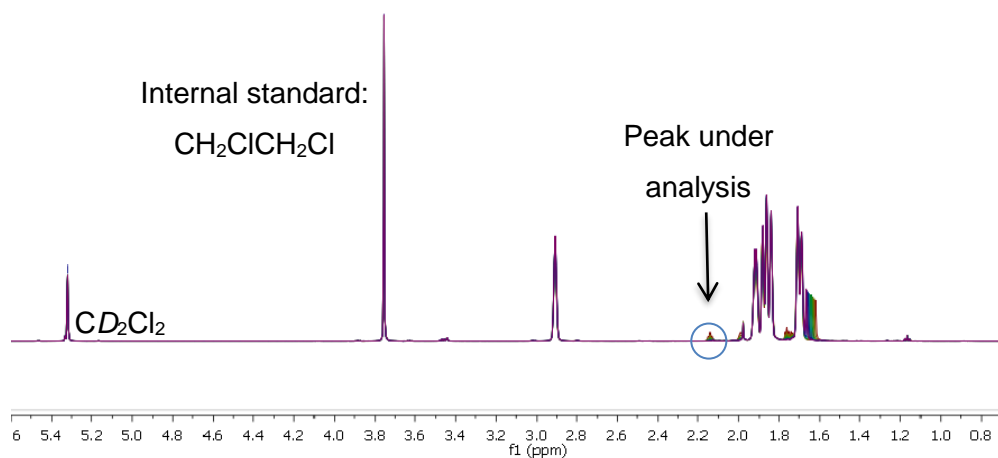
Figure 3.13   ¹H NMR spectrum of a typical reaction mixture containing Ad=Ad, [AdAdBr]⁺[BАr_F]⁻ and SesquiAdAd.
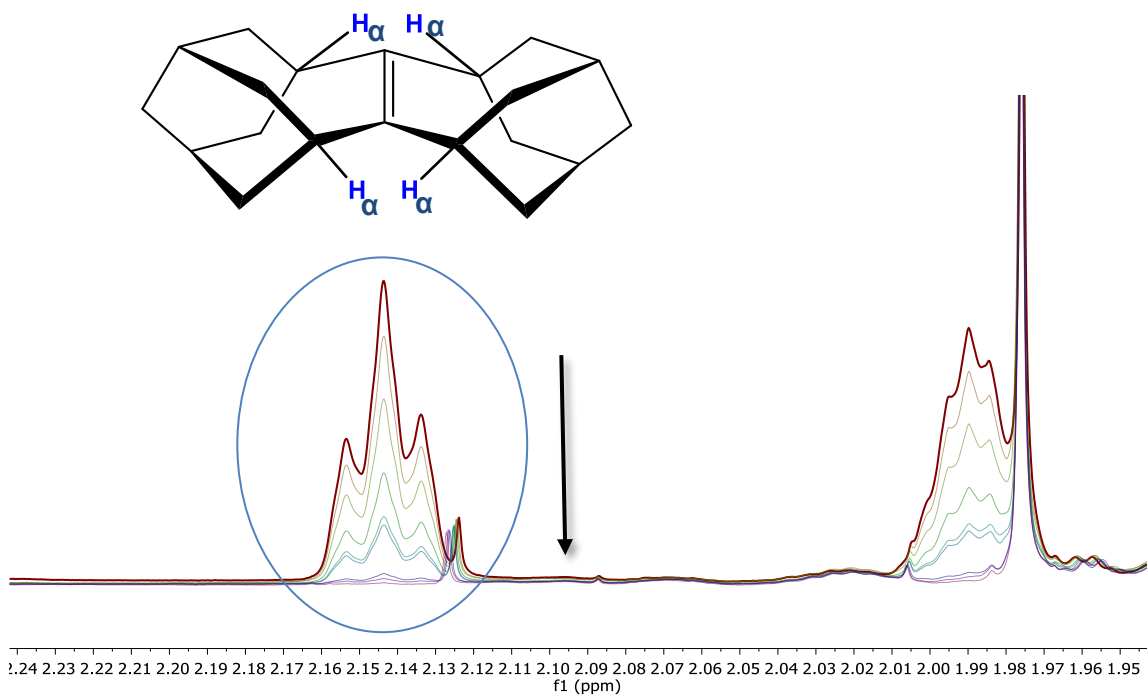
Figure 3.14   Monitoring the disappearance of SesquiAdAd peaks over time by ¹H NMR spectroscopy.

Deconvolution of ^{1}H NMR Spectra

Deconvolution of the SesquiAdAd peaks was required in order to obtain accurate integrals as a function of time. The following procedures were carried out:

a) A minimum of six spectra ranging from the beginning to the end of the experiment were chosen.

b) All spectra were phased and baseline corrected manually using the Mestrenova version 9.1 software.[106]

c) Calibration of the chemical shift scale with reference to CD_2Cl_2 peaks were set at 5.32 ppm.

d) The sesquiAdAd peaks including the impurity singlet peak, were further subjected to a multipoint baseline correction before performing a global spectral deconvolution (GSD) (Figure 3.15). The deconvolution involved line fitting the peaks by adjusting the following parametres: chemical shift, height, width and optimal Lorentzian to Gaussian ratio (L/G) (Figures 3.15 & 3.17).
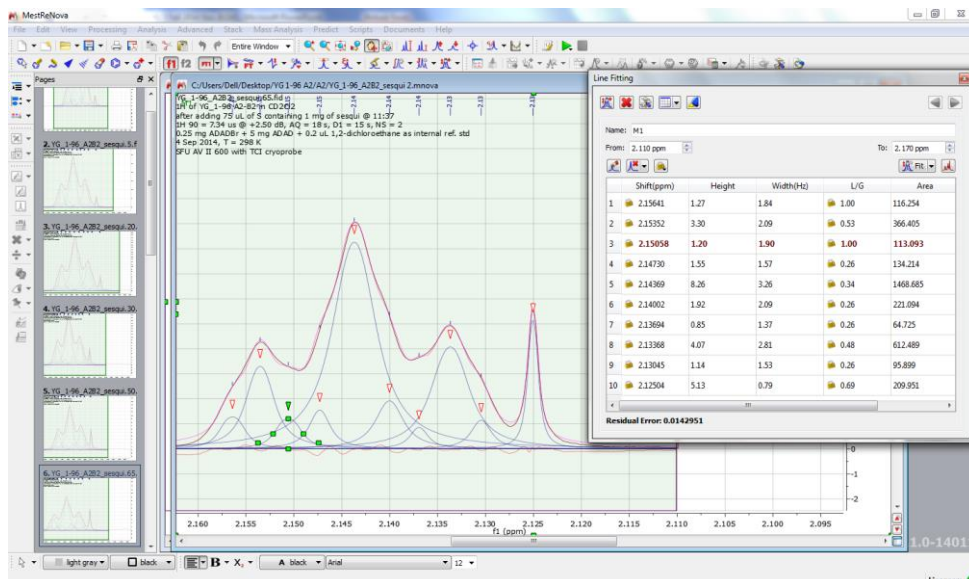
Figure 3.15   Global spectral deconvolution of the sesquiAdAd peaks.

e) Figure 3.16 shows the fitting of the peaks after deconvolution where the red, magnenta and navy lines represent the residuals (goodness of fit), sum of the spectrum and peaks respectively.
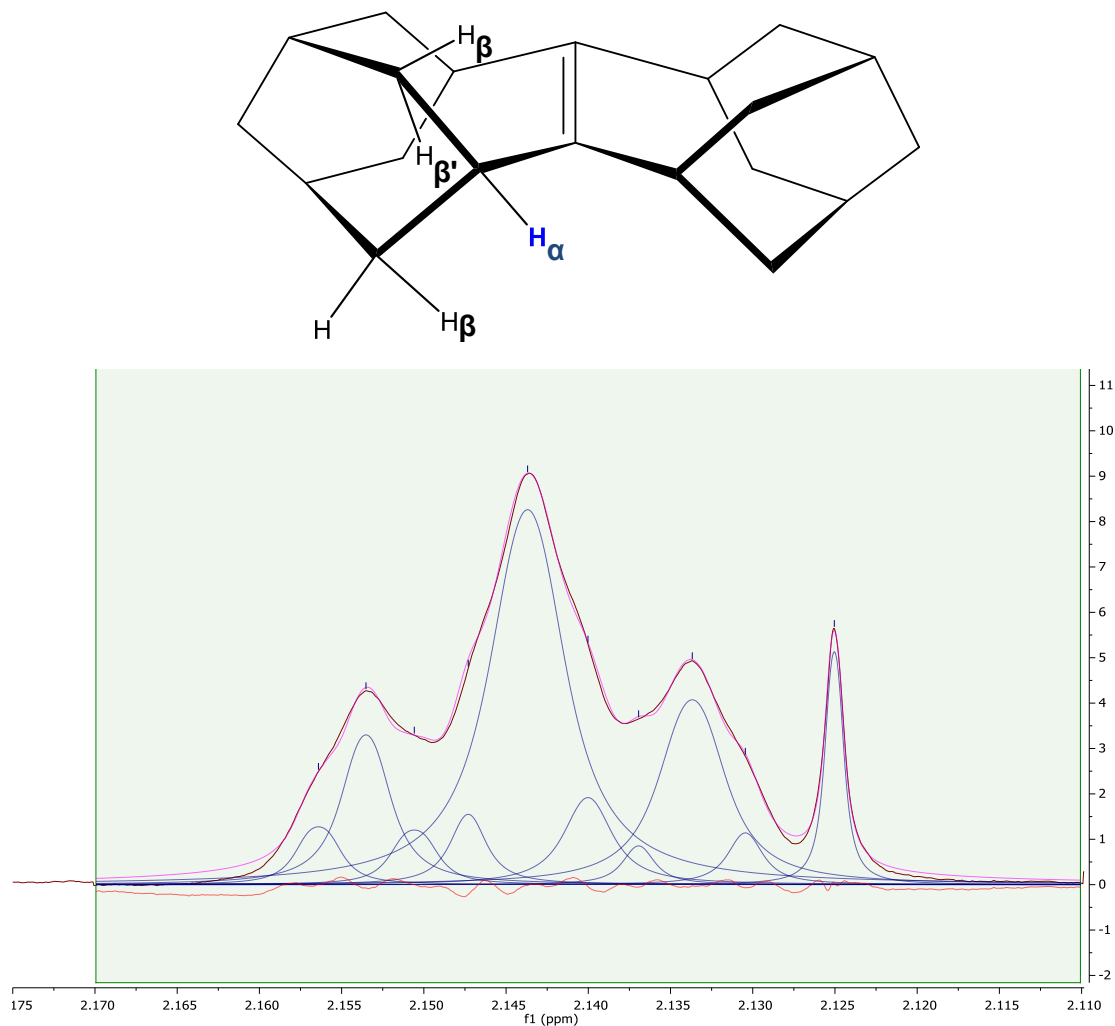
Figure 3.16   Deconvoluted sesquiAdAd peaks.

f) The protons that are being monitored are the H_α nuclei (Figure 3.14 & 3.16, Appendix B), which are adjacent to the double bond. The multiplicity should be a quintet due to the presence of two neighbouring –CH_2 but the hydrogens, notably **H_β and $H_{\beta'}$**, on the CH_2 are different from each other. As such, a triplet of triplets (*tt*) should be observed, which is the result of coupling with two protons with one J value and two protons with another J value. However, from

the deconvoluted peaks (Figure 3.16) and the integrals (Figure 3.17), we deduced that the multiplicity is not a triplet of triplets. This observation can be rationalized by the presence of a second-order effect[107] in the coupling pattern. As a result, the general appearance, chemical shift and multiplicity are affected but the overall integrals of the peaks under analysis do not suffer. Furthermore, line fitting by using a deconvolution protocol takes care of this phenomenon.

g) The resulted integration of SesquiAdAd peaks was determined by the summation of the individual deconvoluted peaks corresponding to SesquiAdAd, that is total area of peaks 1 to 9 (Figure 3.17). The last peak (10) on the deconvolution chart refers to the singlet peak from the impurity which was not considered in the analysis beyond this point.

Line Fitting

Name: M1

From: 2.110 ppm   To: 2.170 ppm

Fit

	Shift(ppm)	Height	Width(Hz)	L/G	Area
1	2.15641	1.27	1.84	1.00	116.254
2	2.15352	3.30	2.09	0.53	366.405
3	2.15058	1.20	1.90	1.00	113.093
4	2.14730	1.55	1.57	0.26	134.214
5	2.14369	8.26	3.26	0.34	1468.685
6	2.14002	1.92	2.09	0.26	221.094
7	2.13694	0.85	1.37	0.26	64.725
8	2.13368	4.07	2.81	0.48	612.489
9	2.13045	1.14	1.53	0.26	95.899
10	2.12504	5.13	0.79	0.69	209.951

Residual Error: 0.0142951

Figure 3.17   Line fitting chart of the deconvoluted peaks and the individual integrals under the curve of the peaks.

h) The internal standard 1,2-dichloroethane peaks of the above corresponding spectra (step a) were also deconvoluted. (Same procedure as in step (d)-(e)). The integration of the internal standard was obtained by the summation of the area of all the individual peaks of the deconvoluted internal standard.

i) The SesquiAdAd peaks were normalized by dividing the area of SesquiAdAd by the area of the internal standard for the same corresponding spectrum (Table 3.2).

Table 3.2   Normalized SesquiAdAd peaks with respect to time of reaction.

Integrals of SesquiAdAd (10^3)	Integrals of IS (10^3)	Ratio of the integral of SesquiAdAd/IS	Time/s (10^3)
10.9	12.9	0.845	0
10.3	13.3	0.774	0.371
8.16	13.1	0.623	1.50
6.81	13.0	0.524	2.26
4.63	12.9	0.359	3.76
3.19	13.1	0.243	4.87
2.24	13.2	0.170	6.00
1.26	13.1	0.0962	7.49

Determination of k_{obs}

The ratio of integrals for the alkene and the internal standard SesquiAdAd/IS against time was fit to a standard first-order rate equation by using a non-linear least squares fit from *Prism 5* software (Table 3.2 & Figure 3.18) and a k_{obs} value was calculated. All fits had r^2 values greater than 0.99.
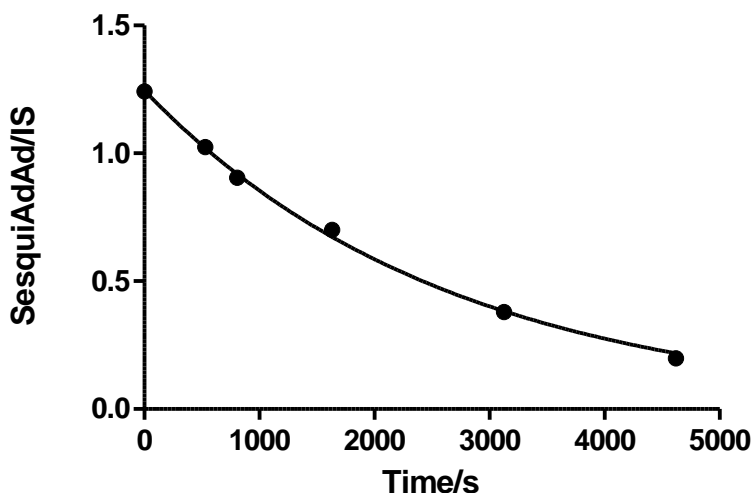
Figure 3.18   Plot obtained (Prism 5 software) from the fitting of experimental data of SesquiAdAd/IS versus time during the rearrangement reaction.

A set of 15 experiments were conducted with different concentrations of Ad=Ad, SesquiAdAd and [AdAdBr]$^+$[BAr$_F$]$^-$ (Table 3.3) at 298.15 K. The rate constant k_{obs} for each experiment was determined as per the above procedure (steps (a)-(h)).

Table 3.3 The rate constant 10^{-4} x k_{obs} / s^{-1} for different concentrations of Ad=Ad, SesquiAdAd and [AdAdBr]$^+$[BAr$_F$]$^-$.

	[AdAdBr]$^+$(1) / mM 0.212	[AdAdBr]$^+$(2) / mM 0.424	[AdAdBr]$^+$(3) / mM 0.847	[AdAdBr]$^+$(4) / mM 1.27	
[Ad=Ad](1) / mM 16.2	3.77 ± 0.11[1]	6.44 ± 0.12	12.4 ± 0.8	Reaction too fast	[SesquiAdAd](1) / mM 3.24
[Ad=Ad](2) / mM 32.4	1.62 ± 0.08	2.49 ± 0.13	6.64 ± 0.17	9.41 ± 0.27	[SesquiAdAd](2) / mM 6.48
[Ad=Ad](3) / mM 48.6	8.98 ± 0.48	6.94 ± 0.08	Technical[2]	10 ± 0.83	[SesquiAdAd](2) / mM 6.48
[Ad=Ad](4) / mM 64.8	5.94 ± 0.41	6.60 ± 0.32	2.33 ± 0.9	17.9 ± 0.59	[SesquiAdAd](2) / mM 6.48

[1] Four different concentrations of [AdAdBr]$^+$[BAr$_F$]$^-$ and [Ad=Ad] along with two different concentrations of [SesquiAdAd] were studied and the rate constant for the corresponding combination of [AdAdBr]$^+$[BAr$_F$]$^-$, [Ad=Ad] and [SesquiAdAd] are recorded. A typical example is entry 3.77 ± 0.11 which represents the observed rate constant (10^{-4} x k_{obs} / s^{-1}) in a kinetic run that contained 0.212 mM [AdAdBr]$^+$[BAr$_F$]$^-$, 16.2 mM [Ad=Ad] and 3.24 mM [SesquiAdAd].

[2] Kinetic run containing [Ad=Ad](3) and [AdAdBr]$^+$(3) was not performed due to technical problem.

Derivation of the Rate Law
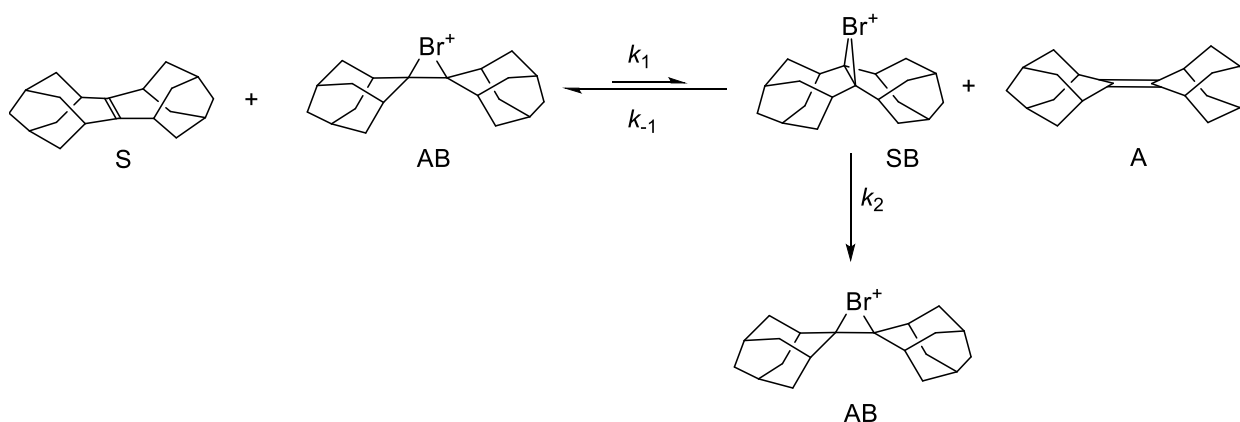
The rate law for this bromonium ion catalyzed rearrangement was determined (Appendix D-Detailed derivation) as follows:

When equilibration is rapid and reversible i.e., the reaction is performed in the presence of excess Ad=Ad:

$$K_{eq} = \frac{[A][SB]}{[S][AB]} = \frac{k_1}{k_{-1}}, \quad \text{and} \quad \frac{d[P]}{dt} = k_2[SB], \quad [SB] = \frac{K_{eq}[S][AB]}{[A]}$$

$$[S]_0 = [S] + [SB] + [P], \quad \text{if} \quad [A]_0 \gg [S]_0 \quad \text{then} \quad [A]_0 \approx [A]_0 + [P]$$

$$[S]_0 - [S] - [SB] = [P], \quad \text{but} \quad [S] = \frac{[A][SB]}{K_{eq}[AB]} \quad \rightarrow \quad [P] = [S]_0 - \frac{[SB]([A] + K_{eq}[AB])}{K_{eq}[AB]}$$

$$[SB] = \frac{K_{eq}[AB]}{[A] + K_{eq}[AB]} \times ([S]_0 - [P]), \quad \text{and} \quad [S]_0 = [P]_\infty$$

$$\frac{d[P]}{dt} = \frac{k_2 K_{eq}[AB]}{[A] + K_{eq}[AB]} \times ([P]_\infty - P_0), \quad \text{therefore} \quad k_{obs} = \frac{k_2 K_{eq}[AB]}{[A] + K_{eq}[AB]}$$

If on the other hand we assume that SB is a high energy intermediate then:

$$\frac{d[A]}{dt} = k_1[S][AB] - k_{-1}[SB][A]$$

$$\frac{d[SB]}{dt} = 0 = k_1[S][AB] - k_{-1}[SB][A] - k_2[SB], \text{ then } [SB] = \frac{k_1[S][AB]}{k_{-1}[A] + k_2}$$

$$\frac{d[A]}{dt} = \frac{k_1[S][AB](k_{-1}[A] + k_2)}{k_{-1}[A] + k_2} - \frac{k_1 k_{-1}[A][S][AB]}{k_{-1}[A] + k_2} = \frac{k_1 k_2[S][AB]}{k_{-1}[A] + k_2}, \text{ so } k_{obs} = \frac{k_1 k_2[AB]}{k_{-1}[A] + k_2}$$

Under conditions of rapid equilibration and if SB [sesquiAdAdBr$^+$] is a high energy intermediate then the same rate law is obtained for both mechanism.

$$k_{obs} = \frac{k_2 K_{eq}[AB]}{[A] + K_{eq}[AB]}, \text{ if } K_{eq}[AB] \ll [A] \text{ then } k_{obs} = \frac{k_2 K_{eq}[AB]}{[A]}$$

$$k_{obs} = \frac{k_1 k_2[AB]}{k_{-1}[A] + k_2}, \text{ if } k_{-1}[A] \gg k_2, \text{ then } k_{obs} = \frac{k_1 k_2[AB]}{k_{-1}[A]} = \frac{k_2 K_{eq}[AB]}{[A]}$$

$k_{obs} = \frac{k_2 K_{eq}[AB]}{[A]}$ is obtained in both cases for rapid equilibrium and high energy intermediate under the assumptions of an excess of [A] and $k_2 << k_{-1}[A]$ respectively, that is, we have a high energy intermediate of [SB] with a rapid equilibrium of the bromonium ions.

Verification of the Rate Law

In order to check whether the predicted rate equation for this mechanistic hypothesis was consistent with the measured kinetic data, the rate law was verified by plotting the rate constant k_{obs} with bromonium ion; [AB] and Ad=Ad; [A] where the former is expected to be first order to [AB] and the latter zero order to [A].

A plot of bromonium ion concentration and k_{obs} was constructed (Figure 3.19). For the two lowest Ad=Ad concentration ([Ad=Ad](1) & [Ad=Ad](2)), a linear correlation is observed. Whereas, at high concentration of Ad=Ad, we observed a deviation from the linear correlation. A plausible explanation for this observation might be the aggregation of Ad=Ad at these high concentrations. As such, it will be necessary to conduct our kinetic studies at lower concentrations of Ad=Ad.
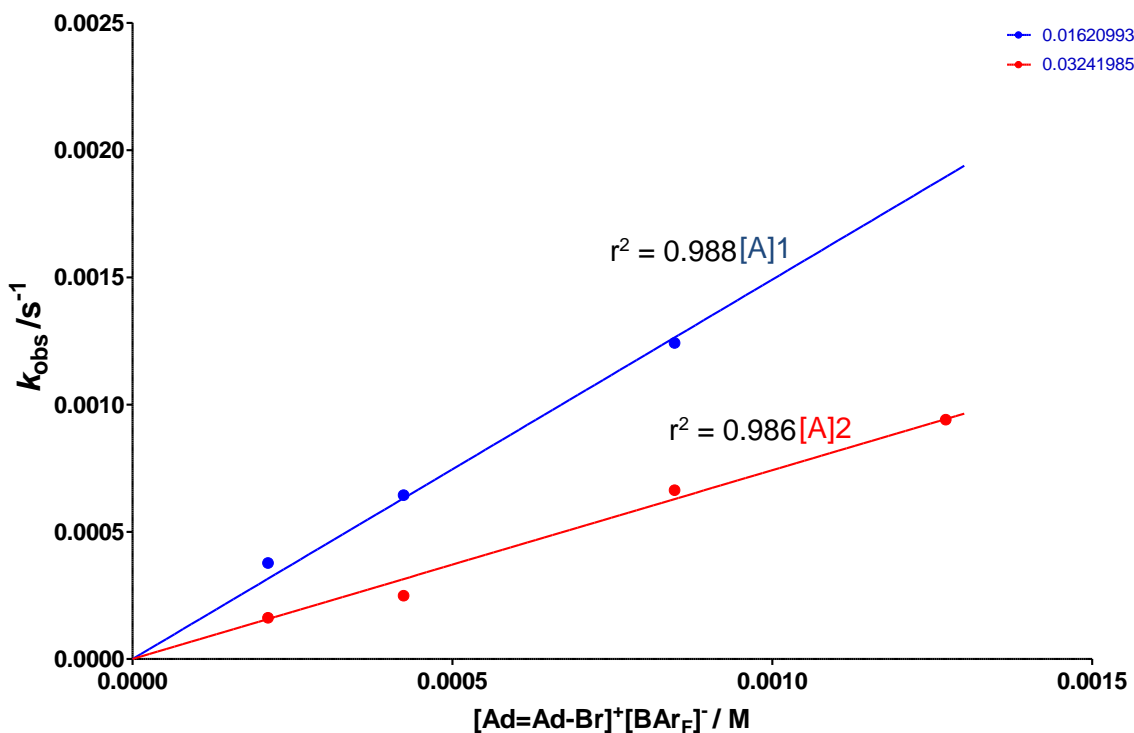
Figure 3.19   Global fit for k_{obs}/s^{-1} versus [AdAdBr]$^+$[BAr$_F$]$^-$; [AB]/M for concentrations of Ad=Ad;[A]1 and [A]2.

Moreover, the second order rate constant from bromonium ion catalysis is reduced as the concentration of Ad=Ad increases, in line with what is expected from the rate law.

Based on this kinetic data, it is proposed that there is a "Br$^+$" transfer from [AdAdBr]$^+$[B(C$_6$F$_5$)$_4$]$^-$ to form the high energy intermediate SesquiAdAdBr$^+$ (Figure 3.20), which then undergoes a skeletal rearrangement to [AdAdBr]$^+$ as shown in Figure 3.21.
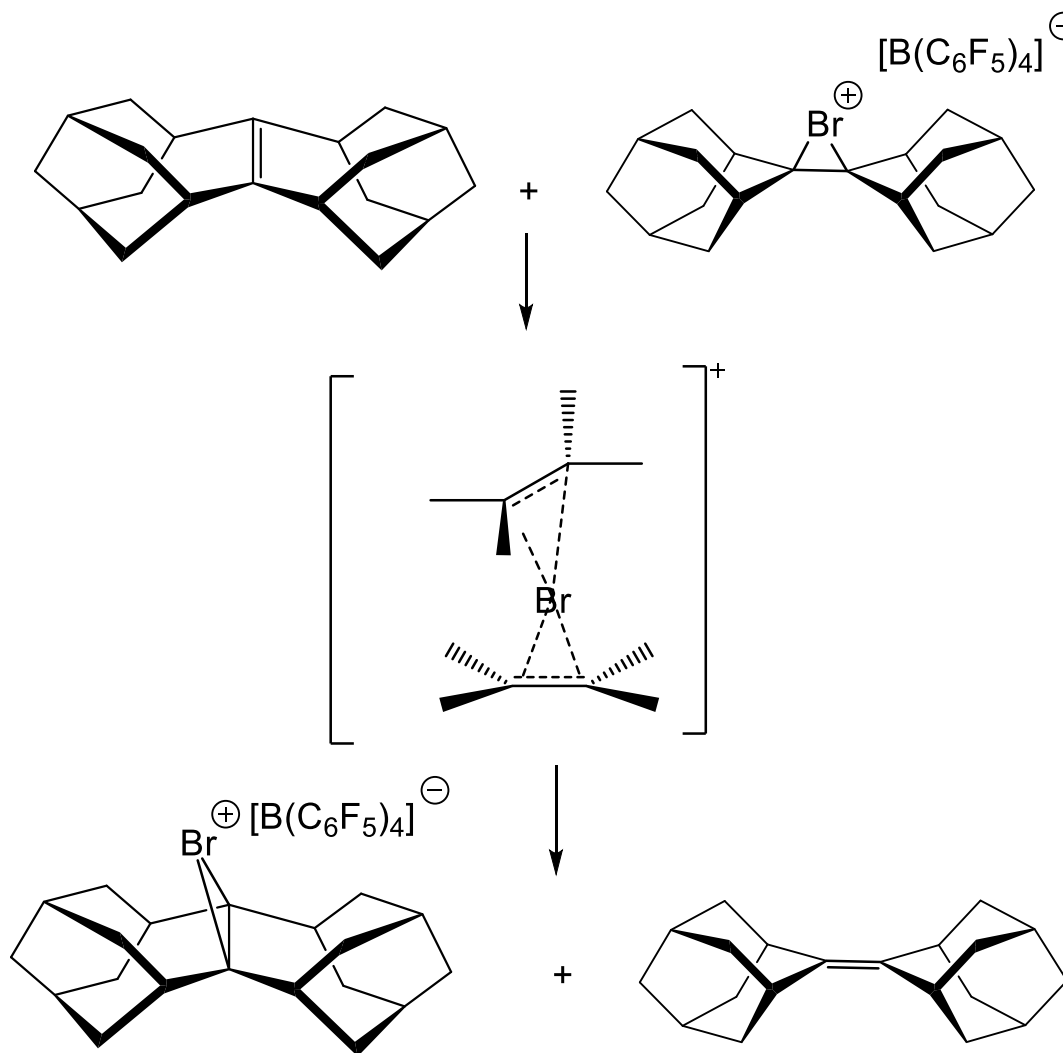
Figure 3.20   "Br$^+$" transfer to the free alkene SesquiAdAd.
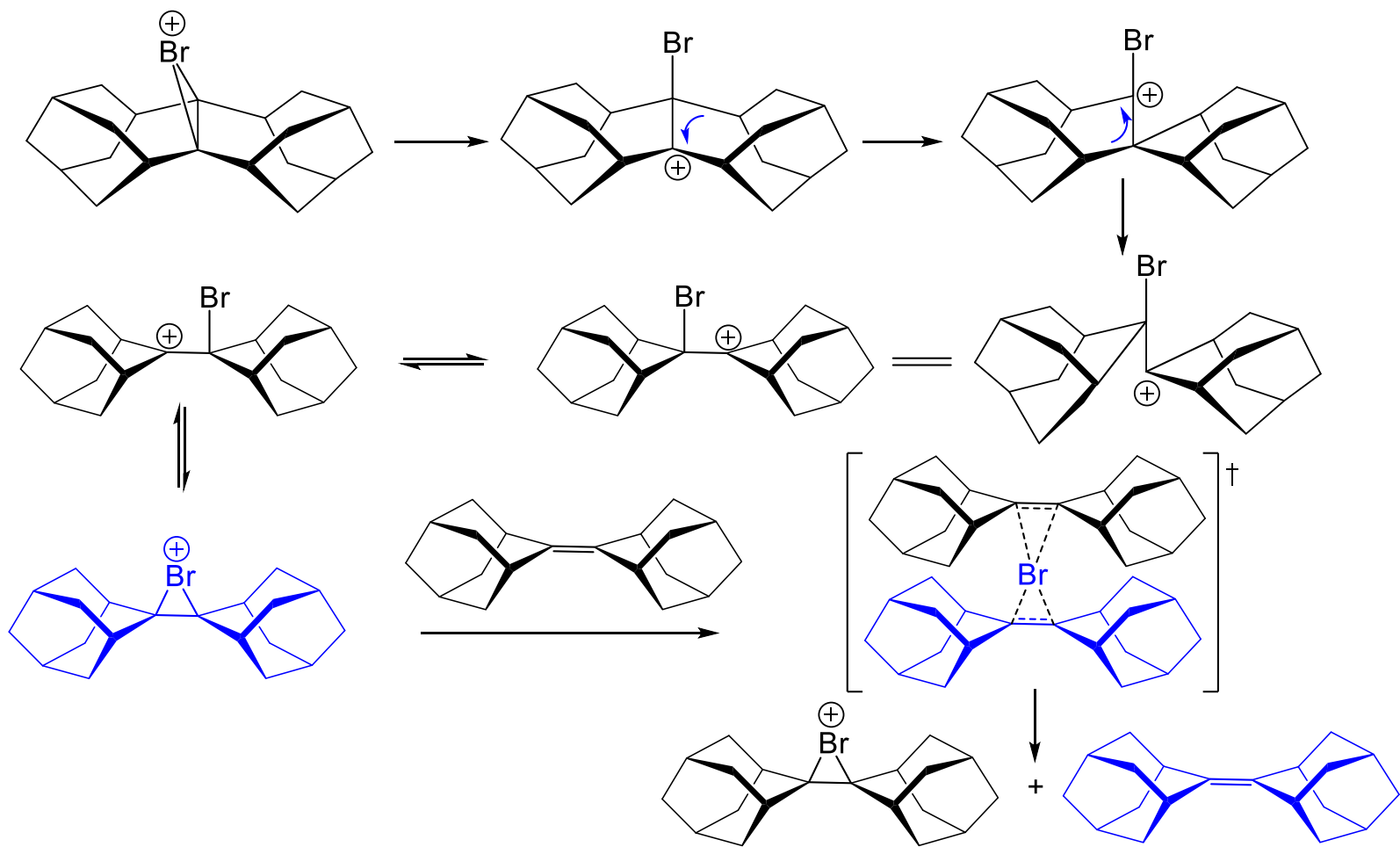
Figure 3.21   The proposed mechanistic rearrangement of SesquiAdAdBr⁺; [SB] to [AdAdBr⁺]; [AB] via a "Br⁺" transfer to Ad=Ad; [A].

From the above proposed rearrangement mechanism, we expect that there will be a "Br$^+$" transfer from the rearranged bromonium ion to the free Ad=Ad present to form the free Ad=Ad and [AdAdBr$^+$] respectively. Since [Ad=Ad] is in excess, this "Br$^+$" transfer is dependent on the rearranged bromonium ions and consequently should be zero order in [Ad=Ad].

3.3. Future Work and Conclusion

The main objective of this project was to probe the potential formation of the high energy intermediate sesquiAdAdBr$^+$ and the rate at which the skeletal rearrangement occurs to form Ad=Ad. As such, the starting materials were synthesized and the reaction was followed by ^{1}H NMR spectroscopy. Due to an impurity peak overlapping with the peaks under analysis, it was necessary to deconvolute the spectra. Preliminary results showed a reaction first order in bromonium ions at low concentrations of Ad=Ad at 25°C. More kinetic runs need to be performed at lower concentration of Ad=Ad to confidently support a first order dependence on bromonium ions and a zero dependence on Ad=Ad. Also, this rearrangement reaction will need to be conducted and monitored at different temperatures to determine the kinetic parameters.

3.4. Experimental

3.4.1. General Remarks

General procedures and materials are as described in Chapter 2. Potassium *Tetrakis*(pentafluorophenyl)borate was purchased as a white powder from *Boulder Scientific Company.*

3.4.2. Synthesis and Experimental Data

Synthesis of compound 14
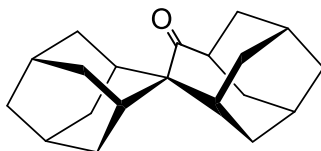
To a mixture of 50% v/v aqueous H_2SO_4 (250 mL) and acetic acid (250 mL) was added compound **12** (5.00 g, 16.5 mmol). After heating for 6 h at 110 °C, the reaction mixture was cooled, poured onto ice water (150 mL) and resulting mixture was extracted with CH_2Cl_2 (3 x 150 mL). The combined organic layer was washed with saturated $NaHCO_3$ (250 mL), brine (250 mL), dried over Na_2SO_4 and evaporated. The crude product was recrystallized from MeOH and hexanes to give pure white crystals of compound **14** (3.81 g, 81%).

^{1}H NMR (400 MHz, CDCl$_3$) δ: 2.70 (m, 1H), 2.52 (m, 3H), 2.12 (m, 24H).

^{13}C NMR (101 MHz, CD$_2$Cl$_2$) δ: δ 220.27, 58.30, 51.51, 40.11, 37.63, 35.72(2C), 34.96(2C), 34.27(2C), 32.80 (2C), 31.43 (2C), 30.53, 28.07, 27.95, 27.3 (2C).

HRMS: *m/z* calcd. for $C_{10}H_{28}ONa$ (M + Na)$^+$: 307.4292; found: 302.2032.

IR: 2899, 2849, 1715, 1450, 1393, 1245 cm^{-1}.

m.p: 174-176 °C (lit.[81] 176-178 °C).

Synthesis of compound 31
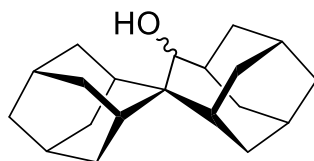
A solution of **14** (12.5 g, 47.9 mmol) dissolved in Et_2O (180 mL) was added dropwise to a stirred slurry of $LiAlH_4$ (1.82 g, 48 mmol) in dried Et_2O (45 mL). After refluxing for 3 hours, the reaction mixture was cooled to room temperature and quenched with EtOAc (100 mL), water (100 mL) and 2 M HCl (100 mL). The organic layer was separated and washed with H_2O (150 mL) and saturated aqueous $NaHCO_3$ (100 mL). The ethereal layer was dried with Na_2SO_4 and concentrated under reduced pressure to afford a white solid (10.9 g, 87%). The crude product was purified by recrystallization from 1:2 hexane-CH_2Cl_2 to obtain the pure alcohol **31** (10.6 g, 84%).

^{1}H NMR (400 MHz, $CDCl_3$) δ: 4.13 (d, J = 5 Hz, 1H), 2.63 – 2.49 (m, 2H), 2.34 – 1.39 (m, 27H).

^{13}C NMR (101 MHz, $CDCl_3$) δ: 79.06, 47.64, 40.81, 40.06, 38.26, 36.58, 35.94, 34.91, 34.90, 33.01, 32.59, 32.33, 32.27, 31.99, 31.06, 29.86, 27.71, 27.61, 27.52, 27.43.

HRMS: m/z calcd. for $C_{20}H_{30}OH$ $(M + H)^+$: 287.2369; found $(M – H_2O)^+$: 269.2266.

IR: 3399, 2896, 2839, 1443, 1215, 1081, 990 cm^{-1}.

m.p: 186-190 °C (lit.[9] 189-192 °C).

Synthesis of SesquiAdAd (3)
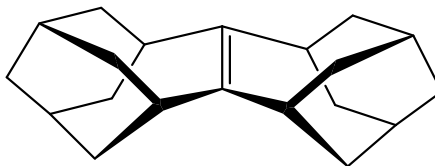
P_2O_5 (14.0 g, 493 mmol) was added portionwise to 14.7 M H_3PO_4 (40 mL) at 0 °C followed by compound **32** (10.0 g, 34.9 mmol). The reaction mixture was heated at 140 °C for 2 hours. The reaction was cooled down and poured onto ice and the precipitate was

extracted using hexanes (3 x 20 mL). The organic layer was washed with H_2O (30 mL), saturated aqueous $Na_2S_2O_3$ (30 mL) and brine (30 mL). It was then dried over Na_2SO_4 and concentrated in vacuo to obtain 9.40 g of a 3:1 mixture of adamantylideneadamantane (**2**) and sesquihomoadamantene (**3**). The mixture was then dissolved in minimum CH_2Cl_2 (200 mL) and an excess of liquid bromine was added dropwise at 0 °C until a dark orange precipitate was obtained, which was stirred for one hour. The resulting precipitate **5** was filtered. The filtrate was extracted with $Na_2S_2O_3$ (100 mL), dried over Na_2SO_4 and evaporated to give crude product **3** (2.10 g, 23%). The crude product was eluted through Florisil with hexanes and recrystallized in acetone to give (1.50 g, 16%) of pure compound **3**.

^{1}H NMR (500 MHz, CDCl$_3$) δ: 2.14 (m, 4H), 1.99 (m, 4 H), 1.88-1.66 (m, 20H).

^{13}C NMR (101 MHz, CDCl$_3$) δ: 149.22, 43.52, 36.77, 35.28, 29.26.

Anal. Calcd for $C_{20}H_{28}$: C: 89.49; H: 10.51. Found: C: 89.46; H: 9.96.

IR: 2906, 2889, 1610, 1436, 1262, 1020 cm^{-1}.

m.p: 197-202 °C (lit.[9] m.p. 199-201 °C).

Synthesis of [AdAdBr]$^+$[BArF]$^-$ (8)
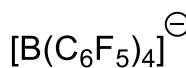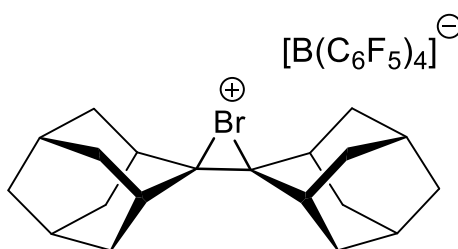
Compound **3** (4.50 g, 7.71 mmol) was dissolved in distilled CH_2Cl_2 (400 mL). $K[B(C_6F_5)_4]$ (5.53 g, 7.71 mmol) was added slowly at room temperature and the reaction mixture was stirred for one hour. The solution was then filtered and the filtrate was evaporated under reduced pressure. A small amount of distilled CH_2Cl_2 (5 mL) was added to obtain a concentrated solution followed by the addition of an excess of hexanes. A beige powder of [AdAdBr]$^+$[B(C$_6$F$_5$)$_4$]$^-$ (**8**) was precipitated out and collected by filtration (7.20 g,

91%). This crude product was crystallized from CH_2Cl_2 by a slow evaporation to afford pure compound **8** (6.64 g, 84%).

^{1}H NMR (500 MHz, CDCl$_3$) δ: 2.14 (m, 4H), 1.99 (m, 4 H), 1.88-1.66 (m, 20H).
Anal. Calcd for $C_{20}H_{28}$: C: 51.46; H: 2.75. Found: C: 51.50; H: 2.40.

Synthesis of Ad=Ad (2)
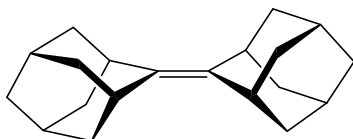
Compound **3** (4.50 g, 7.71 mmol) was dissolved in methanol (500 mL) and the solution was heated under reflux. Cyclohexene (1.60 mL, 15.4 mmol) was added dropwise to the reaction mixture until the orange solution faded. The solution was cooled down and white crystals of Ad=Ad (2.03 g, 98%) formed, was collected by filtration. Further recrystallization in methanol was carried out to afford pure compound **2** (1.76 g, 85%).

^{1}H NMR (400 MHz, CDCl$_3$) δ: 2.90 (s, 4 H), 1.92 (s, 4 H), 1.83-1.86 (m, 12 H), 1.67-1.69 (m, 8 H).
^{13}C NMR (101 MHz, CDCl$_3$) δ: 133.46, 39.8, 37.54, 32.08, 28.74.
Anal. Calcd for $C_{20}H_{28}$: C: 89.49%; H: 10.51%. Found: C: 89.46%; H: 9.96%.
IR: 2902, 2889, 1600, 1450, 1205, 1094 cm^{-1}.
m.p: 185- 186 °C (Lit.[15] 181-182 °C).

3.4.3.   Preparation of Solutions for Kinetics

CD$_2$Cl$_2$ solvent was purchased from Cambridge Isotope Laboratories. The internal reference 1,2-dichloroethane and CD$_2$Cl$_2$ solvents were dried over 4 Å molecular sieves under nitrogen atmosphere. Efforts were made to work under moisture-free conditions as far as possible. The use of glovebox at this point was limited due to the involvement of halogenated solvents.

Stock solutions for different concentrations of Ad=Ad, [AdAdBr]$^+$[B(Ar$_F$)$_4$]$^-$ and SesquiAdAd were prepared:

Ad=Ad ([A])

Four stock solutions of different concentration (Table 3.4) of Ad=Ad were prepared. A typical procedure for preparation of Ad=Ad stock solution of concentration 31.1 mM was as follows:

16.7 mg of Ad=Ad was added to a 2 mL volumetric flask followed by the addition of dried CD_2Cl_2 under nitrogen. The solution was mixed to obtain a homogenous solution and the flask was then capped and wrapped with parafilm.

Table 3.4   Different concentrations of [Ad=Ad] stock solutions.

[Ad=Ad]; [A]	Mass/mg	Concentration /mM
[A]1	16.7	31.1
[A]2	33.3	62.1
[A]3	50.0	93.2
[A]4	66.7	124

[AdAdBr]⁺[B(Ar_F)₄]⁻ ([AB])

The procedure for the preparation of the stock solution was the same as for [Ad=Ad] and solution of four different concentrations of [AdAdBr]⁺[B(Ar_F)₄]⁻ were prepared (Table 3.5).

Table 3.5   Different concentrations of [AdAdBr]⁺[B(Ar_F)₄]⁻ stock solutions.

[AdAdBr]⁺[B(Ar_F)₄]⁻; [AB]	Mass/mg	Concentration /mM
[AB]1	1.25	0.609
[AB]2	2.50	1.22
[AB]3	5.00	2.44
[AB]4	7.50	3.65

SesquiAdAd ([S])

The procedure for the preparation of the stock solution was the same as for [Ad=Ad] and solution of two different concentrations of SesquiAdAd were prepared (Table 3.6).

Table 3.6   Different concentrations of [SesquiAdAd] stock solutions.

[SesquiAdAd]; [AB]	Mass/mg	Concentration /mM
[S]1	26.7	24.9
[S]2	13.3	49.7

References

1.   Fort, R. C.; Schleyer, P. v. R., *Chem. Rev.* **1964**, *64*, 277-300.

2.   Kirchen, R. P.; Sorensen, T. S.; Whitworth. S. M., *Can. J. Chem.* **1993**, *71*, 2016-2027.

3.   Schleyer, P. v. R., *J. Am. Chem. Soc.* **1957**, *79,* 3292.

4.   Landa, S.; Macháček, V., *Collect. Czech. Chem. Commun.* **1933**, *5,* 1-5.

5.   Barton, D. H. R.; Doller, D., *Acc. Chem. Res.* **1992**, *25*, 504-512.

6.   Bone, J. A.; Pritt, J. R.; Whiting, M. C., *J. Chem. Soc., Perkin Trans. 1* **1972**, 2644-2647.

7.   McKervey, M. A., *Chem. Soc. Rev.* **1974**, *3,* 479-512.

8.   Strating, J.; Scharp, J.; Wynberg, H., *Recl. Trav. Chim. Pays-Bas* **1970**, *89*, 23-31.

9.   Boelema, E.; Wynberg, H.; Strating, J., *Tetrahedron Lett.* **1971**, *12*, 4029-4032.

10.   Gill, G. B.; Hands, D., *Tetrahedron Lett.* **1971**, *12*, 181-184.

11.   McMurry, J. E., *Acc. Chem. Res.* **1983**, *16*, 405-411.

12.   Meijer, E. W.; Kellogg, R. M.; Wynberg, H., *J. Org. Chem.* **1982**, *47*, 2005-2009.

13.   Bolster, J.; Kellogg, R. M.; Meijer, E. W.; Wynberg, H., *Tetrahedron Lett.* **1979**, *20*, 285-286.

14.   Huang, X.; Batchelor, R. J.; Einstein, F. W. B.; Bennet, A. J., *J. Org. Chem.* **1994**, *59*, 7108-7116.

15.   Strating, J.; Wieringa, J. H.; Wynberg, H., *J. Chem. Soc., Chem. Commun.* **1969**, 907-908.

16.   Brown, R. S.; Nagorski, R. W.; Bennet, A. J.; McClung, R. E. D.; Aarts, G. H. M.; Klobukowski, M.; McDonald, R.; Santarsiero, B. D., *J. Am. Chem. Soc.* **1994**, *116*, 2448-2456.

17.   Slebocka-Tilk, H.; Ball, R. G.; Brown, R. S., *J. Am. Chem. Soc.* **1985**, *107*, 4504-4508.

18. Bennet, A. J.; Brown, R. S.; McClung, R. E. D.; Klobukowski, M.; Aarts, G. H. M.; Santarsiero, B. D.; Bellucci, G.; Bianchini, R., *J. Am. Chem. Soc.* **1991**, *113*, 8532-8534.

19. Nagra, H. K.; Batchelor, R. J.; Bennet, A. J.; Einstein, F. W. B.; Lathioor, E. C.; Pomeroy, R. K.; Wang, W., *J. Am. Chem. Soc.* **1996**, *118*, 1207-1208.

20. Das, A. K.; Moatazedi, Z.; Mund, G.; Bennet, A. J.; Batchelor, R. J.; Leznoff, D. B., *Inorg. Chem.* **2007**, *46*, 366-368.

21. Boelema, E.; Wieringa, J. H.; Wynberg, H.; Strating, J., *Tetrahedron Lett.* **1973**, *14*, 2377-2380.

22. Chou, D. T.; Huang, X.; Batchelor, R. J.; Einstein, F. W.; Bennet, A. J., *J. Org. Chem.* **1998**, *63*, 575-581.

23. Rathore, R.; Lindeman, S. V.; Zhu, C. J.; Mori, T.; Schleyer, P. v. R.; Kochi, J. K., *J. Org. Chem.* **2002**, *67*, 5106-5116.

24. Koerner, T.; Slebocka-Tilk, H.; Brown, R. S., *J. Org. Chem.* **1999**, *64*, 196-201.

25. Cotton, F. A.; Wilkinson, G.; Murillo, C. A.; Bochmann, M., *Advanced Inorganic Chemistry.* John Wiley & Sons: Rutland, U.K., 1999.

26. Atoji, M.; Richardson, J. W.; Rundle, R. E., *J. Am. Chem. Soc.* **1957**, *79*, 3017-3020.

27. Goh, Y. M.; Nam, W., *Inorg. Chem.* **1999**, *38*, 914-920.

28. King, R. B., *Adv. Chem.* **1967**, *62*, 203-220.

29. Yoon, T. P.; Jacobsen, E. N., *Science* **2003**, *299*, 1691-1693.

30. Ahrland, S.; Chatt, J.; Davies, N. R., *Q. Rev. Chem. Soc.* **1958**, *12*, 265-276.

31. Clevette, D. J.; Orvig, C., *Polyhedron* **1990**, *9*, 151-161.

32. Cotton, F. A., *J. Am. Chem. Soc.* **1968**, *90*, 6230-6232.

33. Power, P. P., *J. Organomet. Chem.* **2004**, *689*, 3904-3919.

34. Storr, T.; Thompson, K. H.; Orvig, C., *Chem. Soc. Rev.* **2006**, *35*, 534-544.

35. Tanabe, K. K.; Cohen, S. M., *Chem. Soc. Rev.* **2011**, *40*, 498-519.

36. Chen, T.-H.; Popov, I.; Kaveevivitchai, W.; Miljanić, O. Š., *Chem. Mater.* **2014**, *26*, 4322-4325.

37. Thompson, K. H.; Orvig, C., *Dalton Trans.* **2006**, 761-764.

38. Leeuwen, P. W. N. M. v., *Homogeneous Catalysis*. Springer: Netherlands., 2004.

39. Noyori, R., *Angew. Chem. Int. Ed. Engl.* **2002**, *41*, 2008-2022.

40. Maier, N. M.; Franco, P.; Lindner, W., *J. Chromatogr. A* **2001**, *906*, 3-33.

41. Knowles, W. S., *Angew. Chem. Int. Ed. Engl.* **2002**, *41*, 1999-2007.

42. Osborn, J. A.; Jardine, F. H.; Young, J. F.; Wilkinson, G., *J. Chem. Soc. A* **1966**, 1711-1732.

43. Knowles, W. S.; Sabacky, M. J., *Chem. Commun. (London)* **1968**, 1445-1446.

44. Ault, A., *J. Chem. Educ.* **2002**, *79*, 572.

45. Colacot, T. J., *Platinum Metal Reviews* **2002**, *46*, 82-83.

46. Blaser, H. U.; Schmidt, E., *Asymmetric Catalysis on Industrial Scale: Challenges, Approaches, and Solutions*. John Wiley & Sons: Weinheim, Germany., 2007.

47. Vineyard, B. D.; Knowles, W. S.; Sabacky, M. J.; Bachman, G. L.; Weinkauff, D. J., *J. Am. Chem.Soc.* **1977**, *99*, 5946-5952.

48. Knowles, W. S., *Acc. Chem. Res.* **1983**, *16*, 106-112.

49. Kagan, H. B.; Dang Tuan, P., *J. Am. Chem. Soc.* **1972**, *94*, 6429-6433.

50. Burk, M. J., *J. Am. Chem. Soc.* **1991**, *113*, 8518-8519.

51. Burk, M. J.; Feaster, J. E.; Nugent, W. A.; Harlow, R. L., *J. Am. Chem. Soc.* **1993**, *115*, 10125-10138.

52. Mosher, H. S.; Tidwell, T. T., *J. Chem. Educ.* **1990**, *67*, 9.

53. Hofmann, A. W., *Ber. Dtsch. Chem. Ges.* **1872**, *5*, 704-719.

54. Kehrmann, F., *Ber. Dtsch. Chem. Ges.* **1888**, *21* (2), 3315-3321.

55. Kehrmann, F., *Ber. Dtsch. Chem. Ges.* **1890**, *23*, 130-136.

56.   Kehrmann, F., *Ber. Dtsch. Chem. Ges.* **1908**, *41*, 4357-4358.

57.   Meyer, V.; Sudborough, J. J., *Ber. Dtsch. Chem. Ges.* **1894**, *27*, 1580-1592.

58.   Meyer, V., *Ber. Dtsch. Chem. Ges.* **1894**, *27*, 510-512.

59.   Conant, J. B.; Blatt, A. H., *J. Am. Chem. Soc.* **1929**, *51*, 1227-1236.

60.   Gleu, K., *Angew. Chem.* **1959**, *71*, 391-391.

61.   Bradley, D. C.; Chisholm, M. H., *Acc. Chem. Res.* **1976**, *9*, 273-280.

62.   Tolman, C. A., *J. Am. Chem. Soc.* **1970**, *92*, 2956-2965.

63.   Tolman, C. A., *Chem. Rev.* **1977**, *77*, 313-348.

64.   Otsuka, S.; Yoshida, T.; Matsumoto, M.; Nakatsu, K., *J. Am. Chem. Soc.* **1976**, *98*, 5850-5858.

65.   Chen, L.; Ren, P.; Carrow, B. P., *J. Am. Chem. Soc.* **2016**, *138*, 6392-6395.

66.   Hvoslef, J.; Hope, H.; Murray, B. D.; Power, P. P., *J. Chem. Soc., Chem. Commun.* **1983**, 1438-1439.

67.   Wolczanski, P. T., *Polyhedron* **1995**, *14*, 3335-3362.

68.   Andersen, R. A.; Coates, G. E., *J. Chem.Soc., Dalton Trans.* **1972**, 2153-2155.

79.   Bochmann, M.; Wilkinson, G.; Young, G. B.; Hursthouse, M. B.; Malik, K. M. A., *J. Chem. Soc., Dalton Trans.* **1980**, 901-910.

70.   Schrock, R. R., *Polyhedrons,* **1995**, *14*, 3177–3195.

71.   Alyea, E. C.; Basi, J. S.; Bradley, D. C.; Chisholm, M. H., *Chem. Commun. (London)* **1968**, 495-495.

72.   Alyea, E. C.; Bradley, D. C.; Copperthwaite, R. G., *J. Chem. Soc., Dalton Trans.* **1972**, 1580-1584.

73.   Bartlett, R. A.; Power, P. P., *J. Am. Chem. Soc.* **1987**, *109,* 7563-7564.

74.   Cummins, C. C., *Chem. Commun.* **1998**, 1777-1786.

75.   Hayes, C. E.; Platel, R. H.; Schafer, L. L.; Leznoff, D. B., *Organometallics* **2012**, *31*, 6732-6740.
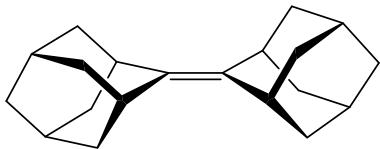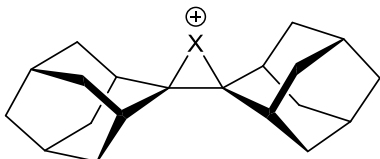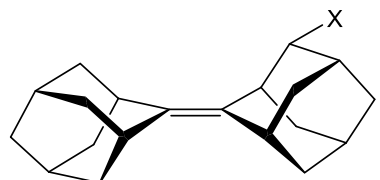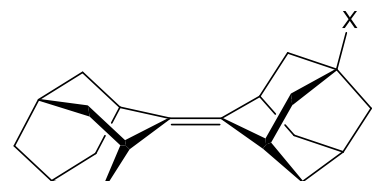
76.   Hayes, C. E.; Leznoff, D. B., *Organometallics* **2010**, *29*, 767-774.

77.   Hayes, C. E.; Sarazin, Y.; Katz, M. J.; Carpentier, J.-F.; Leznoff, D. B., *Organometallics* **2013**, *32,* 1183-1192

78.   Lenoir, D., *Synthesis* **1989**, 883-897.

79.   Huang, X.; Tanaka, K. S. E.; Bennet, A. J., *J. Am. Chem. Soc.* **1998**, *120,* 1405-1409

80.   Clark, T.; Teasley, M. F.; Nelsen, S. F.; Wynberg, H., *J. Am. Chem. Soc.* **1987**, *109*, 5719-5724.

81.   Wynberg, H.; Boelema, E.; Wieringa, J. H.; Strating, J., *Tetrahedron Lett.* **1970**, *11,* 3613-3614.

82.   Luche, J. L.; Rodriguez-Hahn, L.; Crabbe, P., *J. Chem. Soc., Chem. Commun.* **1978**, 601-602.

83.   Schneider, H. J.; Hoppen, V., *J. Org. Chem.* **1978**, *43*, 3866-3873.

84.   Rychnovsky, S. D.; Skalitzky, D. J., *Tetrahedron Lett.* **1990**, *31*, 945-948.

85.   Rohde, J. J.; Pliushchev, M. A.; Sorensen, B. K.; Wodka, D.; Shuai, Q.; Wang, J.; Fung, S.; Monzon, K. M.; Chiou, W. J.; Pan, L.; Deng, X.; Chovan, L. E.; Ramaiya, A.; Mullally, M.; Henry, R. F.; Stolarik, D. F.; Imade, H. M.; Marsh, K. C.; Beno, D. W. A.; Fey, T. A.; Droz, B. A.; Brune, M. E.; Camp, H. S.; Sham, H. L.; Frevert, E. U.; Jacobson, P. B.; Link, J. T., *J. Med. Chem.* **2007**, *50*, 149-164.

86.   Declerq, J.P.; Germain, G.; Meerssche, M. van.; Hajek, M.; Volka, K., *Bull. Soc. Chim. Belg.* **1979**, *88*, 1019-1026.

87.   Huang, X.; Bennet, A. J., *J. Chem. Soc., Perkin Trans. 2* **1994**, 1279-1284.

88.   Huang, X.; Bennet, A. J., *J. Chem. Soc., Perkin Trans. 2* **1997**, 1027-1034.

89.   Dodson, G.; Wlodawer, A., *Trends Biochem. Sci.* **1998**, *23*, 347-352.

90.   B: Mechanisms of enzyme catalysis. (2016, June 28). Retrieved from http://biochem-vivek.tripod.com/id45.html.

91.   Kazlauskas, R. J., *Org. Synth.* **1992**, *70*, 60.

92.   Moncea, O.; Gunawan, M. A.; Poinsot, D.; Cattey, H.; Becker, J.; Yurchenko, R. I.; Butova, E. D.; Hausmann, H.; Šekutor, M.; Fokin, A. A.; Hierso, J.-C.; Schreiner, P. R., *J. Org. Chem.* **2016**, *81*, 8759-8769.

93. Wieringa, J. H.; Strating, J.; Wynberg, H., *Tetrahedron Lett.* **1970**, *11* (52), 4579-4582.

94. Farrugia, L. J., *J. Appl. Crystallogr.* **1997**, *30*, 565-565.

95. Fenn, T. D., *J. Appl. Crystallogr.* **2003**, *36*, 944-947.

96. Brown, R. S., *Acc. Chem. Res.* **1997**, *30*, 131-137.

97. Bellucci, G.; Bianchini, R.; Chiappe, C.; Marioni, F.; Ambrosetti, R.; Brown, R. S.; Slebocka-Tilk, H., *J. Am. Chem. Soc.* **1989**, *111*, 2640-2647.

98. Brown, R. S.; Nagorski, R. W.; Bennet, A. J.; McClung, R. E. D.; Aarts, G. H. M.; Klobukowski, M.; McDonald, R.; Santarsiero, B. D., *J. Am. Chem. Soc.* **1994**, *116*, 2448-2456.

99. Rodebaugh, R.; Fraser-Reid, B., *J. Am. Chem. Soc.* **1994**, *116*, 3155-3156.

100. Rodebaugh, R.; Fraser-Reid, B., *Tetrahedron* **1996**, *52*, 7663-7678.

101. Neverov, A. A.; Brown, R. S., *Can. J. Chem.* **1994**, *72*, 2540-2543.

102. Meijer, E. W.; Wynberg, H., *Tetrahedron Lett.* **1981**, *22*, 785-788.

103. Nagra, H. K.; Batchelor, R. J.; Bennet, A. J.; Einstein, F. W. B.; Lathioor, E. C.; Pomeroy, R. K.; Wang, W., *J. Am. Chem. Soc.* **1996**, *118*, 1207-1208.

104. Strauss, S. H., *Chem. Rev.* **1993**, *93*, 927-942.

105. Seppelt, K., *Angew. Chem. Int. Ed.* **1993**, *32*, 1025-1027.

106. Global Spectral Deconvolution (GSD) Mestrelab Research. (2016, September 22). Retrieved from http://mestrelab.com/resources/gsd/.

107. Stevenson, P. J., *Org. Biomol. Chem* **2011**, *9*, 2078-2084.

Appendix A.   Symmetry of Ad=Ad Derivatives

The molecule framework present in Ad=Ad possesses high symmetry, D_{2h} point group. Substituents at different positions on the molecule alter the symmetry elements and result in lower symmetry. For example, Table 1.1 lists the point groups and symmetry elements present upon introduction of simple functional groups to the Ad=Ad skeleton. Of note, chiral *bis*-adamantane based molecules (C_1) can be accessed by the introduction of a substituent on C-4.

Table A.1   Symmetry of molecules based on Ad=Ad skeleton.

Molecule	Point Group	Symmetry Elements
	D_{2h}	E $C_2(x, y, z)$ $\sigma(xy, xz, yz)$ i
	C_{2v}	E $C_2(z)$ $\sigma_v(xz, yz)$
	C_1	E
	C_s	E $\sigma_v(xz)$
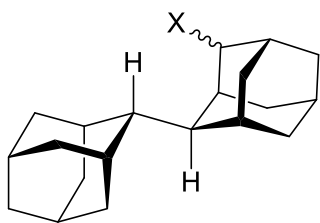
C₁   E

Appendix B.   Optimization of the conditions for benzoate protection and esterification reactions

Table B.1   Optimization of the conditions for benzoate protection.

Entry	Conditions	Observations
1	1.5 eq Benzoyl chloride, 2.5 eq pyridine, CH_2Cl_2, N_2, 4 hours	Reaction incomplete
2	1.5 eq Benzoyl chloride, 2.5 eq pyridine, CH_2Cl_2, N_2, 12 hours	Reaction incomplete
	Extra addition of 2.5 eq of benzoyl chloride and 1.5 eq pyridine to reaction mixture and allowed to stir overnight	Reaction completed 82% yield

Table B.2   Optimization of esterification reaction.

Entry	Conditions	Observation
1	1 eq. Pentanoyl chloride 2 eq. pyridine r.t., 48 h	Reaction not completed
2	3 eq. Pentanoyl chloride 4 eq. pyridine reflux, 3 h	Reaction completed (78% yield)

Appendix C.   Supplementary NMR Spectra
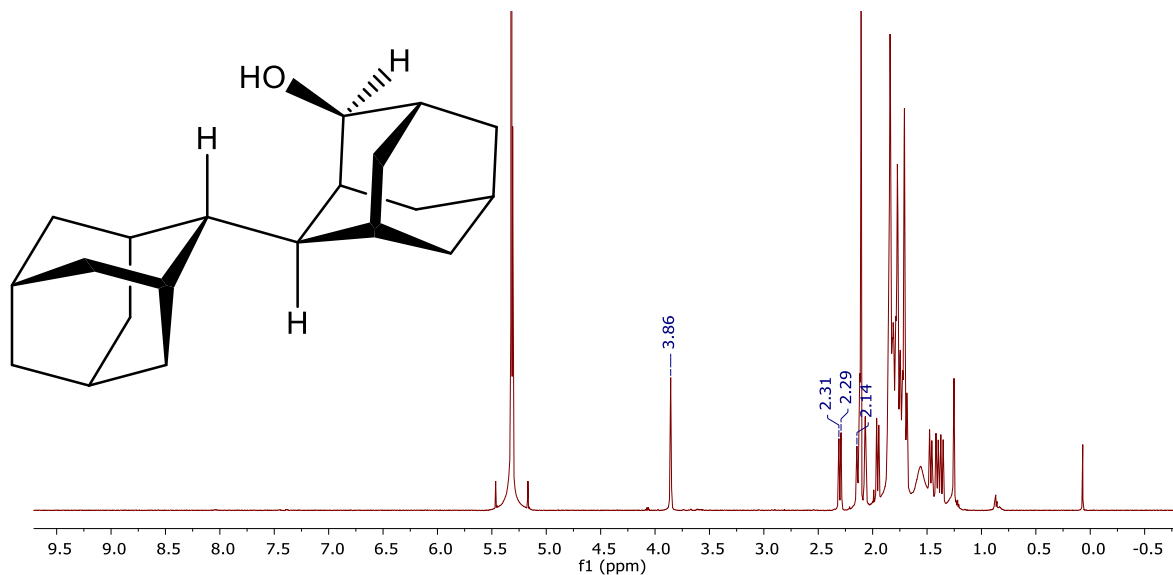
Compound *rac 10-(a)*

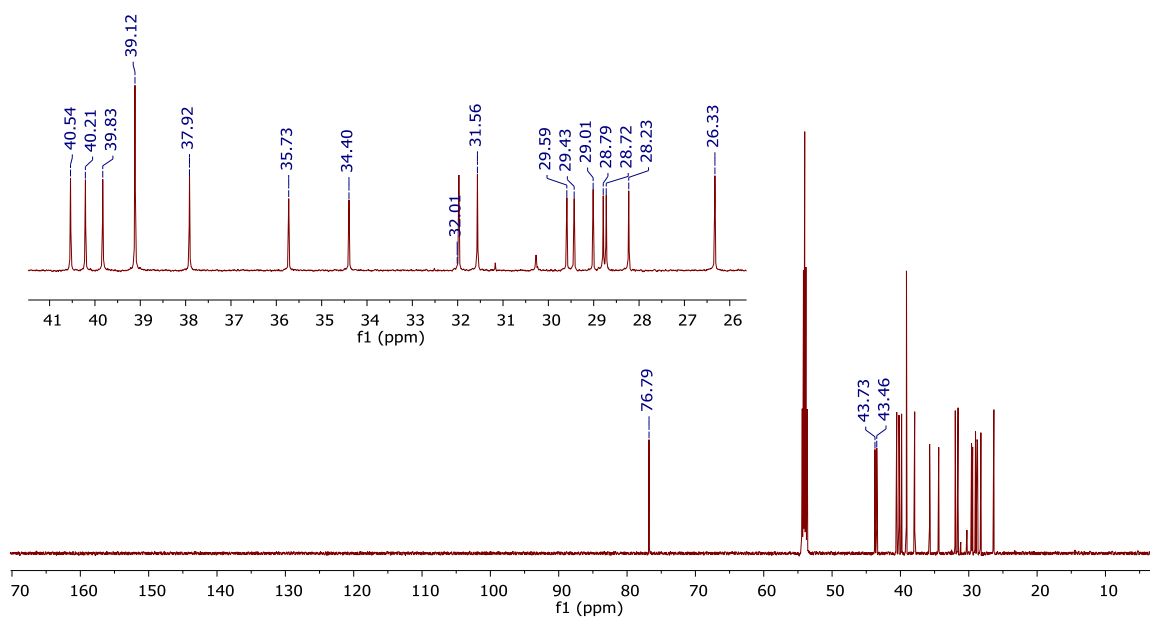Figure C.1   ¹H NMR spectrum of compound *rac 10-(a)* in CD₂Cl₂.

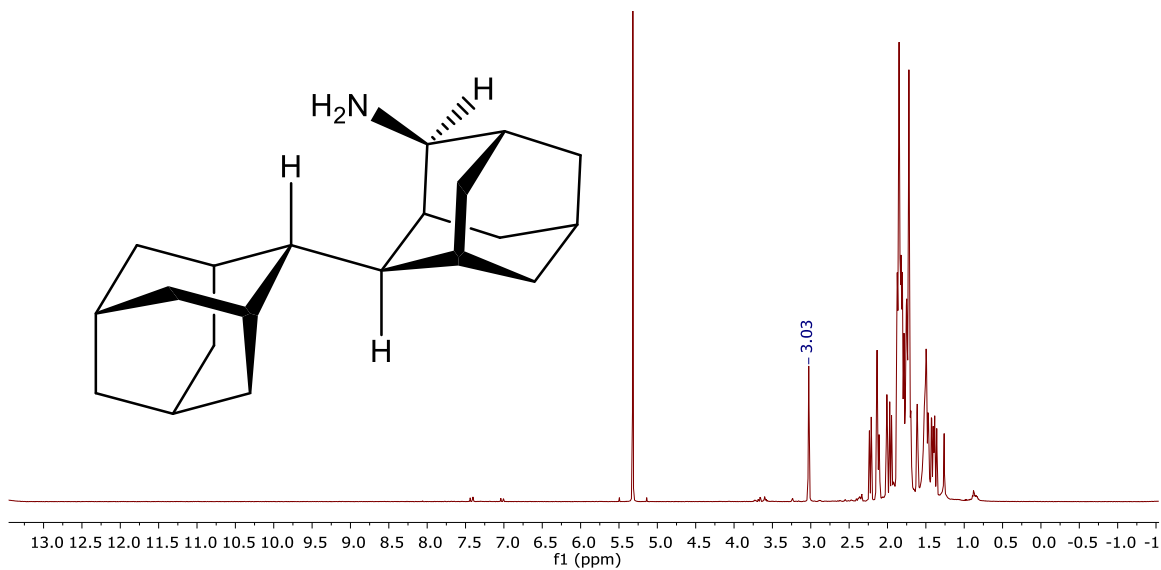Figure C.2   ¹³C NMR spectrum of compound *rac 10-(a)* in CD₂Cl₂.

Compound rac 11-(a)

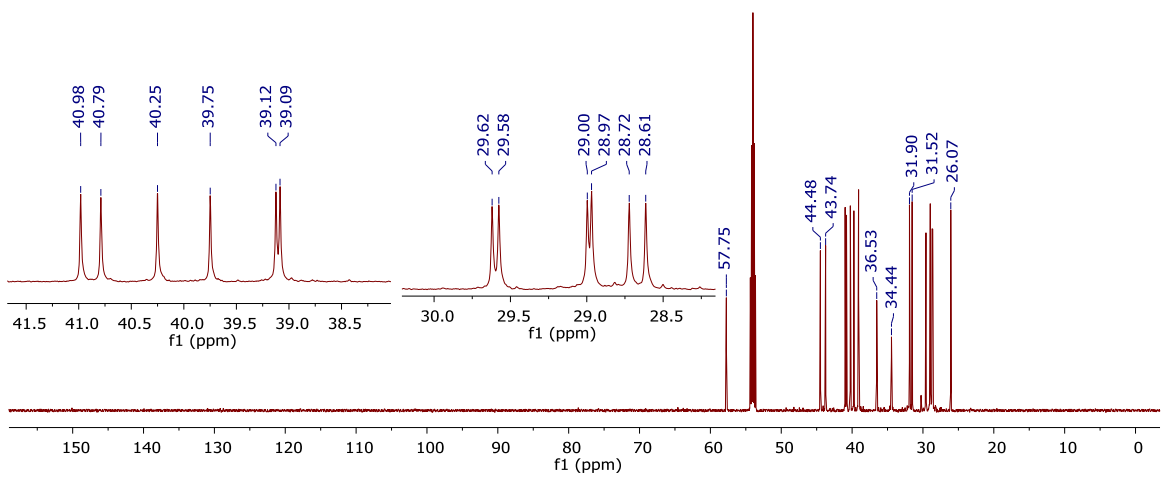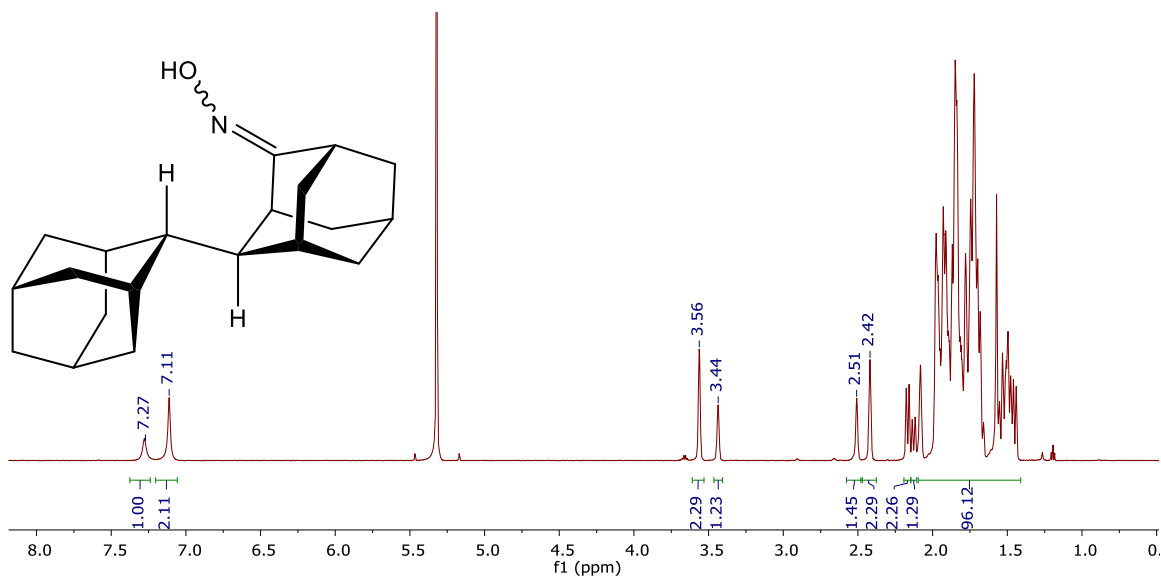Figure C.3 ^{1}H NMR spectrum of compound *rac 11-(a)* in CD$_2$Cl$_2$.

Figure C.4 ^{13}C NMR spectrum of compound *rac 11-(a)* in CD$_2$Cl$_2$.

Compound *17*

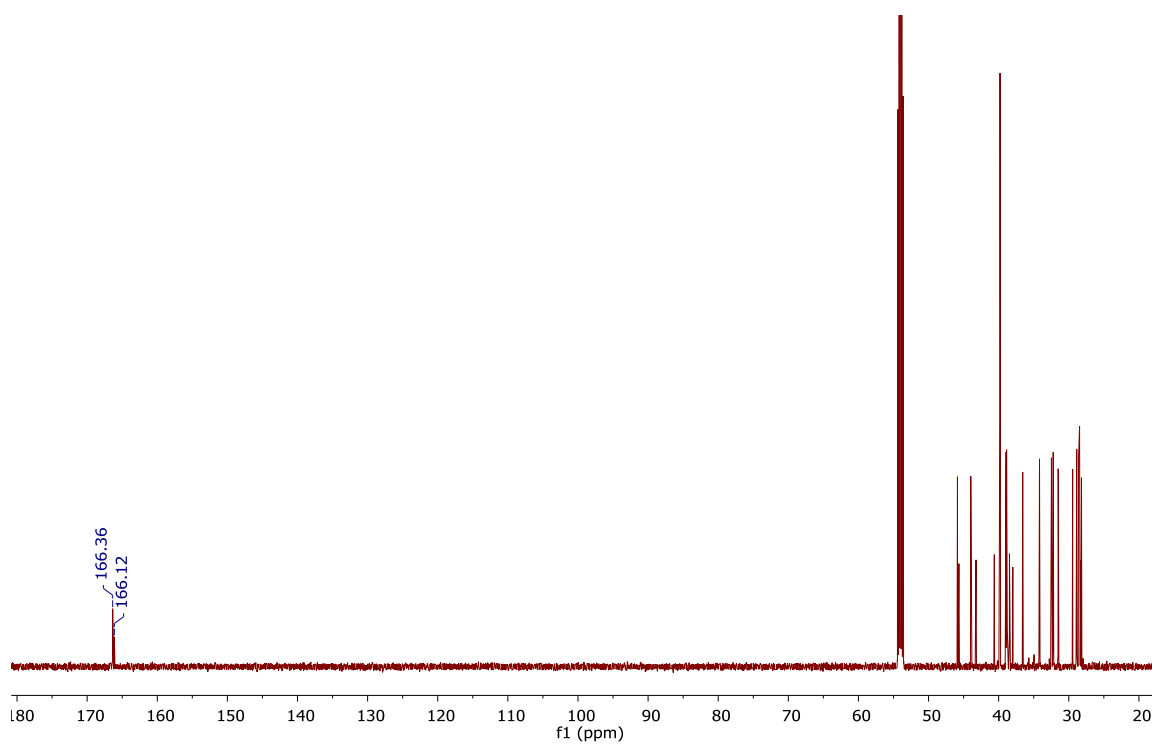Figure C.5   ¹H NMR spectrum of compound *17* in CD$_2$Cl$_2$.

Figure C.6   ¹³C NMR of compound *17* in CD$_2$Cl$_2$.

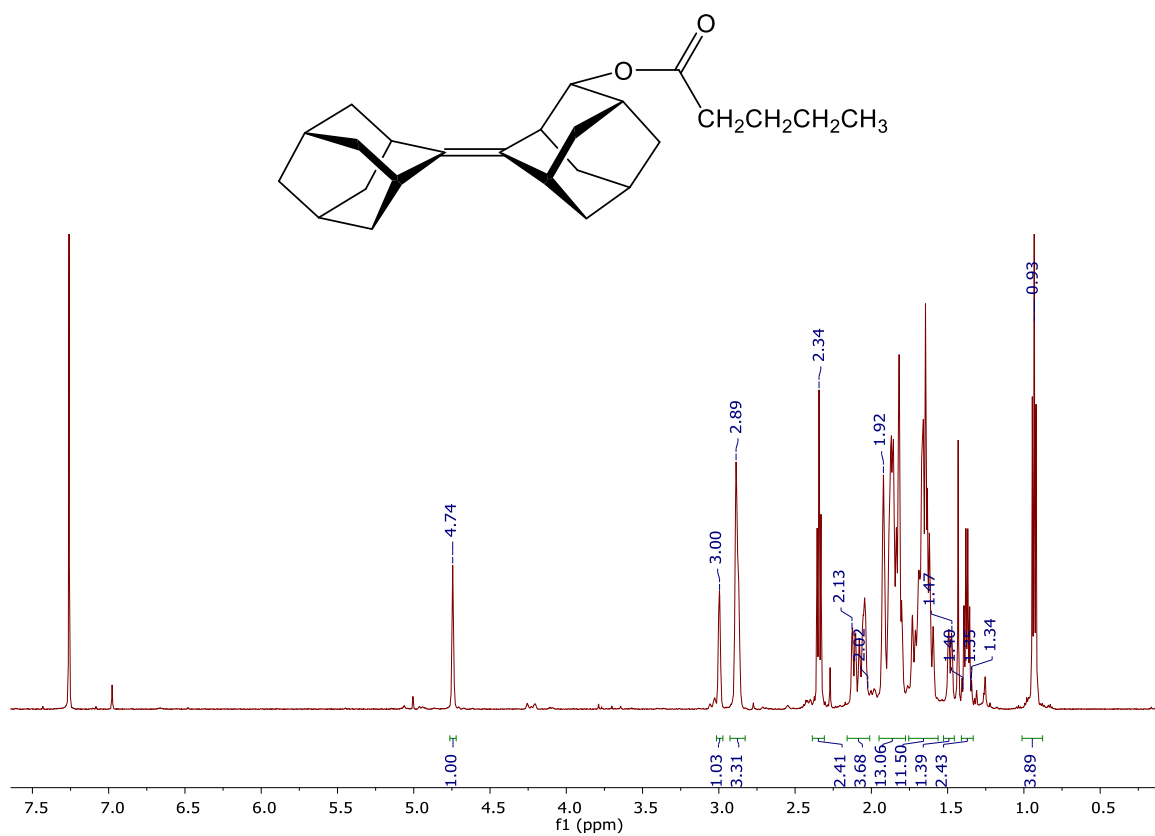**Compound *rac-9***

Figure C.7 ^{1}H NMR spectrum of compound *rac-9* in CDCl$_3$.

Compound *(-)6*
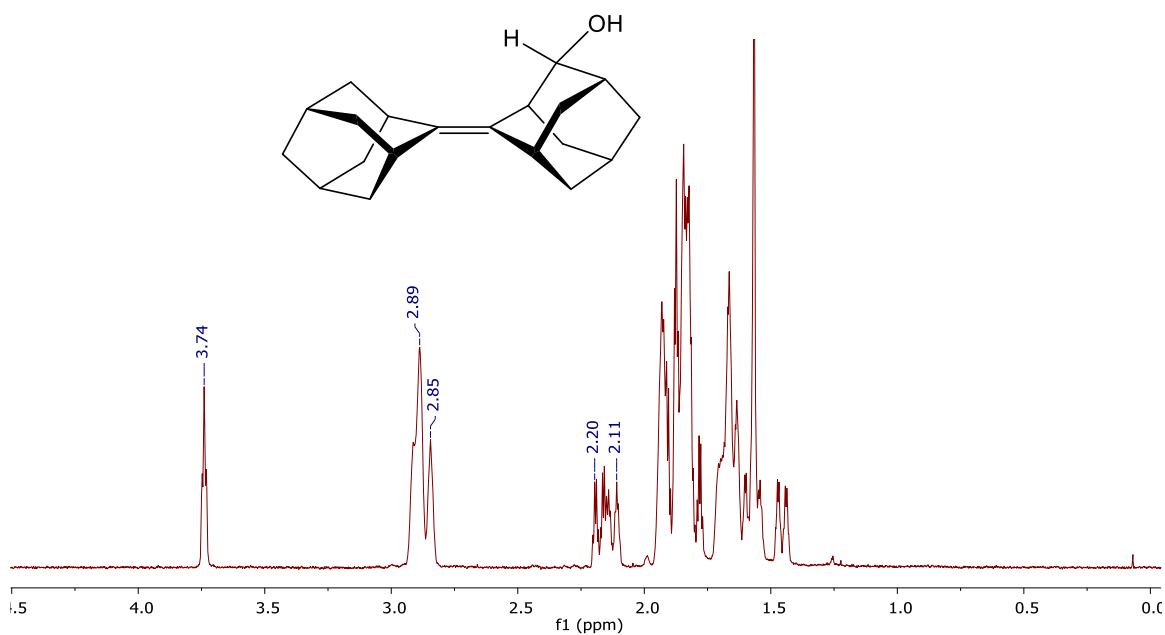

Figure C.8 ^{1}H NMR spectrum of unsaturated chiral alcohol *(-)6*.
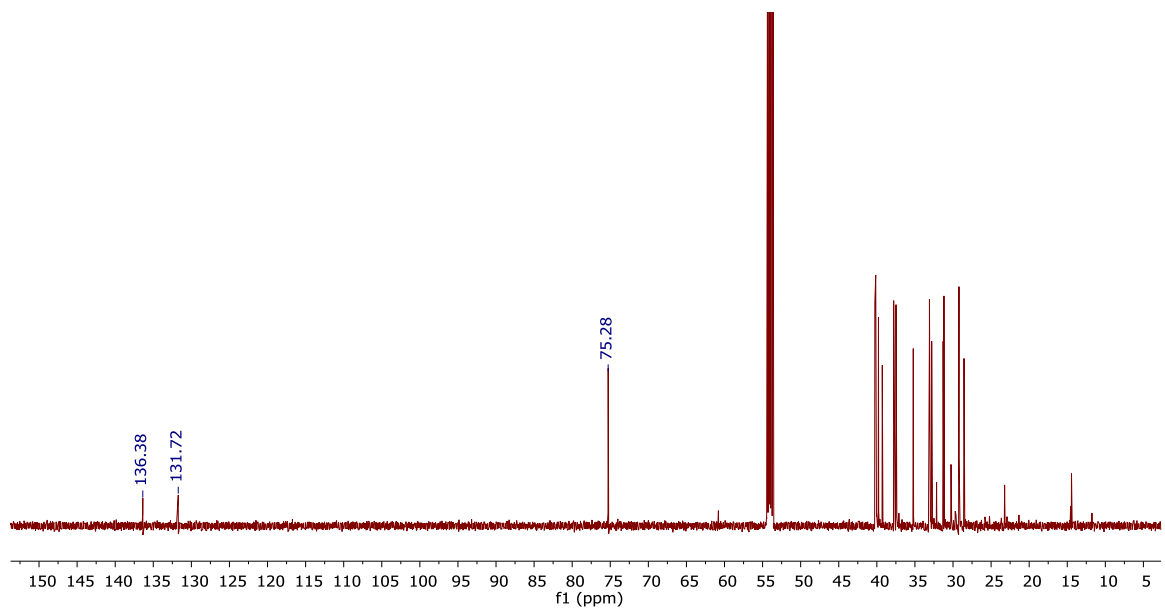
Figure C.9 ^{13}C NMR spectrum of unsaturated chiral alcohol *(-)6* in CD$_2$Cl$_2$.

125

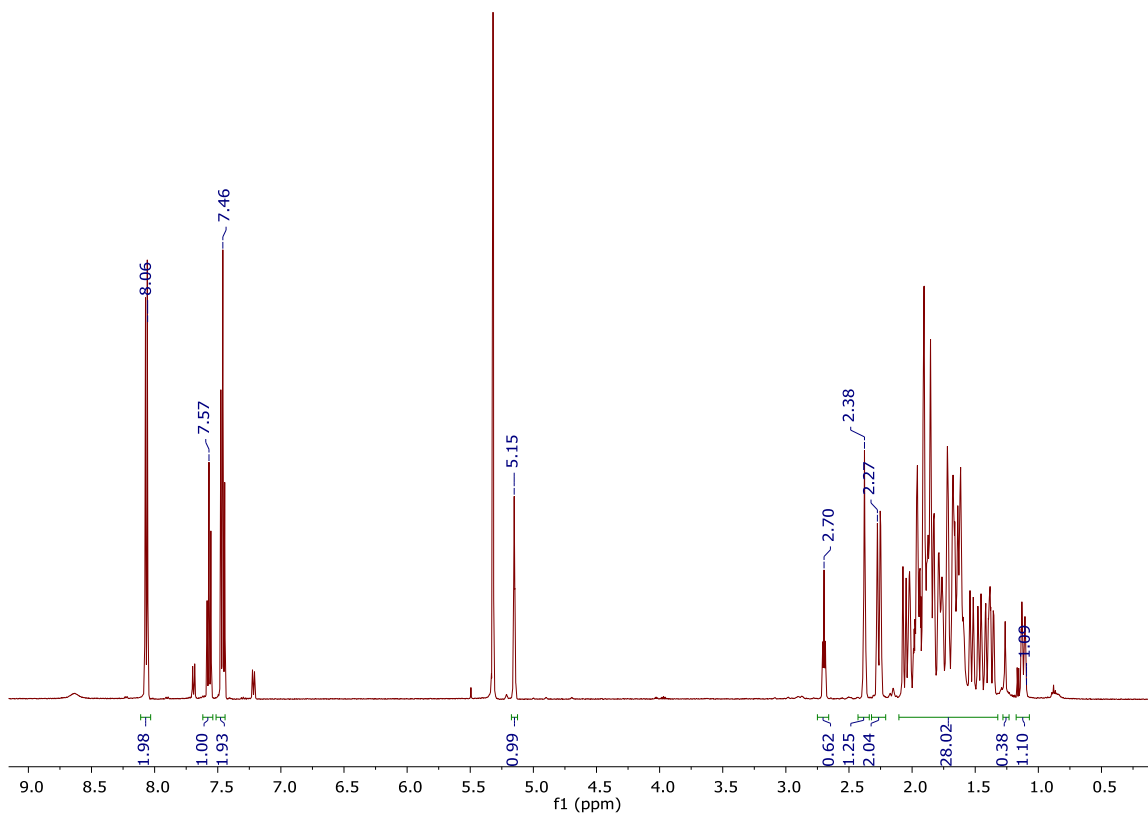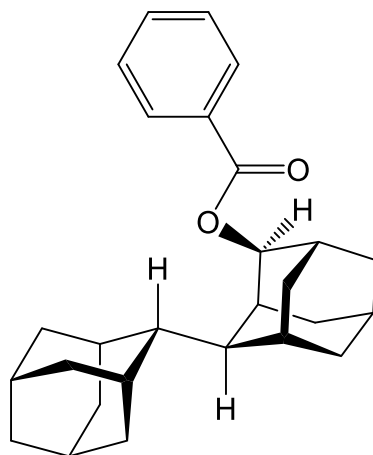**Compound *(+)15-(a)***

Figure C.10   ¹H NMR spectrum of pure major diastereomer *(+)15-(a)* in CD₂Cl₂.
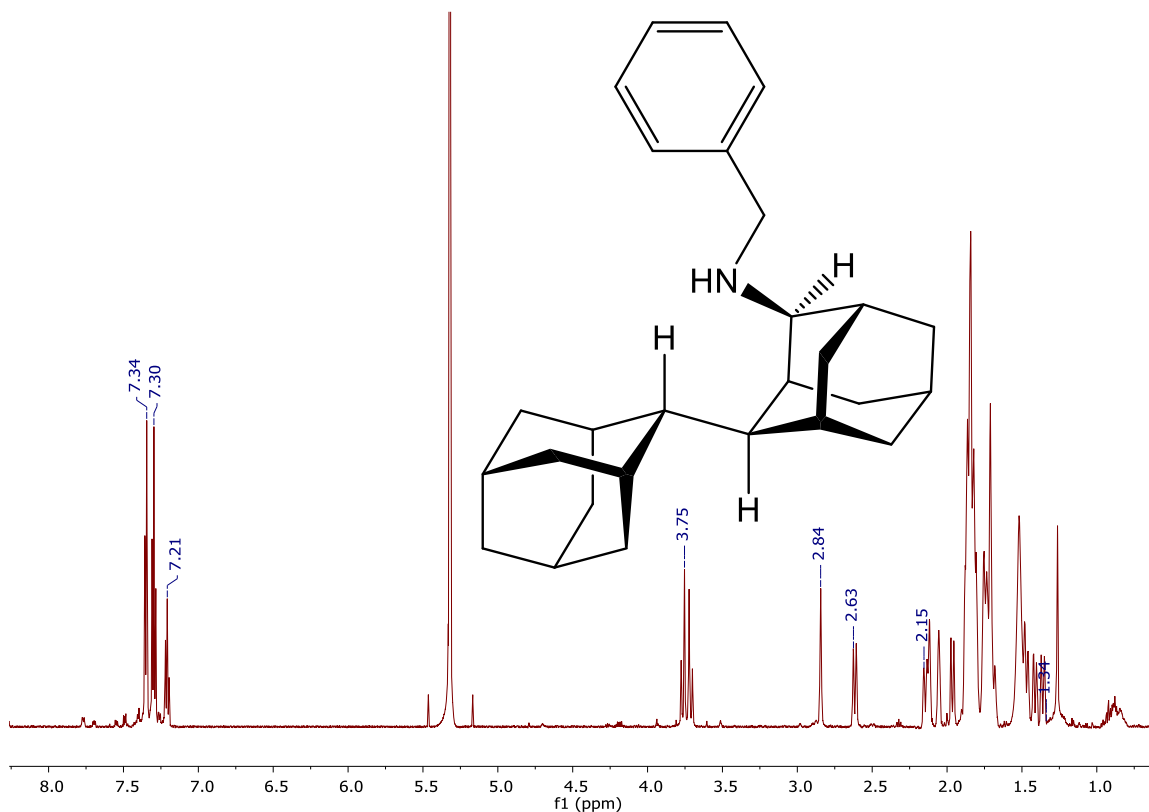
Compound *(+) 16-(a)*

Figure C.11   ¹H NMR spectrum of pure major diastereomer *(+)16-(a)* in CD₂Cl₂.
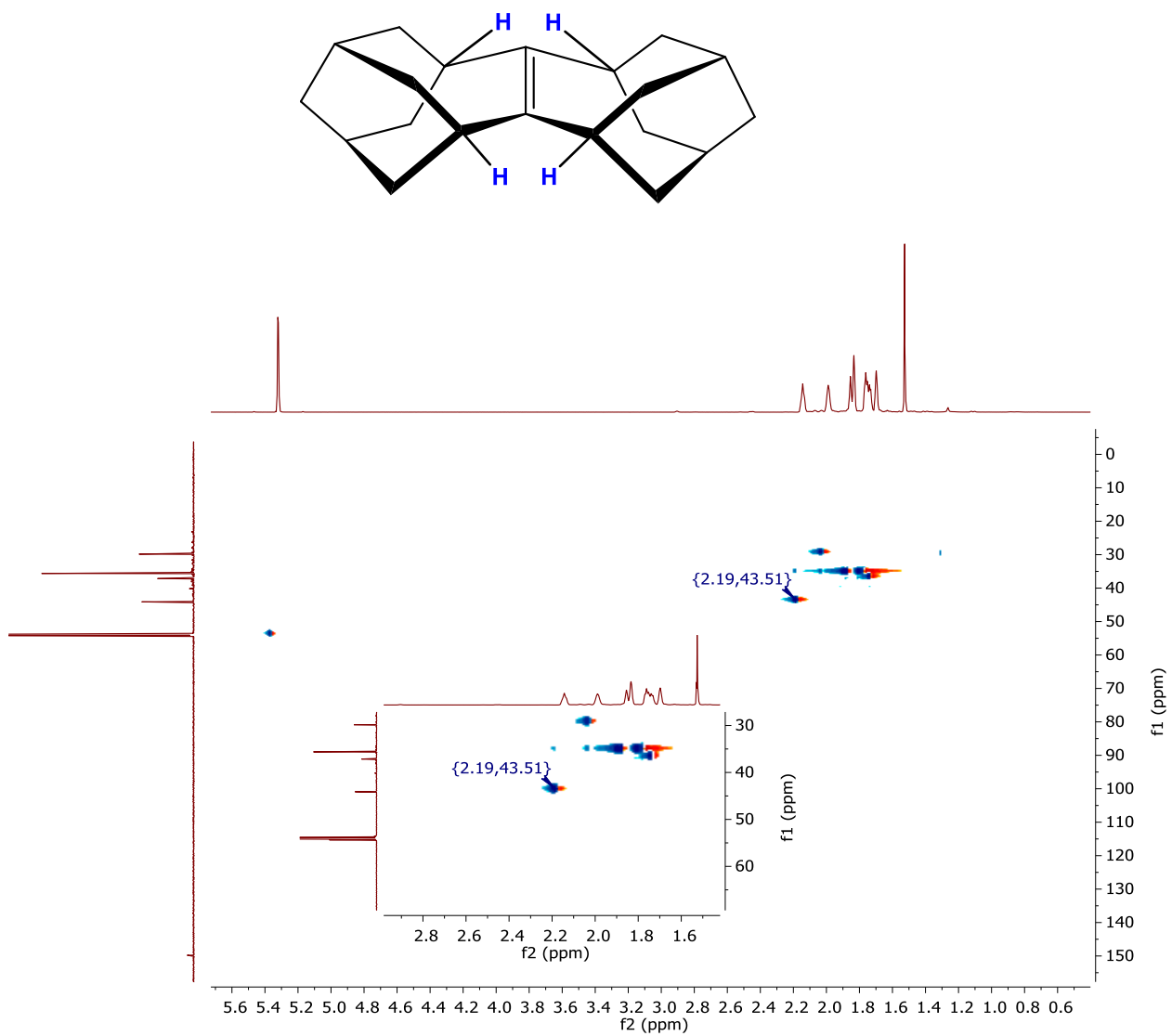
Compound 3

Figure C. 12 ^{1}H-^{13}C HSQC spectrum of SesquiAdAd **(3)** in CD$_2$Cl$_2$.

Appendix D. Supplementary Crystallographic Information

Table D.1   Supplementary crystallographic data for compounds *17, (-)6 and (+)7.*

Compound reference	Compound *17*	Compound *(-)6*	Compound *(+)7*
Chemical formula	$C_{22}H_{35}NO_2$	$C_{20}H_{28}O$	$C_{20}H_{28}O$
Formula Mass	345.51	284.42	284.42
Crystal system	Triclinic	Orthorhombic	Monoclinic
a/Å	6.5948(5)	15.4691(4)	6.5560(4)
b/Å	9.4198(7)	30.4630(8)	12.1153(8)
c/Å	15.3951(11)	6.7400(2)	9.5191(7)
α/°	96.549(4)	90	90
β/°	92.029(4)	90	93.513(3)
γ/°	98.774(5)	90	90
Unit cell volume/Å^3	937.65(12)	3176.12(15)	754.66(9)
Temperature/K	150(2)	296(2)	293(2)
Space group	$P\bar{1}$	$P2_1\,2_1\,2$	$P2_1$
No. of formula units per unit cell, Z	2	8	2
Radiation type	CuKα	CuKα	MoKα
Absorption coefficient, μ/mm^{-1}	0.593	0.535	0.074
No. of reflections measured	3284	29214	11392
No. of independent reflections	3284	5600	2775
R_{int}	0.1317	0.1012	0.0477
Final R_1 values ($I > 2\sigma(I)$)	0.0982	0.0537	0.0622
Final $wR(F^2)$ values ($I > 2\sigma(I)$)	0.2705	0.1233	0.1694
Final R_1 values (all data)	0.1051	0.0744	0.0745
Final $wR(F^2)$ values (all data)	0.2782	0.1342	0.1838
Goodness of fit on F^2	1.229	1.049	1.400
Flack parameter		0.0(2)	1.5(10)

Appendix E.   Derivation of Rate Law for the Bromonium Ion Catalyzed Rearrangement of Sesquihomoadamantene.

Under pre-equilibrium approximation, that is, the first step which is the equilibrium step, is fast and reversible and the second step (k_2) is the slow step.

$$\frac{d[P]}{dt} = k_2[SB] \tag{1}$$

$$K_{eq} = \frac{[A][SB]}{[S][AB]} = \frac{k_1}{k_{-1}} \tag{2}$$

Rearranging equation (2) to make [SB] subject of formula

$$[SB] = \frac{K_{eq}[S][AB]}{[A]} \tag{3}$$

$$[S]_0 = [S] + [SB] + [P] \tag{4}$$

When Ad=Ad is in excess,

$$[A]_0 \gg [S]_0 \quad \text{then} \quad [A]_0 \approx [A]_0 + [P] \tag{5}$$

Rearranging equation (3) to make [S] subject for formula

$$[S] = \frac{[SB][A]}{K_{eq}[AB]} \tag{6}$$

Substituting equation (6) in equation (4) with [P] subject of formula

131

$$\tag{7}$$

$$[P] = [S]_0 - \frac{[SB]\big([A] + K_{eq}[AB]\big)}{K_{eq}[AB]}$$

Rearranging equation (7) to make [SB] subject of formula

$$[SB] = \frac{K_{eq}[AB]}{[A] + K_{eq}[AB]} \times ([S]_0 - [P]), \quad \text{and} \quad [S]_0 = [P]_\infty \tag{8}$$

Substituting equation (8) in equation (1)

$$\frac{d[P]}{dt} = \frac{k_2 K_{eq}[AB]}{[A] + K_{eq}[AB]} \times ([P]_\infty - P_0), \quad \text{therefore} \quad k_{obs} = \frac{k_2 K_{eq}[AB]}{[A] + K_{eq}[AB]} \tag{9}$$

If on the other hand we assume a steady state approximation, that is, SB is a high energy intermediate then:

$$\frac{d[SB]}{dt} = 0 = k_1[S][AB] - k_{-1}[SB][A] \tag{10}$$

Rearranging equation (10) to make [SB] subject of formula

$$[SB] = \frac{k_1[S][AB]}{k_{-1}[A] + k_2} \tag{11}$$

Rate of formation of product Ad=Ad [A]:

$$\frac{d[A]}{dt} = k_1[S][AB] - k_{-1}[SB][A] \tag{12}$$

Substituting equation (11) in equation (12)

$$\frac{d[A]}{dt} = k_1[S][AB] - \frac{k_1 k_{-1}[A][S][AB]}{k_{-1}[A] + k_2}$$

$$= \frac{k_1[S][AB](k_{-1}[A] + k_2)}{k_{-1}[A] + k_2} - \frac{k_1 k_{-1}[A][S][AB]}{k_{-1}[A] + k_2}$$

$$= \frac{k_1 k_{-1}[A][S][AB] + k_1 k_2[S][AB] - k_1 k_{-1}[A][S][AB]}{k_{-1}[A] + k_2}$$

$$\frac{d[A]}{dt} = \frac{k_1 k_2[S][AB]}{k_{-1}[A] + k_2} \tag{13}$$

Under conditions of rapid equilibration and if SB [sesquiAdAdBr⁺] is a high energy intermediate then the same rate law is obtained for both mechanism.

$$k_{obs} = \frac{k_2 K_{eq}[AB]}{[A] + K_{eq}[AB]} \text{ , if } K_{eq}[AB] \ll [A] \text{ then } k_{obs} = \frac{k_2 K_{eq}[AB]}{[A]}$$

$$k_{obs} = \frac{k_1 k_2[AB]}{k_{-1}[A] + k_2}, \text{ if } k_{-1}[A] \gg k_2, \text{then } k_{obs} = \frac{k_1 k_2[AB]}{k_{-1}[A]} = \frac{k_2 K_{eq}[AB]}{[A]}$$

$k_{obs} = \frac{k_2 K_{eq}[AB]}{[A]}$ is obtained in both cases for rapid equilibrium and high energy intermediate under the assumptions of an excess of [A] and $k_2 \ll k_{-1}$[A] respectively, that is, we have a high energy intermediate of [SB] with a rapid equilibrium of the bromonium ions.